Identification of Essential Genes in Hepatocellular Carcinomas using CRISPR Screening

IDENTIFICATION OF ESSENTIAL GENES IN HEPATOCELLULAR CARCINOMAS USING CRISPR SCREENING

A Dissertation Presented

By

Ankur Sheel

Submitted to the Faculty of the

University of Massachusetts Graduate School of Biomedical Sciences, Worcester

in partial fulfillment of the requirements for the degree of

DOCTOR OF PHILOSOPHY

July, 15th, 2019

(MD/PhD, Cancer Biology)

IDENTIFICATION OF ESSENTIAL GENES IN HEPATOCELLULAR CARCINOMAS USING CRISPR SCREENING

A Dissertation Presented

By

Ankur Sheel

This work was undertaken in the Graduate School of Biomedical Sciences

(MD/PhD, Cancer Biology)

Under the mentorship of

Wen Xue, PhD, Thesis Advisor

Victor R. Ambros, PhD, Member of Committee

Thomas G. Fazzio, PhD, Member of Committee

Pranoti Mandrekar, PhD, Member of Committee

Jun Qi, PhD, External Member of Committee

Brian C. Lewis, PhD, Chair of Committee

Mary Ellen Lane, PhD,

Dean of the Graduate School of Biomedical Sciences

July, 15th, 2019

ACKNOWELDGEMENTS

This work would not have been possible without the support and guidance of many people. The first and foremost person I would like to acknowledge is my PI, Wen Xue. Wen's support and mentorship offered a unique perspective on the nuances of biomedical research and scientific thinking. Overall, I have learned a great deal from Wen and look forward to carrying those lessons with me as I move forward in my career. I would also like to thank Darryl Conte and Emily Mohn for their support and teaching me how to communicate my research in a clear and concise manner. I feel fortunate to have completed my graduate studies in the RTI as all the faculty, staff, post-docs and students in this department are not only encouraging but they are willing to teach and help. I would like to thank the members of TRAC including Brian Lewis, Victor Ambros, Dohoon Kim and Tom Fazzio for their time, guidance, and advice during my PhD. I would also like to thank the additional members of my dissertation exam committee, Pranoti Mandrekar and Jun Qi, for their using their time to evaluate my work.

Next, I would like to acknowledge all the current and previous members of the Xue lab. Tingting Jiang, Jordan Smith, Shun-Qing Liang, Zachary Kennedy, Chun-Qing Song and Yueying Cao have provided me with support and mentorship in both my scientific and personal pursuits. Most importantly I would like to thank Suet Yan Kwan for her support and guidance throughout my graduate studies. Suet Yan and I both worked together as a team, and this work could not have been completed without her

relentless efforts. I could not have asked for a better group of lab-mates and friends during my PhD.

I would also like to thank my friends in both the GSBS and the MD/PhD program at UMMS. The PhD can often feel quite isolating, but the comradery that is developed amongst fellow students is galvanizing. Finally, I would like to thank my parents, my brother and my fiancé for being my shoulder to lean on and for teaching me patience, perseverance and discipline.

ABSTRACT

Hepatocellular carcinoma (HCC) is an aggressive subtype of liver cancer with a poor prognosis. Currently, prognosis for HCC patients remains poor as few therapies are available. The clinical need for more effective HCC treatments remains unmet partially because HCC is genetically heterogeneous and HCC driver genes amenable to targeted therapy are largely unknown. Mutations in the *TP53* gene are found in ~30% of HCC patients and confer poor prognosis to patients. Identifying genes whose depletion can inhibit HCC growth, and determining the mechanisms involved, will aid the development of targeted therapies for HCC patients. Therefore, the first half of this thesis focuses on identifying genes that are required for cell growth in HCC independent of p53 status.

We performed a kinome-wide CRISPR screen to identify genes required for cell growth in three HCC cell lines: HepG2 (p53 wild-type), Huh7 (p53-mutant) and Hep3B (p53-null) cells. The kinome screen identified 31 genes that were required for cell growth in 3 HCC cell lines independent of *TP53* status. Among the 31 genes, 8 genes were highly expressed in HCC compared to normal tissue and increased expression was associated with poor survival in HCC patients. We focused on TRRAP, a co-factor for histone acetyltransferases. TRRAP function has not been previously characterized in HCC. CRISPR/Cas9 mediated depletion of TRRAP reduced cell growth and colony formation in all three cell lines. Moreover, depletion of TRRAP reduced its histone acetyltransferase co-factors KAT2A and KAT5 at the protein level with no change at the mRNA level. I found that depletion of KAT5, but not KAT2A, reduced cell growth. Notably, inhibition of proteasome- and lysosome-mediated degradation failed to rescue

protein levels of KAT2A and KAT5 in the absence of TRRAP. Moreover, tumor initiation in an HCC mouse model failed after CRISPR/Cas9 depletion of TRRAP due to clearance via macrophages and HCC cells depleted of TRRAP and KAT5 failed to grow as subcutaneous xenografts *in vivo*. RNA-seq and bioinformatic analysis of HCC patient samples revealed that TRRAP positively regulates expression of genes that are involved in mitotic progression. In HCC, this subset of genes is clinically relevant as they are overexpressed compared to normal tissue and high expression confers poor survival to patients. I identified TOP2A as one of the mitotic gene targets of the TRRAP/KAT5 complex whose inhibition greatly reduces proliferation of HCC cells.

Given that this was the first time the TRRAP/KAT5 complex has been identified as a therapeutic target in HCC, the second half of this thesis focuses on identifying the mechanism via which depletion of this complex inhibits proliferation of HCC cells. I discovered that depletion of TRRAP, KAT5 and TOP2A reduced proliferation of HCC cells by inducing senescence. Typically, senescence is an irreversible state of cell cycle arrest at G1 that is due to activation of p53/p21 expression, phosphorylation of RB, and DNA damage. Surprisingly, induction of senescence after loss of TRRAP, KAT5 and TOP2A arrested cells during G2/M and senescence was independent of p53, p21, RB and DNA damage.

In summary, this thesis identifies TRRAP as a potential oncogene in HCC. I identified a network of genes regulated by TRRAP and its-cofactor KAT5 that promote mitotic progression. Moreover, I demonstrated that disruption of TRRAP/KAT5 and its downstream target gene TOP2A result in senescence of HCC cells independent of p53

status. Taken together, this work suggests that targeting the TRRAP/KAT5 complex and its network of target genes is a potential therapeutic strategy for HCC patients.

TABLE OF CONTENTS

LIST OF FIGURES

LIST OF TABLES

LIST OF COPYRIGHTED MATERIAL PRODUCED BY THE AUTHOR

Chapter II and Chapter III: Most of the text and all figures in Chapter II and Chapter III along with Figure 4.1 are part of a work that has been accepted for publication in *Hepatology* and has preliminarily been published online. Kwan, S., **Sheel, A.**, Song, C., Zhang, X., Jiang, T., Dang, H., Cao, Y., Ozata, D.M., Mou, H., Yin, H., Weng, Z., Wang, X.W., & Xue, W. (2019) Depletion of TRRAP induces p53-independent senescence in liver cancer by downregulating mitotic genes. doi:10.1002/hep.30807. This work is copyrighted by the 2019 American Association for the Study of Liver Diseases. The work is reprinted with permission from John Wiley & Sons Limited.

Appendix II: Figure 1 is adapted from the following manuscript (in submission): Elaimy, A.L., **Sheel, A.**, Brown, C., Walker, M., Amante, J., Xue, W., Chan, A., Baer, C., Goel, H., & Mercurio, A. Real-time imaging of integrin β4 dynamics using a reporter cell line generated by Crispr/Cas9 genome editing. (Accepted at Journal of Cell Science). Portions of the work are reprinted with permission from The Company of Biologists LTD.

Appendix II: Figure 2 is adapted from the following publication (permission granted for use if cited properly): Mou, H., Ozata, D. M., Smith, J. L., **Sheel, A.**, Kwan, S. Y., Hough, S., Kucukural, A., Kennedy ,Z., Cao, Y., & Xue, W. (2019). CRISPR-SONIC: targeted somatic oncogene knock-in enables rapid in vivo cancer modeling. Genome medicine, 11(1), 21.

CHAPTER I

Introduction

Hepatocellular Carcinoma

Liver cancers are the fourth most common cause of cancer related deaths worldwide (1). Primary liver cancers are comprised of distinct histopathological subtypes including Hepatocellular Adenoma (HCA), Hepatocellular Carcinoma (HCC), Intrahepatic Bile Duct Carcinoma (cholangiocarcinoma or CCC), Hepatoblastoma and Hemangiosarcoma (2). HCC is the most common and prevalent subtype, comprising >83% of liver tumors. The number of new cases of HCC in the United States has increased by ~60% over the last 20 years (from 5.4 to 8.6 new cases per 100,000 patients) (3). Likewise, the rate of death due to HCC in the United States has also increased by ~52% (from 4.4 to 6.7 deaths per 100,000 patients) (4). Overall, HCC has a 5-year survival of ~18%, making it the second most lethal tumor type, the first being pancreatic cancer (5).

The majority of HCC occurs in patients with underlying liver disease. These diseases include chronic infection with Hepatitis B virus (HBV) or Hepatitis C virus (HCV), chronic alcohol abuse, non-alcoholic steatohepatitis (NASH) and other pro-inflammatory metabolic diseases (such as hemochromatosis, α1 antitrypsin deficiency and tyrosinemia) in combination with obesity. Overall, these etiologies create a pro-inflammatory environment resulting in hepatic fibrosis. Hepatocytes undergo continuous

rounds of death and regeneration in this deleterious setting. As hepatocytes replicate under this stress, they begin to accumulate genetic and epigenetic aberrations (6). This genetic and epigenetic instability leads to the initiation of hyperplastic nodules, which can progress to malignancy.

Hyperplastic nodules are comprised of regenerating hepatocytes and show normal cytological features; however, these nodules can proceed to dysplastic nodules. Dysplastic nodules are considered to be a pre-malignant lesion for HCC. Dysplastic nodules show abnormal cytological features such as cellular atypia, pseudoglandular structures and evidence of increased stromal invasion (2). Dysplastic nodules may eventually evolve to form invasive hepatocellular carcinomas.

Molecular Characterization

Molecular analysis of human HCC has revealed multiple genetic and epigenetic alterations that are associated with activation of oncogenes and inhibition of key tumor suppressor genes. Mutations in the *TERT* promoter are the most common genetic aberration seen in HCC samples. These mutations (which include amplifications) account for ~60% of HCC cases and can be detected in dysplastic nodules (7). The prevalent theory in the field of HCC genomics postulates that the high presence of *TERT* promoter mutations in HCC is potentially due to viral integration secondary to HBV and HCV infection. Mutations in pathways that regulate cell cycle progression such as *TP53*, WNT signaling, chromatin remodeling , or angiogenesis account for a large number of HCC cases (6). Chromosomal instability (CIN), as assayed by fluorescence-in-situ

hybridization (FISH), demonstrated that CIN can appear in benign lesions but is more frequent in high-grade dysplastic nodules and correlates with HCC tumor progression (8).

Aberrations in pathways responsible for cell cycle progression account for ~30% of HCC cases. These aberrations include mutations in *TP53*, overexpression/amplification of *CCND1*/*FGF19* and silencing of RB1 expression via deletion or promoter methylation (7, 9). Mutations in the tumor suppressor *CDKN2A* are also seen in ~5% of HCC cases and are associated with alcohol abuse (10).

WNT pathway alterations include activating mutations in the β-catenin gene (*CTNNB1*) and inactivating mutations in *AXIN1*. These mutations are seen in 30% and 10% of HCC cases, respectively (6). In addition, promoter hypermethylation of the APC tumor suppressor is also seen in a small subset ~3% of HCC (11). Overall, WNT pathway mutations are rarely seen in dysplastic nodules and are thought to occur later during HCC progression. In terms of correlation with HCC risk factors, *CTNNB1* activating mutations are associated with alcohol abuse (11).

Loss of function mutations in chromatin remodelers such as *ARID1A* and *ARID2* account for ~10% and ~5% of HCC cases respectively (6). Interestingly, mutations in *ARID1A* and *ARID2* were enriched in non-HBV and non-HCV populations (12) suggesting a tumor suppressor role of the SWI/SNF complex in non-viral induced HCC. In line with this, a previous study demonstrated that suppression of ARID1A in hepatocytes promotes fatty liver and steatohepatitis (13)

Finally, amplification of genes required for angiogenesis and growth such as *VEGFA* account for ~5-10% of HCC cases (6, 14). Amplifications in *VEGFA* are seen

more commonly in HCC compared to dysplastic nodules (7). Interestingly, dysplastic nodules receive their vascular supply through the portal system whereas HCC receives its vascular supply from the hepatic artery (2). The role of VEGFA in promoting tumor growth is well established ubiquitously in cancer models. However, given the difference in vascular supply in HCC compared to dysplastic nodules it would be interesting to examine if *VEGFA* amplifications promote "rewiring" from the portal system to the hepatic artery during progression from a dysplastic nodule to HCC.

Epigenetic aberrations are also seen in HCC. DNA methylation profiles between HCC and normal tissue revealed 298 genes which were significantly hypermethylated. These genes were involved in differentiation, stem cell maintenance and were targets of the Polycomb repressive complex (14).

Molecular Subclasses of HCC

As our understanding of HCC genomics has advanced, multiple attempts have been made to identify genetic signatures and use these signatures to cluster HCC patients in order to provide prognostic information.

Profiling of 603 HCC patient tumors from 8 independent patient cohorts revealed three major classes which correlated with tumor size, extent of cellular differentiation, and serum alpha-fetoprotein levels—S1, S2 and S3 (15). Tumors within the S1 class had DNA mutations mainly in the *TP53* tumor suppressor gene and contained genetic signatures associated with TGF-β activation. Tumors within the S2 class also contained *TP53* mutations, however tumors within this class were positive for the stem-like features

such as EPCAM and had increased expression of alfa-fetoprotein (AFP). Furthermore, S2 tumors contained genetic signatures associated with activated Insulin Like Growth Factor 2 (IGF2). Interestingly, tumors within both S1 and S2 classes contained genetic signatures associated with activated WNT signaling (15). However there was no detectable activating *CTNNB1* mutation in these samples suggesting the presence of additional cellular programs that activate WNT signaling. The authors attributed this observation to crosstalk from activated TGF-β signaling. Both S1 and S2 tumors are histologically less differentiated and patients have high rates of recurrence. Finally, S3 tumors are driven by *CTNNB1* mutations, are histologically more differentiated and have lower rates of recurrence. In this classification regimen, patients with S3 tumors had greater survival rates than patients with S1 and S2 tumors (16). Collectively, S1 and S2 tumors are grouped into the 'proliferative' class whereas S3 tumors are in the 'non-proliferative' class (17).

Nearly a decade after the release of this classification scheme, groups are now beginning to test whether these classes are predictive of responses to therapies. For example, by classifying immortalized HCC cell lines into this system, groups were able to demonstrate that S2 HCC cell lines were more sensitive to drugs like JQ1 (18) and the FGFR inhibitors BGJ398 and AZD4547 (19). Of note, out of 25 HCC cell lines validated *in vitro*, no HCC cell line tested corresponded to the S3 tumor subtype (18). The predictive power of the S1, S2 and S3 subclasses on response to therapies in HCC patients remains to be seen. Moreover, although this classification scheme was one of the

first to molecularly characterize HCC tumors, it failed to consider aberrations in copy number, epigenetic changes and the presence of tumor immune infiltrates.

More recently, analysis of HCC tumor samples by The Cancer Genome Atlas (TCGA) group by whole-exome sequencing, DNA copy number analyses, and DNA methylation along with analysis of miRNA and proteome expression revealed three clusters that were not originally captured by in the S1, S2, S3 classification scheme (14). iCluster 1 contained high grade tumors that were poorly differentiated. Of note, the prevalence of TERT promoter amplifications was low, but these tumors had silenced the miR-122a locus. iCluster 2 contained low grade tumors with less microvascular invasion and had high levels of *CDKN2A* inactivation and high incidence of *CTNNB1* mutations. iCluster 3 contained low grade tumors with less microvascular invasion but also displayed high amounts of chromosomal instability. These tumors contained *TP53* mutations and had high prevalence of *TERT* promoter mutations. Immune phenotyping of HCC revealed that a subset of HCC had high levels of immune cell infiltration. However, the composition of the infiltrate did not correlate with HBV/HCV infection or patient survival. Like the S1, S2, S3 classifications, it remains to be seen whether the iCluster classifications are predictive of responses to therapies.

Clinical Management

Management of patients with HCC is divided into surgical and clinical management. Surgical intervention is available for patients with early stage disease. Patients who present with a solitary nodule (<3cm in size) will qualify for surgical

resection whereas patients with 2-3 small nodules (<3cm in size) will qualify for liver transplantation (20). Surgical resection is associated with a survival rate of ~60% after 5 years, however, ~ 70% of these patients have tumor recurrence at 5 years (21). In contrast, transplantation is associated with a survival of ~60-80% after five years and 50% after 10 years. Furthermore, the tumor recurrence rate is <15% after 5 years (6). However, given the large deficit between the demand for and supply of donors, there is a need for alternative therapies while patients wait for transplants.

Ablation therapy provides one such alternative. Ablation therapy utilizes targeted radiofrequency waves in order to induce necrosis by increasing the intra-tumoral temperature. This form of therapy is utilized in patients with single nodules that are large (>3cm) in size (22). Currently, there are no studies that compare outcomes with surgical resection, transplantation and radiofrequency ablation for the management of HCC (20). However, ablation is frequently used to manage patients who are on the wait-list for transplantation. Overall, the only therapies with curative potential available to HCC patients are surgical resection, transplantation and radiofrequency ablation (23).

Non curative therapies consist of transarterial chemoembolization and systemic therapies. Patients who have multi-nodal disease without metastasis may qualify for transarterial chemoembolization. As discussed earlier, HCC derives its vascular supply from the hepatic artery as opposed to the portal system. Transarterial chemoembolization involves delivery of a cytotoxic agent directly into the hepatic artery followed immediately by embolization of the vessels supply the tumors. The toxic effects on normal hepatic tissue from this therapy are low as normal hepatocytes derive their

vascular supply from the portal vein. A recent meta-review comparing 101 studies on transarterial chemoembolization demonstrated a five-year survival of 32.4% with a median survival of 19.4 months and a mortality rate of <1% (24).

Systemic therapies are recommended for patients who have metastatic disease or those who have progressed after transarterial chemoembolization (6). As our understanding of tumor genetics is advancing, targeted therapies are now utilized for therapy as they have greater anti-tumor potential and display less toxicity compared to cytotoxic agents. However, HCC has the fewest genetic aberrations that can be effectively targeted with molecular therapies (6). Hence, there are few targeted therapies for HCC. Studies have examined the efficacy of broad-spectrum receptor tyrosine kinase (RTK) inhibitors in HCC. In 2008, Sorafenib was the first targeted therapy approved for the treatment of HCC. In the hallmark Sorafenib Hepatocellular Carcinoma Assessment Randomized Protocol (SHARP) trial, sorafenib increased overall survival from 7.9 months to 10.7 months compared to placebo (25). Multiple other therapies made it to phase 3 clinical trials but failed to show parallel or superior survival results compared to sorafenib. These agents include the RTK inhibitors Sunitinib and Erlotinib, the Topoisomerase inhibitor, Doxorubicin, and Tivantinib for MET amplified tumors (6). More recently, Lenvatinib, a vascular endothelial growth factor (VEGF) and fibroblast growth factor receptor (FGFR) inhibitor demonstrated a median overall survival of 13.6 months (26) and was approved for the treatment of HCC. In addition, Regorafenib was approved as second-line treatment after sorafenib as it reduced the risk of death by 37% compared to placebo and had a toxicity profile similar to sorafenib (27).

In the last year two anti PD-L1 immunotherapies, Pembrolizumab and Nivolumab were approved for the treatment for HCC. A phase 2 study with Pembrolizumab showed an anti-tumor response in 17% of patient treated with one patient having complete remission. Furthermore, 56% of patients showed no disease progression for greater than one year (28). A phase 2 study with Nivolumab showed a stable disease rate of 44.9%, with 10.2% of these patients achieving a partial response (29). Data from phase 1 trials which combine immunotherapy with other targeted therapies are promising (6), but phase 3 trials are required to fully establish their roles in clinical management. With immunotherapies emerging as an additional drug regimen for the treatment of HCC, HCC therapeutics is a rapidly growing and exciting field. However, there is still a need to identify additional therapeutic targets that show demonstrable anti-tumor potential beyond RTK inhibitors.

Cell Cycle Primer

The mammalian cell cycle is organized into four major phases: G0/G1, S, G2 and M. Proliferation is dependent on progression through these phases. Moreover, progression through the phases can be induced by extracellular signals such as mitogenic factors and intracellular signals such as DNA damage (30).

The G1 phase is characterized by cellular growth and expression of genes required for DNA synthesis. During this phase DNA damage is predominantly monitored by p53 and checkpoint kinase 2 (CHK2) (30). In order to progress from G1 to S, mitogenic signals induce phosphorylation of cyclin D resulting in binding and activation

of CDK4/6 (31). Progression from G1 to S is driven by phosphorylation of the retinoblastoma protein (RB) and subsequent expression of genes regulated by the E2F transcription factor (30). The cyclin inhibitor *CDKN1A*, also known as $P21^{CIP1}$, can bind to and inhibit the activity of the Cyclin D-CDK4/6 complex (32). *Cyclin E,* an E2F target gene, is expressed at the end of G1 and mediates progression into S phase. The Cyclin E/CDK2 complex also phosphorylates Rb thus creating a positive feedback loop to drive expression of genes in order to progress into S phase (33).

S phase is characterized by replication of the genome. During S phase, cyclin E is degraded by the ubiquitin proteasome system (34), cyclin A is rapidly synthesized and associates with CDK2. In order to faithfully replicate the genome in a timely fashion and progress through S phase, the cell monitors for stalled replication forks and DNA damage (35). Replication fork stalling can occur via alterations in histone pools, alterations in nucleotide pools and decreased chromatin accessibility (35). Furthermore, the cell also monitors for DNA damage during replication. The signaling kinases, ataxia-telangiectasia mutated (ATM) and ataxia-telangiectasia and RAD3 related (ATR) are the main detectors of such lesions (36). Progression through S and into G2 is driven by cyclin A binding to CDK1 (33).

G2 is characterized by rapid cell growth and protein synthesis in order to prepare for cell division. Cyclin A is bound to CDK1 and is active until late G2 whereupon Cyclin A is replaced by Cyclin B (33). In addition, cells have another opportunity to detect and resolve residual DNA damage. DNA damage detected during G2 activates checkpoint kinase 1 (CHK1), which induces G2/M arrest via phosphorylation of CDC25

(37). Progression from G2 into M is also regulated by polo like kinase 1 (PLK1) and aurora kinase A/B (AURKA and AURKB) (38). AURKA and AURKB regulate activity of the Cyclin B/CDK1 complex and also localizes to the centrioles during mitosis to aid in cytokinesis (39). During mitosis, CDK1 activity is driven by association with cyclin B. Cyclin B is degraded by the anaphase promoting complex (APC) in late mitosis. Degradation of cyclin B allows for chromosome separation and cytokinesis mediated by microtubules (40).

Targeting Mitosis and the Cell Cycle in HCC

Cancers are characterized by deregulated proliferation resulting from mutations that either hyperactive or inactivate major cell cycle regulators. Furthermore, pathways that regulate cell cycle progression are the second most prominent genetic drivers of HCC making this network an attractive target for therapeutic intervention. Numerous therapeutic strategies have been developed towards targeting cell cycle progression in cancer cells. These include microtubule inhibitors, CDK inhibitors, aurora kinase inhibitors and agents that induce DNA damage. However, the majority of these strategies have failed due to an inefficient therapeutic index or cytotoxic effects on normal cells (41).

Cytotoxic Agents and DNA Damage

Given that DNA damage is considered to be a major inhibitor of cell cycle progression, cytotoxic agents that induce DNA damage and subsequent cell cycle arrest,

have been a mainstay of treatment for multiple cancer types. Doxorubicin, a Topoisomerase inhibitor, and cisplatin, a DNA cross linking agent, have shown therapeutic efficacy in multiple cancer types and are two of the most commonly utilized chemotherapies in HCC. However, response rates are low and neither drug prolongs survival significantly in HCC patients (42). Furthermore, attempts to increase the drug concentration to levels at which there is an anti-tumor response also results in significant toxicities. Studies have demonstrated that transarterial chemoembolization using either doxorubicin or cisplatin can efficiently increase the dose of drug delivered to the tumor without causing significant toxicity to normal hepatocytes (43, 44). Capecitabine, a drug converted to 5-fluorouracil (5-FU), acts on DNA synthesis and can slow tumor growth. It is currently used as an adjuvant therapy post-surgical resection in HCC. Clinical trials showed lower recurrence rate, greater time to tumor recurrence and a near doubling in the 5-year survival rate with adjuvant Capecitabine (45). Overall, although effective *in vitro*, treatment with cytotoxic agents in HCC is limited due to the toxicities associated with treatment.

Microtubule Inhibitors

Microtubule targeting agents disrupt microtubule dynamics and lead to prolonged cell cycle arrest followed by cell death. These drugs target the polymerization dynamics of microtubules which is required for spindle formation. The most commonly used microtubule targeting agents used clinically are either vinca-alkaloids or taxanes. Vinca-alkaloid derived compounds destabilize spindle formation by preventing microtubule

assembly whereas taxanes stabilize spindle formation by preventing microtubule *disassembly*. These drugs are used to manage multiple malignancies including breast, lung, ovarian, prostate, leukemias and lymphomas.

Despite the thorough investigation of vinca-alkaloids in other malignancies, there are limited trials for the use of such agents in HCC (46). A phase 2 study of Vindesine in 16 HCC patients who did not qualify for transplantation did not show any therapeutic effect as median progression-free survival was 3.4 months (47). Contrarily, taxanes, such as docetaxel (48) and paclitaxel (49), exerted an anti-tumor effect *in vitro*. However, these *in vitro* results did not translate to a durable anti-tumor response in phase 2 trials (50).

A major limitation to the use of microtubule inhibitors is due to the fact that they also exert their effects on normal dividing cells. Consequently, patients treated with these drugs often experience severe neurotoxicities that effect movement and sensation. Moreover, these patients may also experience severe myelosuppression (51). Such toxicities limit the use of microtubule inhibitors in cancers.

Pan-CDK Inhibitors

Cyclin inhibitors are also attractive targets in cancer therapeutics as inhibition of cyclins and treatment with anti-CDK agents can induce cell cycle arrest at G1/S and G2/M transitions. Flavopiridol was one of the first CDK inhibitors to enter the clinic. Flavopiridol is considered to be a pan-cyclin inhibitor as it inhibits CDKs 1, 2, 4 and 7. Although it showed a response rate of ~70% in hematological malignancies, flavopiridol

monotherapy failed to show considerable response in solid tumors (41). However, flavopiridol combined with doxorubicin resulted in stable disease in sarcoma patients (52) and flavopiridol in combination with paclitaxel and carboplatin resulted in stable disease in non-small cell lung cancer (53). Yet when Phase 2 trials were conducted in HCC patients, flavopiridol either as monotherapy or when combined with other cytotoxic agents yielded no durable anti-tumor response (54). In general, the first generation CDK inhibitors such as flavopiridol were unable to exhibit an antitumor response due to the fact that they exhibited a low therapeutic index and raising the dose resulted in toxicities.

However, the success of these compounds in some tumor models prompted the discovery of second-generation inhibitors such as Dinaciclib. Dinaciclib, was found by screening individual compounds against an ovarian cancer mouse xenograft model. Dinaciclib was shown to be 16-fold more potent at inhibiting CDKs 1, 2, 5 and 9 and 100-fold more potent at inhibiting Rb phosphorylation than Flavopiridol (55). Dinaciclib showed efficacy in Phase 1 clinical trials in hematological malignancies such as multiple myeloma (56) and chronic lymphocytic leukemia (57), however, like its predecessor it failed to show efficacy as monotherapy in solid tumors such as HER2-negative metastatic breast cancer (58) and NSCLC (59).

A phase 1 study in 2013 assessing safety of Dinaciclib across solid tumor types, showed no anti-tumor activity in the one patient with HCC (60). Hence, more thorough examination of Dinaciclib in HCC was not warranted at the time. However, recent studies revealed that Dinaciclib susceptibility was dependent on MYC overexpression/amplification in Triple Negative Breast Cancers(61), B-Cell Lymphomas

(62), and HCC (63). In light of this new data, perhaps new clinical trials studying Dinaciclib is warranted in which patients are stratified by MYC expression.

CDK4/6 Inhibitors

The development of pan-CDK inhibitors prompted the discovery of CDK selective inhibitors in order to reduce toxicities associated with pan-CDK inhibition. The CDK4/6 inhibitors Palbociclib and Ribociclib showed potent and durable anti-tumor responses in genetic mouse models and pre-clinical studies for both hematological malignancies (64-66) and solid tumors (67). Surprisingly, Palbociclib showed efficacy in Glioblastoma Multiforme (GBM) models as it was able to cross the blood-brain barrier when delivered systemically (68). Palbociclib induced cell cycle arrest in HCC cell lines, in organotypic *ex vivo* cultures from HCC patients and in HCC mouse models (69). Not surprisingly, HCC tumors with RB deletion and cyclin E amplification were resistant to palbociclib and CDK4/6 inhibitors (69, 70). In addition, tumors that had elevated levels of CDK4/6 activity were found to be more resistant to therapy (67). Interestingly, normal cells displayed low toxicity to CDK4/6 inhibitors in pre-clinical models. One possible explanation for this was that normal cells can rely on CDK2 activity in order to progress through the cell cycle after CDK4/6 inhibition (67). Currently, Palbociclib has been approved by the FDA for the treatment of HER2-positive advanced breast cancer and is currently in being tested in phase 2/3 trials for NSCLC, GBM, Melanoma and HCC (71).

AURKA/B Inhibitors

AURKA and AURKB represent a family of kinases which can regulate progression from S phase to G2, cytokinesis and chromosome segregation during mitosis. Treatment of cancer cells with Alisertib, a small molecular inhibitor for AURKA, induced mitotic arrest and polyploidy leading to cell cycle arrest in multiple myeloma (72), apoptosis in mantel cell lymphoma (73), and tumor regression in *MYCN* driven mouse models of neuroblastoma (74). Further studies in an HCC model driven by MYC overexpression and P53 loss, demonstrated that Alisertib resulted in MYC degradation and prolonged survival in this mouse model (75). Small molecule inhibition of AURKB via AZD1152 similarly showed therapeutic benefit as treatment induced apoptosis in HCC cell lines *in vitro* and in orthotopic hepatic xenografts in p53-wildtype, mutant and null cells (76).

Phase 1 studies have been conducted in hematological malignancies (77) and solid tumors (78) using Alisertib and, like previous cell cycle inhibitors, Alisertib exhibits a greater anti-tumor response in hematological malignancies compared to solid tumors. One potential explanation for this trend is that hematological malignancies proliferate faster than solid tumors resulting in more frequent opportunities for the drug to have its effect (41). A phase 2 study with Alisertib showed a 21% response rate in patients with small cell lung cancer and an 18% response rate in breast cancer (72). Alisertib is currently in phase 2 trials for HCC. While AURKB inhibitors showed promise in pre-clinical models, AURKB inhibitors have not shown significant improvements in survival in phase 2 trials (33).

Due to the structural similarities between different kinase families, many AURKA/B inhibitors also inhibit other tyrosine kinases related to angiogenesis and oncogenesis such as VEGFR2 and BCR-Abl (41). ENMD-2076 is one such AURKA inhibitor that also inhibits VEGFR2. This dual action mechanism allows for a sustained anti-proliferative effect with IC50s ranging from 25nM-700nM in breast, colon, melanoma, leukemia and multiple myeloma tumor xenograft models (79). ENMD-2076 showed extremely promising results in a phase 1 study in patients with HCC (80) and was subsequently granted orphan drug designation for HCC by the FDA.

Overall, the discovery of targeted therapies that inhibit mitosis and cell cycle progression have demonstrated significant benefit in multiple tumor type as these molecules have low therapeutic indices and limited toxicities on normal cells. Furthermore, targeting this vulnerability in HCC cells has been shown to be more efficacious than standard chemotherapy. Currently, small molecule inhibitors that target cell cycle progression and mitosis is an exciting frontier in HCC, however, the success of these compounds remains to be seen in future phase 2 clinical trials.

CRISPR as a Tool for Discovery of Novel Therapeutic Targets

Genetic screens enable identification and functional characterization of genes associated with a particular phenotype. Traditionally, genetic screens in cancer cells relied on random DNA mutagenesis induced via DNA damage or retrovirus mediated transposon integration (81). Sleeping beauty-based transposon screens succesfuly identified therapeutic targets and oncogenic drivers in multiple malignancies. These

targets include HDAC7 in hematopoietic malignancies (82), APC, PTEN and SMAD4 in colorectal cancers (83), the PI3K-AKT-mTOR pathway in osteosarcomas (84) and the HIPPO pathway in HCC (85). Although these approaches contributed to a greater understanding of tumor biology, identifying the genetic changes that were associated with a particular phenotype was challenging (81). With the discovery of RNAi, shRNA and siRNA-based screens allowed for loss of function screens in which the genetic perturbation could be easily detected as shRNAs used molecular tags. Although these screens furthered our understanding of tumor biology and revealed novel therapeutic targets, RNAi based screens were limited by a high number of false negatives due to low knockdown efficiency and the off-target effects of the particular sh/siRNA used (86).

CRISPR Function

The discovery of the CRISPR-Cas9 system and advances in modifying it for the genome engineering in mammalian systems allowed for another facile system that could probe gene function and be utilized in genetic screens. Briefly, the Cas9 enzyme homes in on a particular site in the genome using a single 20-nucleotide guide RNA (sgRNA) (87). It subsequently binds DNA and induces a double stranded break (DSB) upstream of a Protospacer Adjacent Motif (PAM) sequence, a short sequence of 2-6 nucleotides that varies depending on the bacterial origin of the Cas9 enzyme (87). The DSBs are repaired by two intracellular repair mechanisms: Non-homologous End Joining (NHEJ) or Homology-directed Repair (HDR). The NHEJ repair pathway is error prone and can introduce small insertions or deletions (indels) that can introduce frameshift mutations

(88). These mutations result in gene silencing owing to the production of truncated polypeptide, and also often nonsense mediated decay of the transcript (88). Conversely, HDR precisely repairs the DSB using a homologous DNA template (89). Of note, NHEJ-based repair occurs more frequently than HDR (89). The programmable and facile nature of Cas9 allows for forward genetic screens to be performed in various models.

High-throughput CRISPR-based screens are performed by infecting cells with lentivirus consisting of a sgRNA library (90, 91). Briefly, CRISPR libraries typically contain multiple sgRNAs that target each gene. sgRNA oligos are pooled together and then cloned into an appropriate vector to create a pooled library. Cells are then transduced at a low multiplicity of infection (MOI) in order to achieving genomic integration rates of one sgRNA per cell (91). Cells can then be subsequently treated with a drug/toxin to produce a phenotype. Alternatively, cells can be passaged long term to identify genes that are required for cell growth. After a phenotype is produced, enriched or depleted sgRNAs are then identified via next generation sequencing.

CRISPR Screens

The first CRISPR based screens were published less than five years ago and identified genes that mediated resistance to the RAF inhibitor, vemurafenib (92), and nucleotide analog, 6-thioguanin (93). Since then CRISPR screening has gained increased popularity as a tool for genetic screens. A search for “CRISPR screening” in PUBMED reveals >600 papers all within the last 5 years. Although numerous CRISPR genetic knockout screens have been reported, it is important to mention that there are screens

utilizing other functions of CRISPR such as base-editing and transcriptional activation using CRISPRa (94-96). Furthermore, conjugating a catalytically inactive Cas9 (dCas9) with transcriptional repressors, such as KRAB, and activators, such as p300, has allowed for identification of regulatory elements at particular genomic loci (97). Finally, CRISPR screens have also been utilize to identify essential non-coding RNAs (98).

Numerous studies have conducted genetic knockout screens using the CRISPR/Cas9 system. These screens have identified genes essential for fitness in human cells (99), genes essential for proliferation of human cancer cell lines and mouse models of cancer (100). Notably, DEPMAP is a recently created publicly available dataset which compiled data from CRISPR screens that were conducted in over 200 human cancer cell lines (101, 102). Of note, CRISPR screens are now beginning to be conducted in vivo. The major limitation to in vivo CRISPR screens is efficient delivery of the library to target cells while maintaining a low MOI and an even representation of sgRNAs. To overcome this barrier, groups have begun transducing cells *in vitro* and injecting the cells *in vivo* (103-105).

CRISPR vs RNAi Screens

CRISPR based screens initially gained traction due to the easy programmable nature of the nuclease and the fact that CRISPR often resulted in greater and more stable knockdown of targets compared to traditional RNAi (106). In line with this, some of the first CRISPR screens were able to identify a greater number of essential genes compared to RNAi screening (99) and exhibited reduced off target effects compared to RNAi

screening (107). Two years after the first CRISPR screen was published numerous studies were published that presented side by side comparisons of CRISPR and RNAi based screens (108, 109).

In the study by Munoz et al., the authors constructed complementary shRNA and sgRNA libraries and screening five cancer cell lines (three of which were diploid and two of which were aneuploid). They found that the sgRNA screen identified 2-5 times more essential genes than the shRNA screen. When analyzing false positive hits, the authors found that there were no false positive hits in the three diploid cell lines but the sgRNA screen did produce false positives in the two aneuploid cell lines. Moreover, the false positive hits mapped to regions of genomic amplifications (108). In a similar study conducted by Aguirre et al., the authors similarly found that CRISPR screens yielded more hits than traditional RNAi screens. However, they unexpectedly found that sgRNAs that target regions within genomic amplifications had a greater decrease in cell proliferation/survival than sgRNAs that targeted genes outside of the amplified regions (109). A later study demonstrated that CRISPR editing activated the DNA damage response resulting in P53 activation and cell death (110). Therefore, the decreased survival of editing in regions of genomic amplifications can be attributed to activation of DNA damage. Taken together the results of the studies by Munoz et al. and Aguirre et al. provided evidence towards the superiority of CRISPR screening in providing targets but cautioned the interpretation of these results in cell lines that harbored copy number/ploidy variations.

Furthermore, other studies have cautioned against the use of CRISPR screening in cell lines that the contain an intact p53 pathway (110), mutations in DNA repair pathways, and editing genomic loci marked with heterochromatin or non-accessible DNA (111) as all these factors can reduce the editing efficiency in cell lines. RNAi methods were demonstrated to be more amenable for synthetic lethal screens since the machinery required for knockdown was cytoplasmic and did not depend on locus accessibility, chromatin conformation or ploidy (112).

Genetic Screening in Hepatocellular Carcinomas

The utility of CRISPR screens allows for discovery of novel therapeutic targets, this is particularly important for diseases such as HCC which have limited therapeutic targets. Unbiased screening for drug targets in HCC via transposon, RNAi and CRISPR have revealed novel targets in HCC. Transposon based screening allowing for insertional mutagenesis identified Ubiquitin Conjugating Enzyme E2 H (*UBE2H*) and a truncated EGFR variant as drivers of HCC tumorigenesis (111). RNAi based screening identified HCC implicated exportin (*XPO4*) and 13 other genes as tumor suppressors in HCC (113), and also identified *Mapk14* (p38a) as a mediator of sorafenib resistance in a mouse model of HCC (114). More recently a genome wide RNAi screen identified Mitochondrial-Processing Peptidase Subunit Beta (*PMPCB*) as a therapeutic vulnerability in HCC as knockdown inhibited proliferation and also decreased expression of stem cell genes that are associated with the S2 HCC subclass (115). An ex vivo CRISPR screen conducted in our lab reported *NF1* as a novel tumor suppressor gene in HCC (104). Furthermore,

another group conducting a CRISPR kinome screen in HCC cells identified CDK7 as a therapeutic target in MYC driven HCCs (116). In this thesis, I utilize a CRISPR kinome screen to identify Transformation/Transcription Domain Associated Protein (TRRAP) as a therapeutic target in HCC.

TRRAP

TRRAP is a large (3828 amino acids) multidomain protein of the phosphoinositide 3-kinase-related kinases (PIKK) family. TRRAP was first identified as an interacting partner of c-MYC and E2F1 and is required for the transformation ability of c-MYC (117). TRRAP is highly conserved in evolution and has homologs found in many model systems utilized today (Table 1.1). Analysis of TRRAP sequences across species revealed multiple conserved domains: a nuclear localization domain, two tetratricopeptide repeat (TPR) motifs, multiple Huntingtin, elongation factor 3, PR65/A, and TOR (HEAT) domains, a FATC domain, a Leucine zipper and a PIK-like domain.

Firstly, TRRAP contains a functional nuclear localization domain (118). Next, TRRAP contains two TPR domain, which each encode two anti-parallel α helices separated by a turn (119), and a number of HEAT domains. Mutagenesis of these domains in *Tra1*, the Saccharomyces cerevisiae homolog of TRRAP, demonstrated that these domains aid in the assembly of the two TRRAP containing multi-subunit complexes (120). Furthermore, mutations within these domains reduced viability (120). Additional studies demonstrated that the HEAT domains were required for interaction with c-MYC (121) and p53 (122). TRRAP also contains a leucine zipper that promotes TRRAP-DNA interactions (118). The FATC domain is important for binding with the

histone acetyltransferases KAT5 and ATM signaling (123). Finally, like all PIKK family members, TRRAP contains a PIK-like domain. This domain is a highly conserved across evolution and resembles the catalytic domain of PI3kinases. However, sequence analysis of this domain revealed that it lacked the conserved amino acids required for phosphate transfer activity. Therefore, TRRAP is a pseudokinase which largely functions as a scaffold protein (99). Interestingly, a recent study in *S. cerevisiae* demonstrated that deletion of the pseudokinase domain of *Tra1* disrupted nuclear localization presumably though decreased binding of TRRAP to its two Histone Acetyltransferase (HAT) complexes (124). Furthermore, this domain was also required for Myc mediated transformation (121).

Given that *TRRAP* contains multiple HEAT and other protein binding domains, it was important to identify which proteins TRRAP interacted with. Upon its discovery, TRRAP was demonstrated to interact with c-MYC. Subsequent studies demonstrated that TRRAP also interacted with other factors involved in the DNA damage response including p53, E1a, PPARγ, LXR, FXR, β-catenin and BRCA1 (118). TRRAP was also found to regulate ras signaling and drive cell fate decisions in *Caenorhabditis elegans* (106). This diverse range of binding partners suggested that TRRAP controls multiple cellular processes.

TRRAP Functions

Genetic studies have begun to elucidate the role biological role of TRRAP. Early studies demonstrated that loss of *Tra1* in yeast resulted in decreased cell viability (125)

whereas loss of TRRAP in mice resulted in embryonic lethality as embryos did not survive past the blastocyst stage (126). Similarly, loss of function mutations in *Trr-1* in *C. elegans* resulted in developmental defects, specifically vulval cell fates (127) and mutations in Nipped-A, the *Drosophila melanogaster* (*D. melanogaster)* homolog, resulted in defects in wing development (128). Taken together the studies suggest TRRAP plays an integral role in development.

In order to further investigate the functions of TRRAP during embryogenesis, inducible TRRAP loss models were generated. Depletion of TRRAP in Mouse Embryonic Fibroblasts (MEFs) resulted in loss of clonogenicity and mitotic arrest (129). Analysis of differentially expressed genes in TRRAP depleted cells revealed that TRRAP regulated expression of genes responsible for cell cycle progression, cell adhesion, protein synthesis, metabolism and signal transduction via changes in histone H3 and H4 acetylation (130). Later studies demonstrated that TRRAP loss in mouse ES cells resulted in premature differentiation associated with loss of chromatin acetylation and subsequent heterochromatin formation resulting in decreased expression of stemness master genes Oct4, Sox2 and Nanog (131).

Tissue specific analysis of TRRAP loss in vivo demonstrated an integral role for TRRAP in cell cycle progression. TRRAP depleted hepatocytes were unable to regenerate after CCl4 induced damage due to failure to induce expression of cyclin A (132). Depletion of TRRAP in the central nervous system resulted in impaired differentiation of neuronal progenitor cells due to failure to induce timely expression of E2F related cell cycle targets (133).

TRRAP-HAT Complexes

Mass spectroscopy, cross linking and FRET studies revealed that TRRAP was a component in two major HAT complexes: the SAGA complex containing KAT2A (also known as GCN5) and the H2A/H4 HAT complex centered around p400 and KAT5 (also known as TIP60) (134-136). TRRAP was also shown to form a third complex with p400 and BAF53. This complex also had HAT activity, but it was independent of KAT5 (137). Later studies demonstrated that each TRRAP containing complex had distinct functions granted to the complex by the HAT effectors KAT2A and KAT5.

The TRRAP-KAT2A complex also plays major roles in development. Loss of KAT2A alone is embryonic lethal. However, interestingly, deletion of individual components of the of the TRRAP-KAT2A complex has different effects—deletion of KAT2A resulted in embryonic lethality after the blastocyst stage (embryonic day 10.5) (138) whereas deletion of PCAF was compatible with full development (139). This suggested that components within this complex had some overlapping functions.

The TRRAP-KAT2A complex can regulate expression of genes via histone acetylation preferentially on histone H2B residues K11 and K16 and histone H3 residues K9 and K14 (140). CHIP analysis of the KAT2A complex revealed that it was responsible for regulating expression of genes involved in telomere maintenance and mRNA export (141, 142). The KAT2A complex can also acetylate non-histone substrates such as Nfκ-B, c-Myc and Cyclin A (143). KAT2A has also been implicated in transformation as the HAT activity of KAT2A was required for c-MYC mediated

transformation (144). Moreover, KAT2A has also been implicated in acetylating Pygo2, a component of the WNT signaling pathway (145).

Like KAT2A, KAT5 also plays a major role in development as disruption of p400/KAT5 complex results in impaired ESC differentiation (146). However, the TRRAP-KAT5 complex plays a distinct role from the KAT2A complex in that it detects and aids in the resolution of DNA damage. After a double strand DNA break (DSB), the TRRAP-KAT5 complex is recruited to the break site along with ATM. ATM phosphorylates the histone H2A.X to form γH2A.X to recruit other DNA repair proteins to repair the break. Meanwhile, KAT5 acetylates histone tails to facilitate chromatin relaxation around the break site (147). As mentioned earlier, the TRRAP-KAT5 complex is also responsible for regulating gene expression by acetylating residues H2AK5, H3K14 and H4K5/8/12/16 (140). Similar to KAT2A, KAT5 has also been implicated in acetylation and activation of non-histone substrates including MYC, ATM, E2F1 and p53 in order to regulate cell fate decisions (148).

Senescence

Observations of serially passaging primary cells in culture by Leonard Hayflick revealed that cells have a finite replicative capacity after which they have limited proliferative capacity (149). Hayflick later proposed that this arrest was due to “aging or senescence at a cellular level” (150). Cellular senescence is a stable, essentially irreversible, state of cell arrest that can occur during the normal aging process but can also occur in response to a number of toxic stressors such as growth factor withdrawal,

DNA damage, oncogene activation, tumor suppressor inactivation and oxidative stress (151). Consequently, there are a number of markers that are both specific and unique to senescence.

Senescent cells display a number of characteristics that allows for their detection. Morphologically, senescence cells have a large flattened morphology which resembles a sunny-side up egg when observed under a light microscope. In addition to the unique morphology, Senescence Associated β-Galactosidase (SA-β-Gal) is a commonly used biomarker for senescent cells (152). SA-β-Gal staining takes advantage of the fact that senescent cells have increased lysosomal β-galactosidase activity due to expansion of the lysosomal compartment. Lysosomal β-galactosidase is encoded by the *GLB1* gene, however, interestingly, GLB1 plays no role in the senescence response as cells depleted of GLB1 still undergo senescence (153). A critical ingredient in the SA-β-Gal staining solution is X-gal. When cleaved by β-galactosidase, X-gal produces a blue precipitate that is detectable via light microscopy (152). The specificity of detecting lysosomal β-Gal in senescent cells compared to normal cells occurs via pH. Lysosomal β-Gal is typically detected at pH 4, however since senescent cells have an expanded lysosomal compartment, β-Gal in senescent cells can be detected at pH 6 (154).

Additional molecular markers of senescence take advantage of the fact that these cells are arrested during the cell cycle. Senescent cells exhibit increased expression of the Cyclin Dependent Kinase Inhibitors (CDKI) $p15^{INK4B}$, $p16^{INK4A}$, and $p21^{CIP1}$. Increased expression of these CDKIs will result in hypo-phosphorylation of Rb (151).

Changes in global chromatin structure are also associated with senescence. Senescence associated heterochromatin formation (SAHF) are readily detectable in senescent cells as distinct DAPI-dense foci mediated by deposition of H3K9me3 marks(155). Furthermore, in order to mediate some of the nuclear changes associated with senescence, senescent cells also have reduced expression of Lamin B1 (156). However, the role of Lamin B1 reduction in senescence remains unclear. Finally, senescence is also accompanied with secretion of pro-inflammatory cytokines such as IL1, IL6 and IL8. This phenomenon is known as the Senescence Associated Secretory Phenotype (SASP). Overall, senescence can be induced by a wide variety of insults to the cell. Depending on the mechanism of induction, senescent cells will exhibit additional markers that are unique to that mechanism.

Replicative Senescence

Hayflick's original observation, now termed the cell's *Hayflick limit*, was found to be due to telomere attrition (157). Functional telomeres prevent DNA repair machineries from recognizing chromosome ends as DNA DSBs. When telomeres reach a critical length, their protective function during DNA replication is compromised and a DNA damage pathway mediated by ATM and ATR is activated (158). ATM and ATR signaling converge on p53 and result in hypophosphorylation of Rb and senescence. In line with telomere regulation, additional studies have demonstrated that cells deficient in the enzyme telomerase (TERT), which is responsible for telomere repair, undergo senescence (159). Interestingly, expression of TERT was unable to reverse replicative

senescence but silencing of p53 and p16 allowed a subset of cells to re-enter the cell cycle (160).

The functional role of senescence was debated for many years after Hayflick's discovery as some suggested that senescence was a barrier to tumorigenesis whereas others suggested that senescence was merely a state of "cellular exhaustion." However work by Manuel Serrano in Scott Lowe's lab later revealed the role of senescence in tumorigenesis (described below)

Oncogene Induce Senescence (OIS)

After the discovery of the Ras oncogene, Weinberg and colleagues began to test its tumorigenic potential. Weinberg was able to demonstrate that DNA isolated from carcinomas driven by *RAS* mutations could transform *immortalized* cell lines (161), however, oncogenic RAS alone was insufficient to transform *primary* cell lines (162). Work by Manuel Serrano later demonstrated that overexpression of oncogenic RAS in primary cells dramatically reduced cell growth and induced senescence via activation of p53, increased expression of the CDKIs p21, p15 and p16, and hypophosphorylation of Rb. The cells were arrested during G1 and stained positive with SA-β-Gal. To further support Weinberg's initial findings, he demonstrated that immortalizing the cell line with E1A reduced the cell cycle arrest induced by oncogenic Ras (163). Later studies demonstrated that the DNA damage response also reinforced the senescence program triggered by oncogenic RAS(164). Interestingly, overexpression of TERT to "near-immortalization" levels did not rescue senescence suggesting that OIS was distinct from

replicative senescence (165). Serrano concluded that senescence was a tumor-suppressive mechanism and served as a barrier to transformation.

Additional evidence that distinguishes OIS is seen in melanoma literature. A large portion of melanomas are driven by the oncogenic mutant of BRAF V600E (166). Melanocytic nevi, more commonly known as moles, are benign tumors that have low propensity to develop into melanomas. However, a large portion of nevi contain the same $BRAF^{V600E}$ mutation (167). In vitro and in vivo studies in mice demonstrated that these nevi expressed elevated levels of $p16^{INK4A}$ and stained positive with SA-β-GAL (168). Furthermore, it was found that there was no difference in telomere length between nevi and normal skin fibroblasts (169).

Bypass of OIS generally involved the activation of an oncogene or inactivation of a tumor suppressor gene. In line with this, genetic screens have identified several oncogenes that can mediate bypass from OIS. Studies demonstrated that expression of DRIL1, TBX2, BCL6, and KLF4 can bypass OIS (170). Furthermore CXCR2-binding chemokines by senescent cells can reinforce senescence via activation of P53 (171). Furthermore, recent studies have demonstrated that OIS cells can indeed "escape" their senescent state (172). Implications of this escape, along with the mechanisms implicated in this process will be discussed in a later section.

Chromatin Reorganization During Senescence

Work by Masashi Narita demonstrated that OIS was accompanied by global changes in chromatin structure—specifically there was global induction of

heterochromatin formation mediated by Rb and p16 (155). These heterochromatin foci were detectable by intense DAPI staining. Moreover, the DAPI foci stained positive for repressive epigenetic marks such as H3K9me3, HP1γ, macroH2A and loss of the linker histone H1 (173, 174). While overexpression of H3K9 methylation "erasers" such as LSD1 and JMJD2C eventually led to reduced levels of the H3K9me3, deletion of *SUV39H1*, a H3K9 methylation "marker," could reverse OIS (175). SAHF formation was also characterized by accumulation of HMGA proteins on heterochromatin (176). Interestingly, SAHF formation is predominantly seen in OIS as opposed to DNA damage induced senescence and replicative senescence (177). Furthermore, after transformation occurs via inactivation of p53 or ATM depletion, SAHF-like structures are retained (177). This is in line with the observation that cancers typically have higher levels of heterochromatin compared to normal tissue (178).

It was initially thought that SAHFs function to repress expression of cell cycle genes in order to maintain cell cycle arrest (176), however, Fabrizzo d'Adda di Fagagna's group also demonstrated that the SAHF hampered the DNA damage response mechanism suggesting that SAHF does not simply function as a mechanism to regulate gene expression (177).

Senescence Associated Secretory Phenotype (SASP)

SASP was first described as a milieu of pro-inflammatory cytokines secreted after senescence induced by DNA damage, replicative exhaustion and oncogenic RAS by Judith Campisi's group (179). All three pathways share similarity in that senescence is

mediated through the DNA damage response, suggesting that the DNA damage response was required for SASP activation. In line with this, they demonstrated that neither p53 nor p16 was required for the initiation and maintenance of the SASP (179). Furthermore, additional studies demonstrated that ectopic expression of p21 and p16 did induce senescence but without SASP induction (180).

The SASP program is thought to be largely activated by two transcription factors- NFκB and C/EBPβ (178). The major target genes implicated in the SASP are IL1, IL6 and IL8. Once secreted, IL1, IL6 and IL8 have both autocrine and paracrine roles. The autocrine signaling effects reinforce NFκB and C/EBPβ activation and initiate a positive feedback loop for expression of SASP genes. The paracrine signaling has two major effects. First, the SASP-excreted-interleukins induce senescence in neighboring cells. Interestingly, this senescence was dependent on p21, p16 and p53. Second, the presence of these interleukins recruits immune cells in vivo to clear senescent cells (181). Clinically, this is relevant in that senescence induction can lead to immune mediated tumor clearance in patients. In line with this, Scott Lowe's group was the first to show that senescence in HCC cells, induced via p53 restoration, resulted in tumor regression via Natural Killer (NK) cell mediated tumor clearance (182).

However, studies are now demonstrating that although the SASP can promote tumor clearance, the SASP can also have a pro-inflammatory effect and can promote tumorigenesis in some models (183). Initial studies demonstrated that when tumor cells were injected with senescent fibroblasts into nude mice, tumor growth was accelerated compared to when tumor cells are injected with normal fibroblasts (184). The pro-

tumorigenic effect of the SASP along with reversal of senescence will be further discussed in a later section.

Thesis Preview

The work described in this thesis will utilize a CRISPR screen to identify TRRAP as a therapeutic target in HCC. Loss of TRRAP and its cofactor, KAT5, results in decreased proliferation of HCC cells. I will identify a network of genes regulated by TRRAP and KAT5 that are responsible for mitotic progression in HCC and further identify TOP2A as TRRAP/KAT5 target gene. Furthermore, I will demonstrate that loss of TRRAP, KAT5, and TOP2A results in senescence of HCC cells during G2 that is independent of traditional mediators of senescence such as p53, p21, Rb, heterochromatin formation and DNA damage.

Organism	**TRRAP Homolog**
Mus Musculus	Trrap (117)
Saccharomyces cerevisiae	Tra1 (134)
Caenorhabditis elegans	Trr-1 (127)
Drosophila melanogaster	Nipped-A (128)
Arabidopsis thaliana	TRRAP (117)

Table 1.1 TRRAP homologs identified in other model systems

CHAPTER II

CRISPR Screening identifies TRRAP as a therapeutic target in HCC

Preface

The screen conducted in this study was performed by two other members of the Xue Lab, Dr. Suet-Yan Kwan and Dr. Chun-Qing Song.

Introduction

Liver cancer accounts for more than 27,000 deaths in the United States and more than 700,000 deaths worldwide each year (17, 185). The 5-year survival rate for liver cancer patients is 18% and the major subtype of liver cancer is hepatocellular carcinoma (HCC) (6). Current approved advanced HCC treatments include multi-kinase inhibitors regorafenib, lenvatinib and sorafenib, which extend patient survival by several months only, and the immune checkpoint inhibitors Nivolumab and Pembrolizumab, which show ~20% response rates as a second line of therapy (6). The clinical need for more effective HCC treatments remains unmet partially because HCC is genetically heterogeneous and because HCC driver genes amenable to targeted therapy are largely unknown(17, 186). Identifying genes whose depletion can inhibit HCC growth, and determining the mechanisms involved, will aid the development of targeted therapies for HCC patients.

Using a kinome CRISPR screen in three HCC cell lines, we identified transformation/ transcription domain-associated protein (TRRAP) as the top-ranking candidate gene required for HCC cell growth. TRRAP, a pseudokinase member of the

PI3 kinase-like family, acts as a scaffold protein in histone acetyltransferase (HAT) complexes (118, 187-189) that regulate transcription, DNA repair, and replication (118). TRRAP is also a key regulator of cell cycle progression and stemness in embryonic stem cells and cortical apical neural progenitors(131, 133).

TRRAP is mutated and amplified in different cancer types, including melanomas, gastric, and uterine cancers (190-192), and has been implicated in oncogenic transformation. Indeed, the TRRAP S722F hotspot mutation in melanomas can transform NIH3T3 cells (190). Moreover, wildtype TRRAP is required for transformation by c-myc/Hras and E1A/Hras in rat embryo fibroblasts (117) and MYC-dependent tumor initiation in a breast cancer model (193). By contrast, depletion of TRRAP can induce apoptosis and differentiation in lymphoma and brain-tumor initiating cells (194, 195). Given its role in diverse cellular processes, it is possible that TRRAP and its regulated pathways are altered in cancer. However, the extent of TRRAP alterations and its function in cancer cells, particularly in the context of HCC, is not established.

Results

CRISPR screen identifies potential therapeutic vulnerabilities for HCC

To identify genes that are required for cell growth in HCC, we infected three HCC cell lines (Huh7, HepG2, and Hep3B) with a kinome CRISPR library that targets 763 kinases with 8 single guide RNAs (sgRNAs) per gene. To determine changes in sgRNA representation, we harvested genomic DNA from cells of an early passage and after 10 passages, then amplified and identified sgRNAs using PCR and deep sequencing,

respectively. Of the 763 kinases challenged with sgRNA, we found that 31 genes were significantly depleted in all three HCC cell lines (Figure 2.1A, 1D). This result provides in-vitro support to the current theory in the field surrounding HCC therapeutics- few unique molecular targets exist for HCC due to its heterogeneity between patients. GO analysis of the 31 depleted genes revealed that the major pathways that were depleted revolved around P53 and cell cycle regulation (Figure 2.1A). Among these 31 genes, 8 genes (AURKB, BUB1B, CDC7, DTYMK, PGK1, TPR, TRRAP, VRK1) were expressed at least 1.5-fold higher in HCC compared to non-tumor tissue (Figure 2.1B). High expression levels of these genes were associated with poor survival in HCC patients (Figure 2.1C). Of note, previous studies have shown that AURKB, DTYMK, PGK1, TPR, and VRK1 promote HCC tumorigenesis (196-200).

Out of the 8 genes, TRRAP is the top depleted gene in all three cell lines (Figure 2.1D). Using additional published patient data sets, we confirmed that TRRAP expression is higher in tumor compared to matched normal tissue (Figure 2.2A), and increased TRRAP expression is correlated with poor survival (Figure 2.2B). Analysis of the TCGA data set revealed that 12% of HCC patient samples have increased TRRAP mRNA expression, amplification and/or mutations in the TRRAP gene (Figure 2.2D). We also investigated whether TRRAP expression is correlated with certain gene signatures in HCC. We performed Ingenuity pathway analysis and found that TRRAP expression is positively correlated with expression of genes that are involved in ‘molecular mechanisms of cancer’, ‘role of BRCA1 in DNA damage response’ and growth factor

signaling pathways (Figure 2.2E). These results suggest that TRRAP may have an oncogenic role in HCC.

TRRAP and its co-factor KAT5 are required for cell growth in HCC

To understand the function of TRRAP in HCC, we depleted TRRAP expression in Huh7, Hep3B and SNU-475 cells using CRISPR (sgTRRAP) (Figure 2.3A). Loss of TRRAP resulted in decreased cell growth and colony formation in these cell lines (Figure 2.3B and 2.3C). For the subsequent mechanistic studies we utilized the HUH7 and SNU-475 cell lines as these cells had the greatest and most consistent knockdown of TRRAP protein after lentiviral infection.

TRRAP is an adaptor protein in several HAT complexes. In mammalian cells, TRRAP predominantly binds to KAT2A and KAT5(187-189). We found that TRRAP and KAT5 co-localized to the nucleus in Huh7 and SNU-475 cells (Figure 2.4A). We found that TRRAP depletion resulted in decreased KAT5 and KAT2A expression at the protein, but not mRNA level, in Huh7 and SNU-475 cells (Figure 2.4B and Figure 2.4C). Loss of KAT2A and KAT5 was more dramatic in Huh7 cells compared to SNU-475 cells as knockdown of TRRAP protein was greater in HUH7 cells after lentiviral infection with sgTRRAP (Figure 2.3A). To investigate whether KAT2A and KAT5 protein become unstable due to increased protein degradation in the absence of TRRAP, we inhibited proteasomal and lysosomal protein degradation in sgTRRAP cells with MG132 and chloroquine respectively. However, we found that MG132 and chloroquine could not rescue KAT2A and KAT5 protein expression in sgTRRAP cells compared to the positive

control proteins utilized in this study (Figure 2.4D), suggesting a degradation-independent mechanism.

To determine whether TRRAP depletion reduces cell proliferation due to loss of KAT2A or KAT5 expression, we depleted KAT2A and KAT5 using CRISPR (sgKAT2A and sgKAT5) in Huh7 and SNU-475 cells (Figure 2.5A and Figure 2.5B). We found that depletion of KAT5, but not KAT2A, reduced cell growth and colony formation similarly to TRRAP-depleted cells (Figure 2.5C).

To investigate whether depletion of TRRAP, KAT2A, and KAT5 affect tumor growth in vivo, we injected nude mice subcutaneously with Huh7 cells expressing sgTRRAP, sgKAT2A, or sgKAT5. TRRAP- and KAT5-depleted tumors were significantly smaller than tumors in non-targeting controls. However, KAT2A depletion did not have any effect on tumor size at the end point of the study (Figure 2.6A). To investigate the role of TRRAP in HCC tumor in initiation, we injected C57/BL6 mice with three plasmids which encoded for sgTrrap or sgNT, sgP53 and a sleeping beauty based Myc transposase system (Figure 2.6B) via hydrodynamic tail vein injection. Overexpression of Myc along with P53 loss in hepatocytes is a well-established murine model of HCC (104, 201). After four weeks there were no gross liver tumors in mice injected with sgTrrap whereas mice injected with sgNT developed multiple tumors in the liver. Furthermore, clusters of immune cells were present in liver sections injected with sgTrrap. These clusters were negative for the lymphocyte marker CD4 and positive for the macrophage marker F480 (Figure 2.6C).

Identification of genes repressed and activated by TRRAP in HCC and Glioblastoma

The function of TRRAP in transcriptional regulation has been well described (118). To identify genes that are regulated by TRRAP to promote HCC cell growth, we performed RNA-sequencing in sgTRRAP Huh7 cells to identify differentially-expressed genes. Gene ontology (GO) analysis of genes that were down-regulated in sgTRRAP cells were enriched in cell cycle processes, including mitosis, chromosome segregation, and cell division (Figure 2.7A). Genes that were up-regulated in sgTRRAP cells were enriched in nucleic acid processing (Figure 2.7B).

Next, we cross referenced our RNA-sequencing results with published data sets to identify candidate genes that are activated by TRRAP in HCC. We looked for genes that: firstly, were down-regulated in sgTRRAP cells from our RNA-sequencing data (fold change<0.5), secondly, were positively correlated with TRRAP expression in the TCGA HCC data set (Spearman's correlation≥0.3), thirdly, were overexpressed in HCC compared to non-tumor tissue in the GSE14520 data set (fold change≥2), and finally predict poor survival in HCC patients when highly expressed (Figure 2.7C). We also performed this analysis in the opposite direction to identify genes that were repressed by TRRAP. Using these criteria, we identified 22 HCC-relevant genes that were activated (Table 2.1, Figure 2.8, Figure 2.9). Moreover, 19 of the 22 TRRAP-activated genes were involved in either 'cell cycle' or 'mitotic cell cycle' from the GO analysis (Figure 7D). Using our criteria we also identified 3 genes that were repressed by TRRAP (Table 2.2). The 3 TRRAP-repressed genes (BAAT, ITIH1 and RDH16) were liver specific (Figure 2.10). A similar pipeline was utilized to identify SLC7A11 as a BAP1 target gene across

multiple human cancers (202). When the authors of this pervious studied performed their overlapping analyses, they identified one target gene, SLC7A11, whereas our analyses yielded 22 potential TRRAP target genes in HCC.

We focused on TRRAP-activated genes for further analysis as they might be potential targets for inhibiting HCC growth. To assess whether TRRAP may regulate the same genes in another cancer type, we analyzed gene expression data from the TCGA glioblastoma multiforme (GBM) data set. TRRAP is required for restricting differentiation of brain tumor-initiating cells that were derived from human GBM samples (190). We found that 14 of the 22 genes activated by TRRAP in HCC were positively correlated with TRRAP expression in GBM (Spearman's correlation≥0.3, (Table 2.3), suggesting that TRRAP regulates a similar set of genes in both cancer types.

TRRAP and KAT5 activate transcription of mitotic genes in HCC

Since TRRAP- and KAT5-depleted cells display a similar phenotype, we asked whether TRRAP target genes were also regulated by KAT5. We analyzed previously published ChIP-sequencing data in mouse embryonic stem cells for KAT5 binding sites (203) and found that KAT5 binds to the transcriptional start sites of 19/22 genes activated by TRRAP (Figure 2.11A and Figure 2.12). After validating our RNA-sequencing data by confirming the downregulation of 6 genes after TRRAP depletion using qRT-PCR (Figure 2.11B and Figure 2.11C), we investigated the effect of KAT5 and KAT2A depletion on the expression of TRRAP target genes. We found that mRNA expression of TRRAP-activated genes was downregulated in sgKAT5 cells, but not in sgKAT2A cells

(Figure 2.11B and Figure 2.11C). In summary, TRRAP and KAT5 are required for transcriptional activation of mitotic genes. In HCC, these genes are clinically relevant since they are overexpressed and confer poor survival to patients.

TOP2A is a downstream target of TRRAP and KAT5

Based on our RNA-sequencing and bioinformatic analyses, we hypothesized that TRRAP depletion induces senescence by down-regulating mitotic genes. To investigate this, we focused on a downstream target of TRRAP and KAT5—Topoisomerase II alpha (TOP2A) (Table 2.1). TOP2A is highly expressed at G2/M phase and a key regulator of DNA decatenation during mitosis (204). We found that TOP2A expression was positively correlated with TRRAP expression in HCC and GBM patient samples (Figure 2.13A and Figure 2.13C) suggesting that TRRAP regulation of TOP2A was conserved between HCC and GBM. Moreover, TOP2A was overexpressed in HCC compared to non-tumor tissue, and its increased expression was associated with poor survival in HCC patients (Figure 2.13B). We confirmed that TRRAP and KAT5 depletion reduced TOP2A at the mRNA and protein level (Figures 2.11B, 2.11C, 2.13D).

Analysis of published ChIP-sequencing data (203) revealed KAT5 binding to the transcriptional start site of TOP2A (Figure 2.11A). Using the ChIP-sequencing data, we predicted the KAT5 binding site in the human TOP2A promoter. We cloned a 500 bp (-133/+367) region spanning the transcriptional start site of TOP2A to a luciferase promoter reporter and found that overexpression of TRRAP and KAT5 induced TOP2A promoter activity (Figure 2.14A). Previous studies have reported that TRRAP can bind

DNA directly independent of its HATs (118). However, we observed that KAT5 overexpression alone was sufficient to drive promoter activity suggesting that TRRAP alone cannot bind the TOP2A promoter. Instead it is KAT5 mediated binding at the TOP2A promoter which drives transcription of TOP2A. Next, we depleted TOP2A with CRISPR (sgTOP2A) and found the reduced colony formation (Figures 2.14B and 2.14C), resembling those of TRRAP or KAT5 depletion. Together, our results suggest that TOP2A is a key mitotic target of TRRAP and KAT5 in regulating HCC cell growth.

Discussion

Here, we demonstrate that TRRAP functions in HCC cell proliferation by promoting mitotic progression. Previous studies in other cell types have identified several cell cycle genes that are regulated by TRRAP, including cyclins A2, D1, D2 and E, Mad1, Mad2, and MKI67 (126, 129, 132, 194). We found that the majority of TRRAP-activated genes in HCC are involved in mitosis, and include genes not previously known to be TRRAP targets. Transcriptional activation of TRRAP-activated genes also required KAT5, indicating a specificity in recruitment of chromatin factors by TRRAP. Other TRRAP-interacting transcription factors, such as Myc and β-catenin, are frequently altered in HCC (14, 118). Investigations into whether these factors are important for TRRAP-dependent cell cycle control in HCC are warranted.

The oncogenic roles of mitosis genes in tumorigenesis have been reported. Over-expression of genes that regulate DNA replication and chromosomal segregation are involved in promoting chromosomal instability, a phenotype of aggressive cancers (205).

In HCC, YAP and FOXM1 promote chromosomal instability, and predict poor prognosis in patients (206). Of note, our study has identified FOXM1 is one of the TRRAP-activated genes. We also found that 11 of our 22 TRRAP-activated genes overlapped with the chromosomal instability gene signature (205). Thus, TRRAP overexpression may contribute to chromosomal instability in HCC.

Lineage tracing studies in both toxin-induced and genetic mouse models of HCC revealed that the cell of origin for HCC was hepatocytes (207). As cells transform from hepatocytes into HCC, normal hepatocytic functions are repressed—CYP450 levels and activities are suppressed (208), bile acid homeostasis is disrupted (209) and fatty acid metabolism is dysregulated (210). Interestingly our RNA-seq analysis identified Bile Acid-CoA:Amino Acid N-Acyltransferase (BAAT), Inter-Alpha-Trypsin Inhibitor Heavy Chain 1 (ITIH1), and Retinol Dehydrogenase 16 (RDH16) as genes that are repressed by TRRAP expression in HCCs.

BAAT is responsible for the final step in bile acid synthesis (211) and also shuttles unconjugated bile salts through the peroxisome as it enters the enterohepatic circulation (212). Studies regarding BAAT and tumorigenesis are limited. One sequencing based study comparing the transcriptome in Intrahepatic cholangiocarcinoma (ICC) to normal tissue identified that BAAT levels were significantly decreased in ICC tissues (213). Furthermore another study demonstrated that bile acid synthesis is downregulated in HCC due to decreased expression of enzymes responsible for bile acid synthesis secondary to RAS/ERK activation (214). Yet, no studies have implicated the

role of BAAT in HCC tumorigenesis. Furthermore, studies have not implicated TRRAP in regulating bile acid synthesis.

One of the major functions of the liver is the storage and metabolization of the soluble vitamins: Vitamin A, D, E and K. RDH16 is an enzyme responsible for the first step of synthesis of all-trans-retinoic acid (ATRA) from Vitamin A. ATRA has been demonstrated to have anti-tumor properties in HCC and cotreatment with sorafenib can result in synergy (215). Furthermore, RDH16 expression is decreased in alcohol induced HCC (216). However the function of RDH16 has not been studied in HCC. Studies in gliomas revealed that RDH16 could regulate differentiation as overexpression inhibited the expression of the stem cell markers Nestin, Oct4 and Sox2 and induced the differentiation of oligodendrocyte cells into stem-like gliomas (217). This suggests that TRRAP regulation of RDH16 is also conserved in Gliomas as TRRAP has also been demonstrated to promote differentiation in glioma models (133). However, this correlative relationship requires investigation in future studies.

ITIH1 encodes a component of the heavy chain of the inter-alpha-trypsin inhibitor complex, which is secreted by hepatocytes into the blood to prevent aberrant protease activity (218). Expression of ITIH1 was found to be downregulated in tumor compared to normal tissue in a cohort of ICC patients (219). Loss of ITIH1 is implicated in a myriad of inflammatory diseases including Rheumatoid Arthritis, Crohn's Disease and Ulcerative Colitis (218). Functional studies have not elucidated the function of ITIH1 in hepatocytes, however based on the low expression of ITIH1 in other inflammatory diseases, we hypothesize that loss of ITIH1 in hepatocytes can trigger a pro-inflammatory

environment that can contribute to HCC tumorigenesis. This hypothesis can be tested in future studies.

Given that BAAT, RDH16 and ITIH1 are required for integral hepatocyte functions, increased expression of TRRAP perhaps represses these genes in order to mediate the transformation from normal hepatocytes into HCC. Furthermore, increased expression of all three genes confers a favorable prognosis to HCC patients. Taken together the data suggests that all three genes can contribute to tumorigenesis when repressed by TRRAP in HCC cells.

The function of TRRAP in other cancer types is unclear. A previous study found that TRRAP depletion induces differentiation of brain tumor-initiating cells derived from GBM patients, partially due to reduced cyclin A2 expression and S/G2 progression (194). We found that cyclin A2 is also a TRRAP-activated gene in HCC, although we did not observe a strong positive correlation between cyclin A2 and TRRAP mRNA expression in TCGA GBM patient samples. However, we found an overlap in TRRAP-activated genes (14 of the 22) between GBM and HCC. Thus, TRRAP may regulate a similar set of genes between different cancer types. However, unlike in HCC, TRRAP mRNA expression is not a prognostic predictor in either GBM or other cancers (Figure 2.13C and based on data from the Human protein atlas). TRRAP mutations are reported in several cancer types, but their effects have not been studied.

In this chapter, we also demonstrate that loss of TRRAP results in loss of the HAT cofactors KAT2A and KAT5. Interestingly, there was no change in mRNA levels of both KAT2A and KAT5. Studies have demonstrated that KAT2A can be ubiquitinated

and degraded by the ubiquitin proteasome system (220) and that P300 degradation resulted in lysosomal degradation of KAT5 (221). Given that both KAT2A and KAT5 form complexes with TRRAP we hypothesized that loss of TRRAP resulted in destabilization of the complex and subsequent degradation of KAT2A and KAT5. However, this was not the case as treating cells with the MG132, a proteasome inhibitor, and chloroquine, a lysosomal degradation inhibitor, failed to rescue protein levels of both KAT2A and KAT5.

Taken together with the fact that mRNA levels of both KAT2A and KAT5 remain steady, the data suggested that the decreased protein expression of KAT2A and KAT5 may be due to failure to translate the transcripts. However, further experiments are needed to test this hypothesis. Given that other transcripts are being translated, it is reasonable to speculate that this regulation is not due to loss of a universal translation factor such as EIF4 and was instead transcript specific. Specificity for translational regulation can be conferred via the 5' and 3' UTRs. 5'UTR and 3'UTRs of transcripts contain binding sites for RBPs. Binding of RBPs at the 5'UTR or 3'UTR mediates capping, polyadenylation, export out of the nucleus and recruitment to the ribosome for translation (222). Additionally, aberrations in levels of RNA Binding Proteins (RBPs) can also reduce translation in a transcript specific manner. One possibility is that TRRAP loss results in decreased expression of an RBP that is responsible for translation of the KAT2A and KAT5 transcripts.

The loss in KAT2A and KAT5 protein but not mRNA could also be due aberrations in polyadenylation and in UTR lengths. Previous studies have demonstrated

that an increase in the 3'UTR length, due to aberrant polyadenylation, can decrease translation of a transcript (223). Future studies can determine changes in the 3'UTR length of the KAT2A and KAT5 transcripts after TRRAP depletion via 3' RACE.

Overall future studies can utilize two experiments to understand how translation of these transcripts is disrupted. The first experiment would be to determine localization of the transcript via RNA-FISH or polysome isolation. If the transcripts are localized predominantly in the nucleus, it suggests that TRRAP depleted cells are unable to cap and tail KAT5 and KAT2A transcript or require another RBP to mediate efficient nuclear export. If the transcripts are found within the polysome, it suggests that TRRAP depleted cells are unable to initiate translation of these transcripts. The second study needs to analyze the 3' and 5' UTR sequences of KAT2A and KAT5 in order to identify putative RBP domains or microRNA binding domains and identify the RBP protein(s) and/or microRNAs that can bind to the transcript and regulate its translation. Once a candidate list is generated, this list can be cross referenced with the RNA-seq data from TRRAP depleted cells to further home in on the candidate RBP(s).

The work in this chapter also identified that depletion of KAT5 reduces proliferation of HCC cells. KAT5's main function is as a histone acetyltransferase however work in mouse ES cells also shows that KAT5 plays a repressive role in differentiation and development via binding of the P400-KAT5 complex to H3K4me3 marks (146). In line this HAT independent function, mutation of two residues (Gln-377 and Gly-380) to glutamic acid in the acetyl CoA binding site of KAT5 abolishes its HAT catalytic activity (189). Previous studies have demonstrated that the HAT activity of

KAT5 is required for DNA damage sensing via ATM (224) as acetylation, firstly, relaxes the chromatin thereby making it more accessible for DNA repair enzymes (147) and, secondly, mediates activation of ATM to initiate signaling of the DNA damage response (224). However recent studies have demonstrated that because of the large size of the KAT5 complex, catalytically inactive KAT5 can still repress gene expression by binding DNA thereby limiting chromatin accessibility (225).

The role of catalytically inactive KAT5 in tumorigenesis remains unclear. Analysis of TCGA data reveals that the major aberration of KAT5 in HCC, comprising 5% of cases, is amplification. Missense mutations are found in <1% of HCC and the mutations that do occur are not within the acetyl CoA binding site (data not shown)(14). In this chapter I demonstrate that in the absence of KAT5, HCC proliferation is impaired by decreased expression of key genes involved in mitotic progression. Given that KAT5 *activates* transcription of mitotic progression genes in our model, I would expect that the catalytic HAT function of KAT5 would be required for HCC progression.

Overall in this chapter I identify TRRAP and KAT5 as a mediator of proliferation in HCC cells. The results provide an important discovery for a role for TRRAP and its co-factor KAT5 in activating downstream mitotic genes in HCC cell growth. Our mechanism identifies the TRRAP complex as a potential therapeutic target in HCC. Given that the crystal structure of the TRRAP/KAT5 complex was recently characterized in yeast, it may be possible to target the interaction between TRRAP and KAT5 and disrupt the histone acetyltransferase activity of the complex (226). Moreover, small molecule inhibitors targeting KAT5 and mitotic proteins are currently under development

(41, 227). Future work should determine how TRRAP overexpression and mutations affect its function to understand the extent and significance of TRRAP alterations in other cancers. Moreover, because in vivo models of TRRAP consist of only genetic knockouts, it will be critical to establish constitutively-active TRRAP and mutant TRRAP models to further characterize its role in tumor development.

Materials and Methods

Cell culture

Huh7 and SNU475 cells were provided by Dr. Scott Lowe. Huh7 cells were cultured in DMEM. SNU-475 cells were cultured in RPMI supplemented with 10 mM HEPES, 1 mM sodium pyruvate, and 4500 mg/L glucose. Hep3B and HepG2 cells were provided by Dr. Junwei Shi and cultured in MEM. All cell lines were grown in media supplemented with 10% FBS and 1% penicillin-streptomycin and maintained in a 37□C incubator with 5% CO2. Huh7, HepG2, Hep3B and SNU-475 cells were authenticated using ATCC's cell authentication service. MG132 and chloroquine were purchased from Millipore Sigma.

Kinome CRISPR screen

The human kinome CRISPR pooled library was a gift from John Doench and David Root (Addgene #1000000083). The library was amplified according to Addgene's library amplification protocol. Lentivirus containing the kinome library was packaged using 293fs cells. For each cell line, duplicates were performed. For each replicate, 2 ×

10^7 cells were infected with lentivirus. Huh7 and Hep3B cells were selected with 2 μg/mL puromycin for 3 days and HepG2 cells were selected with 4 μg/mL puromycin for 4 days. For each sample, genomic DNA was harvested from at least 6 × 106 cells using the PureLink Genomic DNA mini kit (Thermo Fisher Scientific, Waltham, MA). sgRNA was amplified using Phusion flash high-fidelity PCR master mix (Thermo Fisher Scientific). All sequencing datasets were evaluated using FastQC (version 0.11.2) to ensure high quality. Depleted genes were identified as previously described (228).

Bioinformatics analysis

To analyze gene expression levels between tumor and non-tumor tissues, the GSE14520 (20) and TCGA HCC data sets were used. Gene expression data of tumor (n=225) and non-tumor tissue (n=220) in the GSE14520 data set were analyzed using GEO2R (https://www.ncbi.nlm.nih.gov/geo/geo2r/). Briefly, P-values were calculated using moderated t-statistics and adjusted using the Benjamini-Hochberg method. Gene expression data of TCGA HCC tumors and matched non-tumors (n=50) were obtained from the UCSC Xena Browser (http://xena.ucsc.edu/) and analyzed using the Wilcoxon signed-rank test. The list of genes that predict prognosis of HCC patients was obtained from the Human Protein Atlas (version 18, https://www.proteinatlas.org/) . For survival analysis, FKPM values and survival data were obtained from the Human Protein Atlas and cBioPortal (http://www.cbioportal.org/) respectively. The LEC data is available on GEO with accession numbers GSE1898 and GSE4024 (229, 230). FKPM values were grouped in tertiles and the highest and lowest tertiles were designated as ‘high

expression' and 'low expression' groups. P-values were calculated using the log-rank Mantel-Cox test with GraphPad Prism. TRRAP mutations and copy-number alterations in HCC were obtained from cBioPortal. For gene correlation analyses, correlation data from the TCGA HCC (n=360) and GBM (n=136) data sets were obtained from cBioPortal. Briefly, gene expression data were analyzed using Spearman's correlation analysis. For GO analyses, the list of genes was analyzed using the PANTHER overrepresentation test and annotated with the GO Ontology database (released 2018-10-08). P-values were calculated using Fisher's Exact test and corrected by the Benjamini-Hochberg method. To determine KAT5 binding sites, we analyzed ChIP-sequencing data from GSE69671 (203).

sgRNA design and lentivirus infection

sgRNAs were designed using https://portals.broadinstitute.org/gpp/public/analysis-tools/sgrna-design, cloned into the LentiCRISPRv2 backbone (Addgene #52961) and packaged into lentivirus using 293fs cells. HCC cells infected with lentivirus were selected with puromycin for 2-4 days. Sequences of sgRNAs are listed in Table 2.4.

Immunoblot Analysis

Cells were washed twice with ice-cold PBS and harvested in RIPA buffer (Boston Bioproducts, Ashland MA) supplemented with protease (Roche, Indianapolis, IN) and phosphatase inhibitor cocktails (Thermo Fisher Scientific). The concentration of protein

was measured using the BCA assay (Thermo Fisher Scientific). For each sample, 25 µg of protein was loaded onto an SDS-PAGE gel. The following antibodies were used to probe against: TRRAP (#3967; Cell Signaling Technology, Danvers, MA), KAT2A (#3305; Cell Signaling Technology), KAT5 (sc-166323; Santa-Cruz Biotechnology, Dallas, TX), NIK (#4994; Cell Signaling Technology), LC3B (#2775; Cell Signaling Technology), TOP2A (#12286; Cell Signaling Technology), GAPDH (MAB374; Millipore Sigma, Burlington, MA), Hsp90 (#610419; BD Bioscience, San Jose, CA), and Flag (#2368; Cell Signaling Technology and #F1804; Millipore Sigma). Bands were visualized with an immunofluorescent secondary antibody (LICOR) using the Odyssey Imaging system.

Cell growth and colony formation assays

To measure cell growth, cells were seeded onto 96-well plates. CellTitre-glo assay (Promega, Madison, WI) was performed according to the manufacturer's protocol. The growth of cells at day 3 and day 5 was normalized to measurements taken one day after the cells were plated. Each repeat was averaged between 6 wells. For colony formation assays, Huh7 and SNU-475 cells were seeded at 3000 and 2000 cells per well respectively onto 6-well plates. After 11 days, cells were fixed with 4% formalin and stained with 0.5% crystal violet. All experiments were repeated three times.

RNA extraction and RT-qPCR

RNA was extracted from cells using the RNeasy mini kit (Qiagen, Germantown, MD) and DNA was removed by on-column DNase digestion (Qiagen) according to the manufacturer's protocol. One microgram of RNA was used to synthesize cDNA using the high-capacity cDNA reverse transcription kit (Thermo Fisher Scientific) according to the manufacturer's protocol. RT-qPCR analyses were performed using SsoFast EvaGreen supermix (Bio-Rad, Hercules, CA) according to the manufacturer's protocol and GAPDH was used as a control. Primer sequences used for qRT-PCR are listed in Table 2.5.

Animal Studies

Female 6-week-old NCRNu/Nu mice were purchased from Taconic Bioscience (Rensselaer, NY) and injected in the right or left flank with 1x106 TRRAP stable knockdown Huh7 cells. Cells were resuspended in PBS and mixed in a 2:1 ratio with matrigel (Westnet Inc., Canton, MA) to a final volume of 200 μL. Tumor size was measured by calipers and volume was calculated using the formula Volume=((π)(Length)〖(Width^2))/6.

For induction of HCC in vivo, sgRNAs against p53 and Trrap were cloned into a previously described Sleeping Beauty Cas9 plasmid (231). Plasmids were delivered in vivo via Hydrodynamic tail vein injection into 6-week-old female C57/Bl6 mice as previously described (104).

All mice were housed in JAG75 (Allentown) ventilated cage systems with 1/4″ Bed-o'Cobs (Andersons Lab Bedding) in facilities accredited by the American Association for Laboratory Animal Care (AALAC) at the University of Massachusetts (UMass) Medical School. Mice were provided with nestlets (Ancare) and Bed-r'Nests (Andersons Lab Bedding) and maintained in a pathogen-free animal facility at 22°C under the 12-hour light/dark cycle. Mice were injected during the light cycle and were not fasted prior to injection. Mice were maintained on a standard diet of Prolab Isopro RMH 3000 (LabDiet) throughout the course of the experiment. All animal protocols were approved by the UMass Medical School Institutional Animal Care and Use Committee (IACUC) and comply with all relevant federal guidelines and institutional policies.

Immunohistochemistry

Murine livers were fixed in 4% or 10% (v/v) formalin overnight and embedded in paraffin. 4 μm liver sections were stained with hematoxylin and eosin (H&E) or with antibodies using standard immunohistochemistry protocols. The following antibodies and dilutions were used: 1:100 anti-CD4 (Thermo-fisher) and 1:400 anti-F4/80 (CST).

RNA-sequencing and bioinformatics analysis

Ribosomal RNA was depleted and RNA-sequencing libraries were prepared as previously described (25). The libraries were quantified using the KAPA Library Quantification Kit (Kapa Biosystems, Wilmington, MA) and sequenced using the Illumina NextSeq 500 system. RNA-seq reads from each sample were aligned using

STAR (version 2.5.2b) (232) against the GRCh37/hg19 human reference genome. Gene expression was quantified through RSEM (v1.2.31) (233) with GENCODE V19 gene annotation. DESeq2 (1.22.0) (234) was employed to identify differentially expressed genes using raw read counts quantified by htseq-count(235).

Immunofluorescence

Cells were plated onto glass coverslips overnight and fixed with 4% Paraformaldehyde (Fisher Scientific) for 15 minutes and permeabilized with 0.3% Triton X-100 (Millipore Sigma) for 10 mins. Coverslips were blocked with blocking solution comprised of 7% Fetal Bovine Serum (Thermo Fisher) and 3% Bovine Serum Albumin (Millipore Sigma) for 1 hour at room temperature. Coverslips were then incubated with the following antibodies at 1:100 for 1 hour at room temperature: Rabbit-anti-TRRAP (#PA5-65866; Thermo Fisher Scientific) and mouse-anti-TIP60 (#sc-166323; Santa Cruz). Coverslips were then incubated with the following secondary antibodies for 1hour at room temperature at 1:500: Alexa Fluor 488 goat anti-mouse IgG (#A11001; Life Technologies) and Alexa Fluor 568 donkey anti-rabbit IgG (#A10042; Life Technologies). Cells were then stained with 5 µg/mL DAPI (#D1306; Fisher Scientific). Images were captured at 63x using a Leica DMi8 microscope.

Luciferase promoter assay

A 500 bp region spanning the transcriptional start site of TOP2A promoter from Huh7 cells was cloned using primers listed in Table 2.6 and ligated to the pBV-luc vector

(Addgene #16539). A 500bp region of the TOP2A ORF was also cloned using primers listed in Table 2.6 into the pBV-luc vector and served as a negative control. Flag-TRRAP was purchased from Addgene (#32103). Flag-KAT5 was purchased from Genecopoeia (#EX-Z5325-Lv101) and the Flag-KAT5 sequence was subcloned into lentiCas9-blast (Addgene #52962) to replace the Cas9 sequence. 293fs cells were plated onto 6-well plates and transfected with 1 µg each of the indicated plasmids and pRL-SV40P (Addgene #27163) using lipofectamine 3000 (Invitrogen) for 48 hours. Cells were then trypsinized and re-plated onto 96-well plates, and luciferase activity was measured using the Dual-glo luciferase assay system (Promega) according to the manufacturer's protocol. For each sample, luciferase activity was measured by normalizing firefly luciferase activity to Renilla luciferase activity and averaged between 6 wells. Fold change was calculated with respect to a pBV-luc negative control plasmid

Figures

A

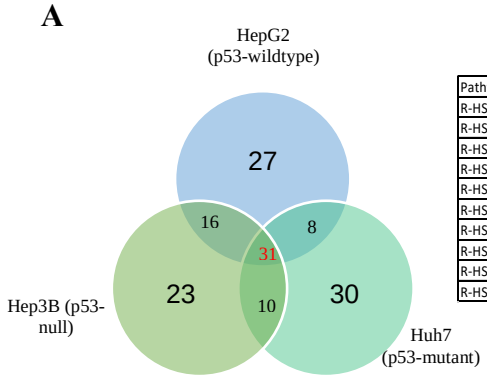

Pathway Identifier	Pathway Name	Entities pValue	Entities FDR
R-HSA-5633007	Regulation of TP53 Activity	4.82E-07	8.10E-05
R-HSA-3700989	Transcriptional Regulation by TP53	5.06E-07	8.10E-05
R-HSA-6804756	Regulation of TP53 Activity through Phosphorylation	5.90E-06	6.25E-04
R-HSA-1640170	Cell Cycle	1.03E-05	8.25E-04
R-HSA-69278	Cell Cycle, Mitotic	1.74E-05	0.00111462
R-HSA-2426168	Activation of gene expression by SREBF (SREBP)	4.15E-05	0.002198627
R-HSA-74160	Gene expression (Transcription)	7.81E-05	0.003342725
R-HSA-1655829	Regulation of cholesterol biosynthesis by SREBP (SREBF)	9.16E-05	0.003342725
R-HSA-69620	Cell Cycle Checkpoints	1.04E-04	0.003342725
R-HSA-6796648	TP53 Regulates Transcription of DNA Repair Genes	1.04E-04	0.003342725

B

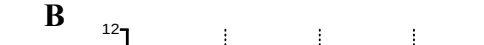

Figure 2.1. A kinome CRISPR screen identifies genes essential for HCC cell growth. **A)** Venn diagram depicting overlapping depleted gene in three HCC cell lines and table of 10 most significant annotation clusters from GO analysis of the 31 depleted genes **B)** mRNA levels of candidate genes in non-tumor and tumor samples in the GSE14520 data set. P-values were calculated using moderated t-test. Black lines indicate the geometric mean of each group. **C)** Kaplan Meier curves of TCGA liver cancer patients with high or low expression of the candidate genes in **A**. P-values were calculated using the log-rank Mantel-Cox test. **D)** Genes from the CRISPR screen were ranked by their false discovery rate, the 8 candidate genes are indicated.

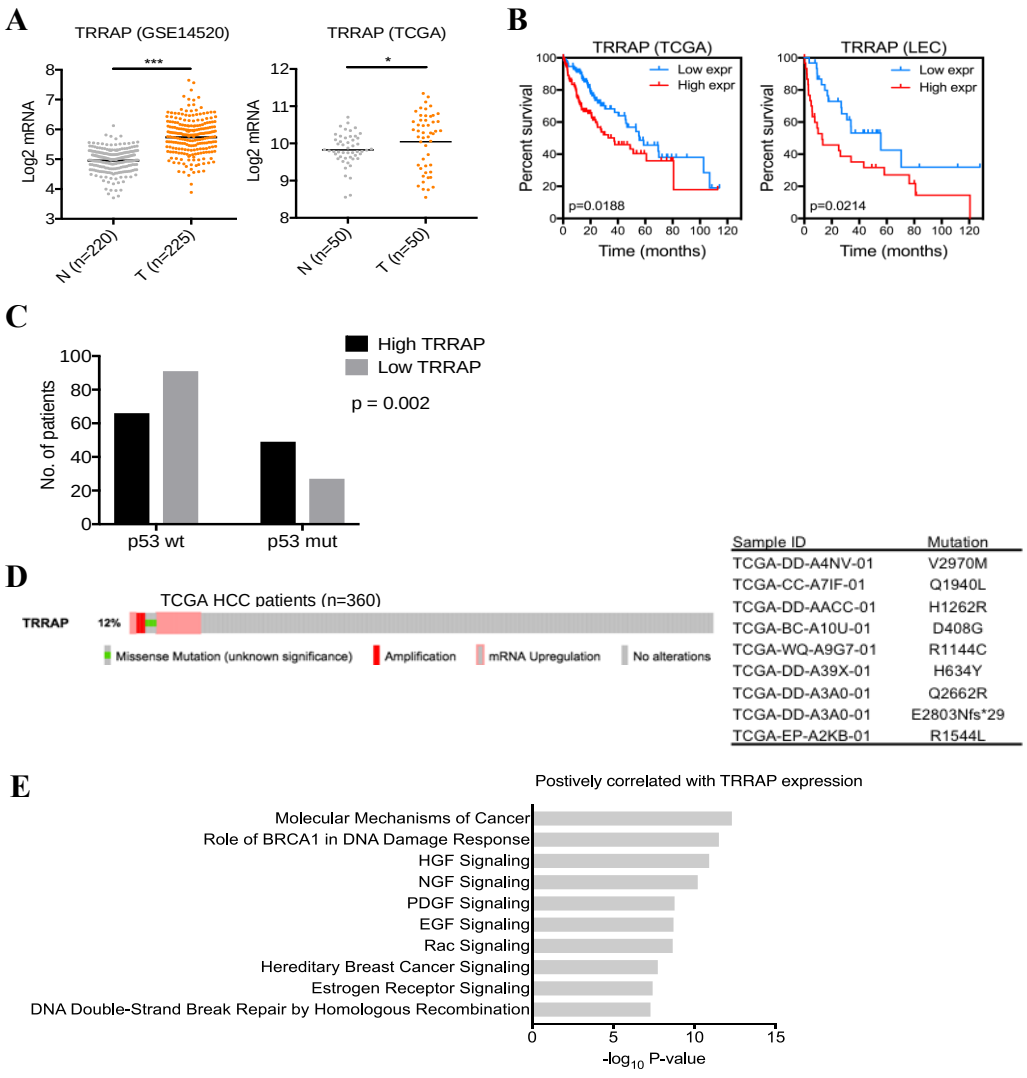

Figure 2.2. Identification of TRRAP as a potential oncogene in HCC.
A) mRNA levels of TRRAP in non-tumor and tumor samples from the GSE14520 (left) and TCGA (right) data sets, p-values were calculated using moderated t-test and Wilcoxon signed-rank test respectively. Black lines indicate the geometric mean of each group. **B)** Kaplan Meier curves of HCC patients from the TCGA (left) and NIH Laboratory of Experiment Carcinogenesis (LEC, right) cohorts with high (TCGA n=115 and LEC n=31) or low (TCGA n=118 and LEC n=31) TRRAP expression. P-values were calculated using the log-rank Mantel-Cox test. *$p < 0.05$, ***$p < 0.001$. **C)** p53 status in TRRAP high (n=115) and TRRAP low (n=118) TCGA HCC patient samples. P-value was calculated by Fisher's exact test. **D)** TRRAP mRNA up-regulation, copy-number alterations and/or mutations in TCGA patient HCC samples. **E)** Ingenuity Pathway

analysis of genes that were positively correlated with TRRAP expression (Spearman's correlation> 0.3) in TCGA HCC samples.

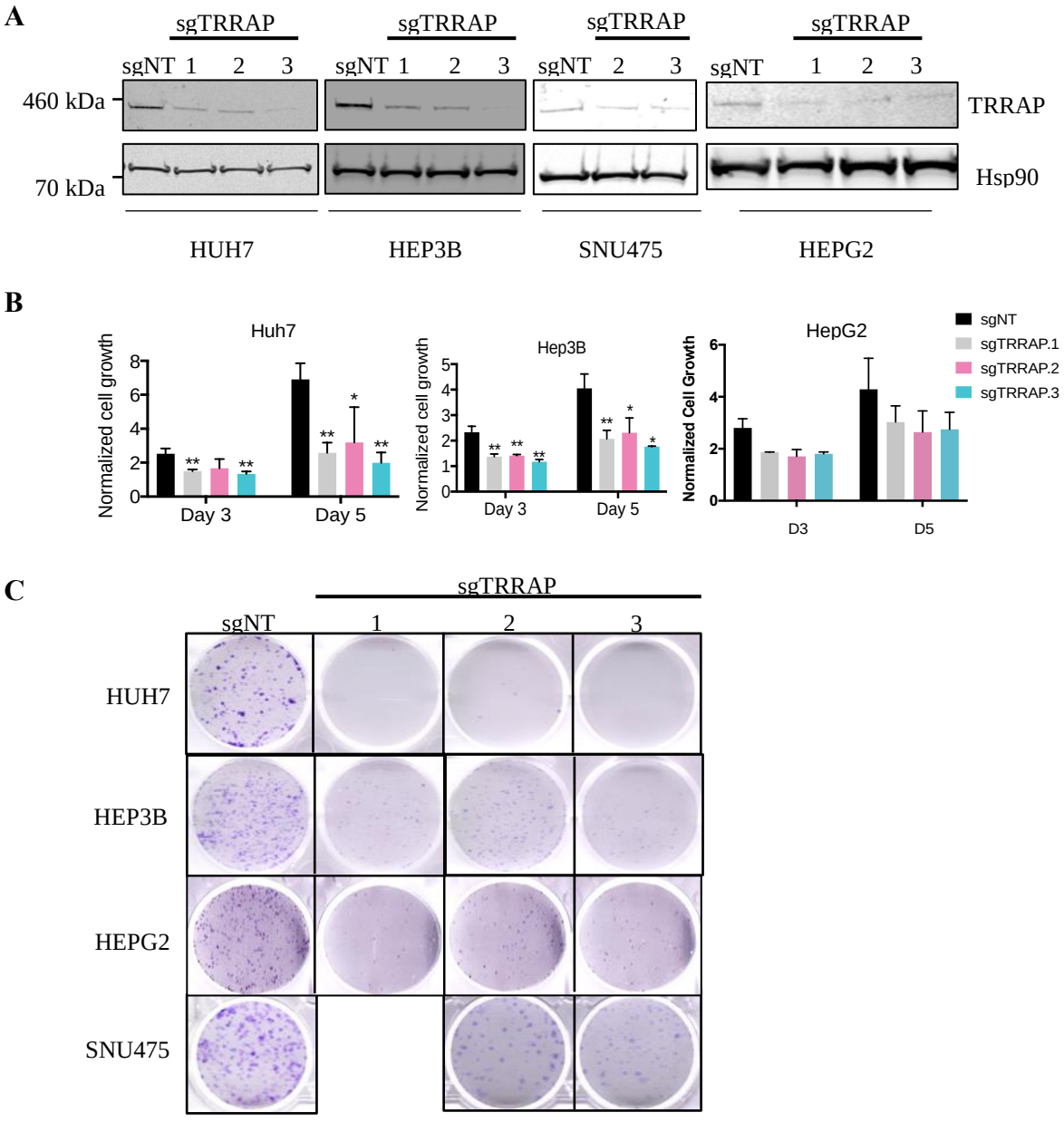

Figure 2.3. Loss of TRRAP impairs cell growth in HCC cells.
A) TRRAP protein expression in Huh7, Hep3B, SNU-475 and HEPG2 cells infected with non-target (sgNT) and 3 individual TRRAP sgRNAs (sgTRRAP). HSP90 was used as a loading control. **B and C)** Cell growth and colony formation of Huh7, Hep3B, and SNU-475 and HEPG2 cells infected with sgNT and sgTRRAP. **B)** Cell growth was measured at 1, 3, and 5 days after plating using the CTG assay and normalized to day 1. **C)** Cells

were stained with crystal violet. Data was presented as mean ± SD; p-values were calculated by comparing to sgNT, *p < 0.05, **p < 0.01, ***p < 0.001 (student's t test).

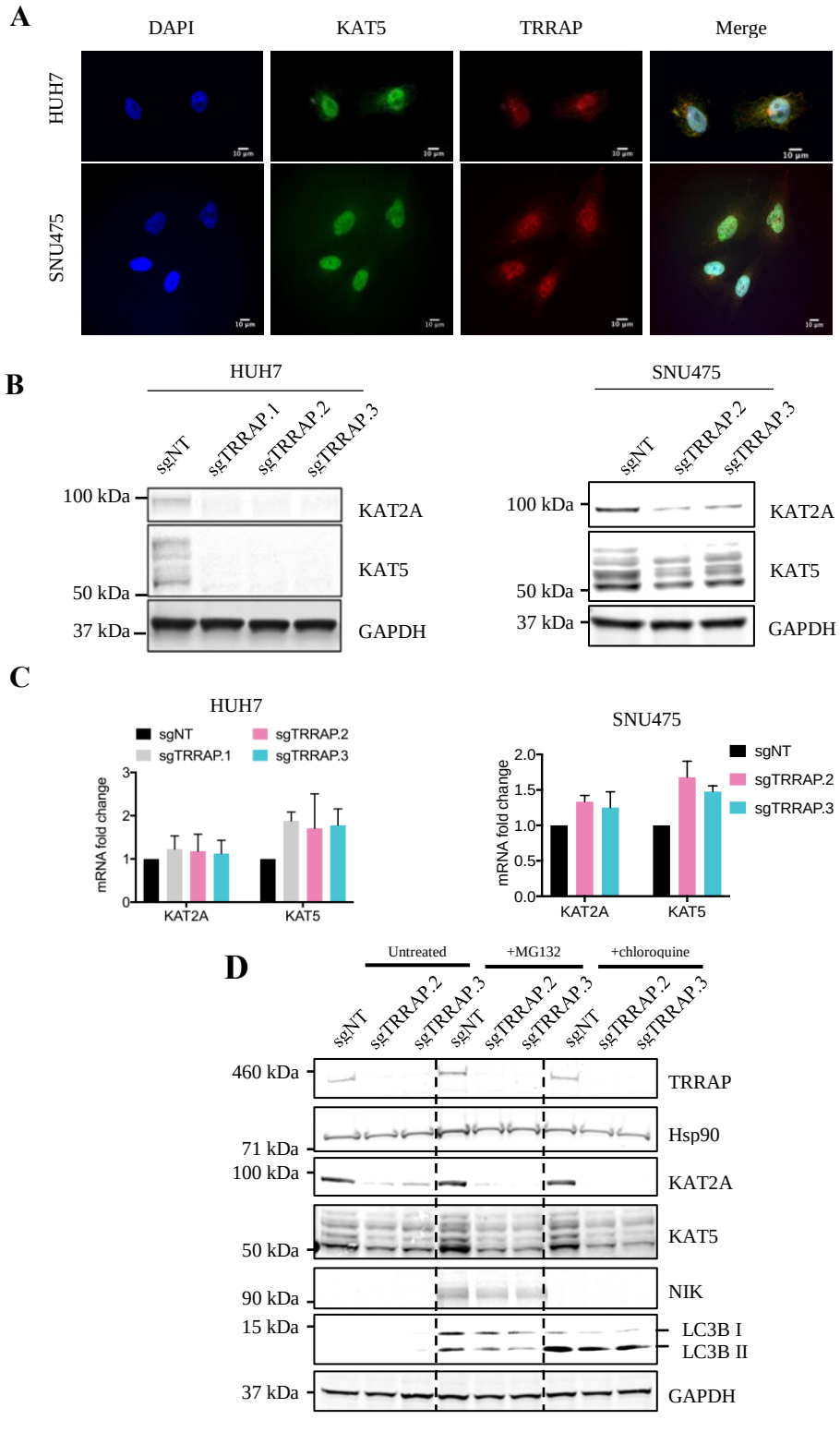

Figure 2.4. Loss of TRRAP results in loss of HAT cofactors KAT2A and KAT5. **A)** Immunofluorescence images of Huh7 and SNU-475 cells stained with DAPI (blue), anti-KAT5 (green) and anti-TRRAP (red) antibodies. **B)** Protein levels of KAT2A and KAT5 in HUH7 and SNU-475 cells infected with sgNT and sgTRRAP. GAPDH was used as a loading control. **C)** mRNA levels of KAT2A and KAT5 in HUH7 and SNU-475 cells infected with sgNT and sgTRRAP. **D)** Huh7 cells were infected with the indicated sgRNAs, then treated with 2.5 μM MG132 or 50 μM chloroquine for 17 hours. Increased expression of NIK and LC3B were used as positive controls to show inhibition of proteasomal and lysosomal protein degradation. GAPDH was used as a loading control.

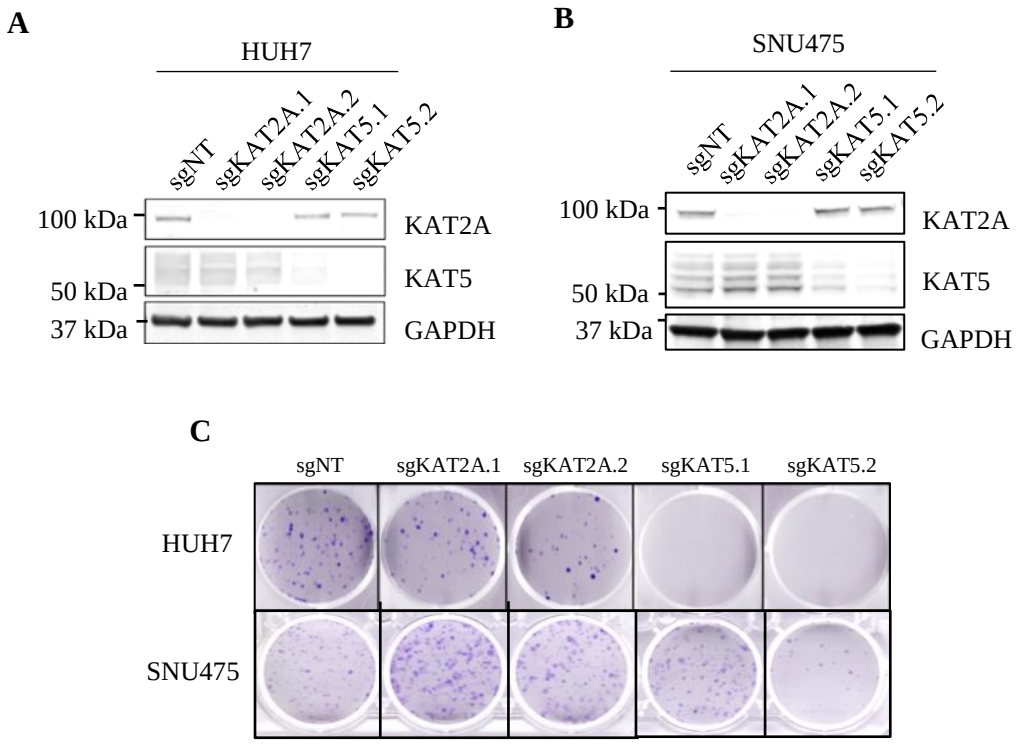

Figure 2.5. Loss of histone acetyltransferase KAT5 impairs growth in HCC cells. **A)** Western blot of KAT2A, KAT5 levels in Huh7 cells infected with sgNT, sgKAT2A and sgKAT5. GAPDH was used as a loading control. **B)** Western blot of KAT2A, KAT5 levels in SNU475 cells infected with sgNT, sgKAT2A and sgKAT5. GAPDH was used as a loading control. D) Colony formation, of Huh7 and SNU475 cells infected with sgNT, sgKAT2A, and sgKAT5. Cells were stained with crystal violet.

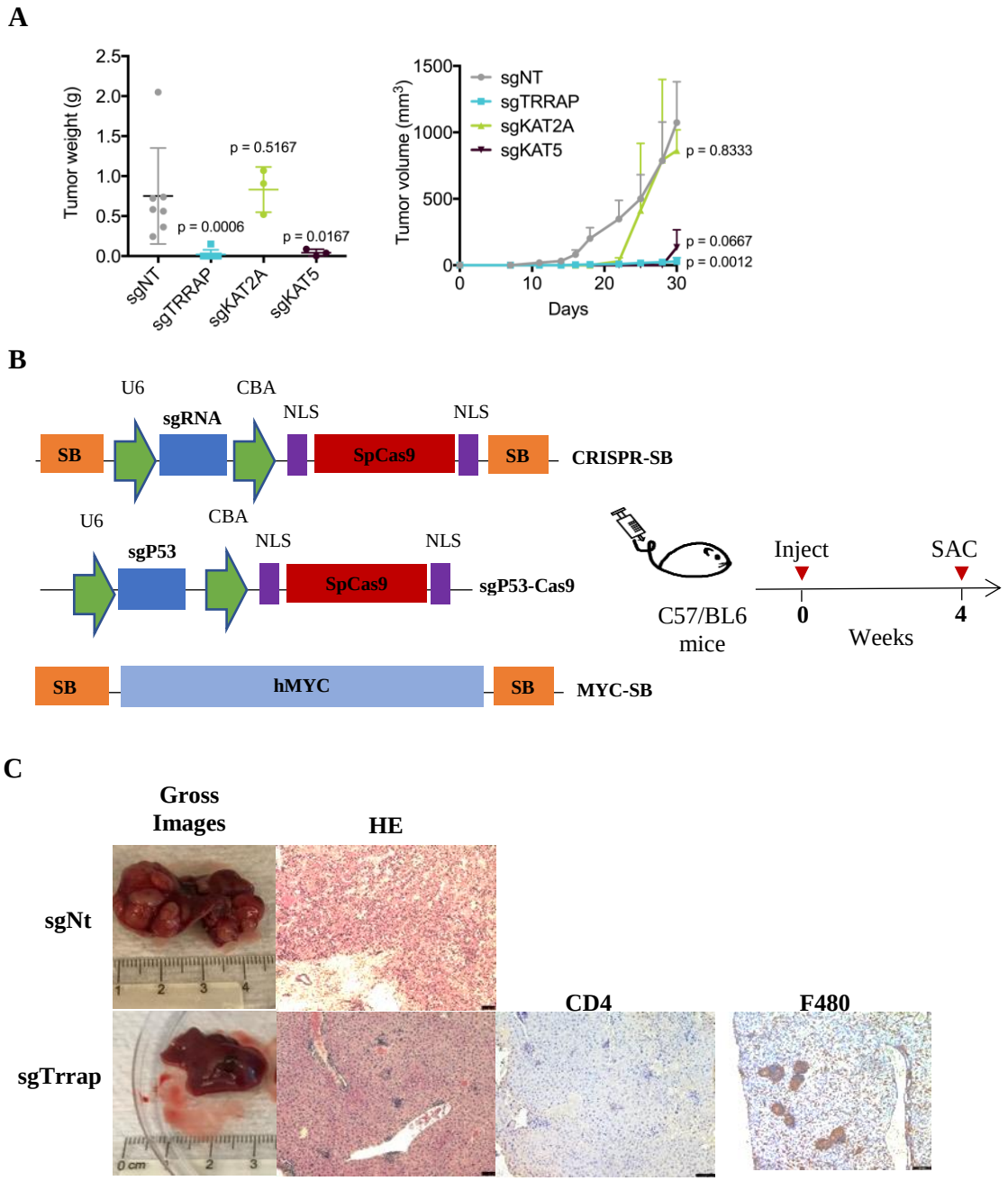

Figure 2.6. Loss of TRRAP and KAT5 impairs HCC growth and initiation in vivo. **A)** Tumor weight at day 30 (left) and tumor sizes (right) in nude mice subcutaneously injected with Huh7 cells. P-values were calculated using Mann-Whitney test against the sgNT group. Data was presented as mean ± SD; p-values were calculated by comparing to sgNT, *p < 0.05, **p < 0.01, ***p < 0.001, NS = not significant (student's t test). **B)**

Overview of three plasmids injected into mice via hydrodynamic tail vein injection to generate HCC tumors. The CRISPR-sleeping beauty plasmid plasmid contains S. pyogenes Cas9 (SpCas9) flanked by two nuclear localization signals (NLS) that is driven by a chicken beta-actin promoter (CBA) and an sgRNA (encoding either a Non-Target or Trrap sgRNA) driven by a U6 promoter. This entire construct is flanked by two sleeping beauty (SB) cassettes for integration. A second plasmid contains an sgRNA against P53 driven by a U6 promoter and a S. pyogenes Cas9 (SpCas9) flanked by two nuclear localization signals (NLS). The third plasmid contains the human MYC cDNA flanked by two SB cassettes. **C)** Gross images of the entire liver and H&E staining of liver sections four weeks after injection with sgNT or sgTRRAP along with IHC analyses of CD4 and F480 in sgTRRAP tumors.

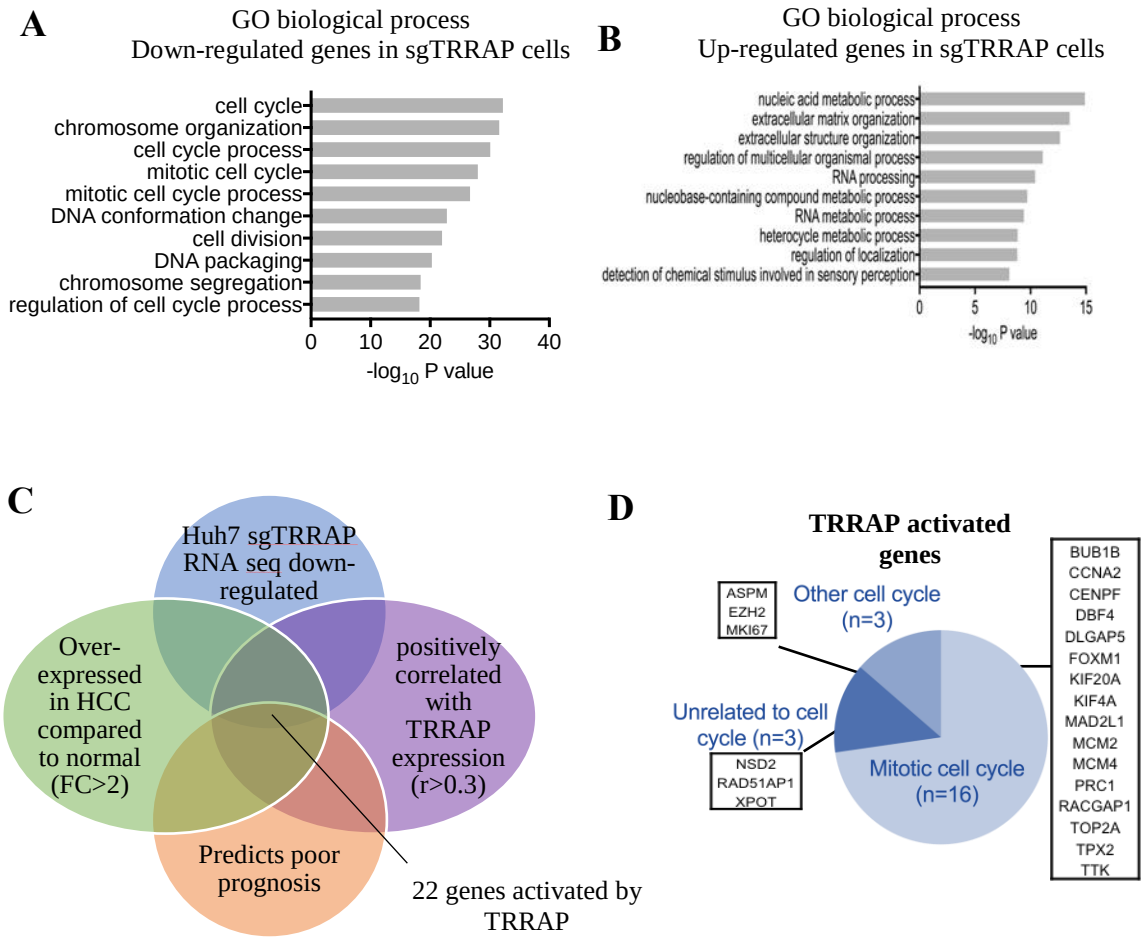

Figure 2.7. Analysis of genes regulated by TRRAP in HCC
A) Gene ontology (GO) analysis of down-regulated genes in sgTRRAP cells compared to non-targeting control. The 10 most significant annotation clusters are shown here. **B)** Gene ontology (GO) analysis of up-regulated genes in sgTRRAP cells compared to non-targeting control. The 10 most significant annotation clusters are shown here. **C)** Pipeline for identifying HCC-relevant TRRAP target genes. **D)** GO analysis of the 22 TRRAP-activated genes identified in B.

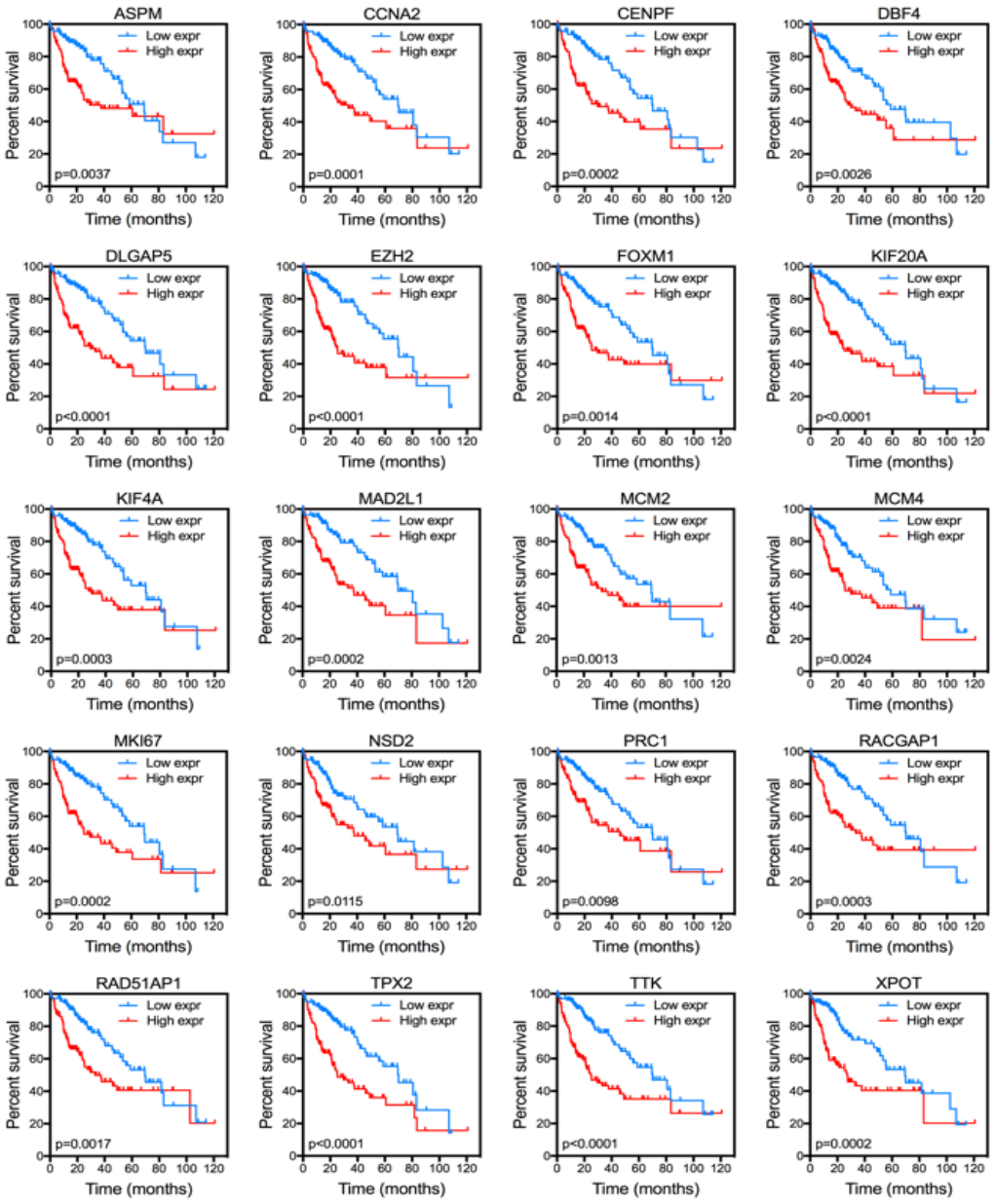

Figure 2.8. Increased expression of TRRAP-activated genes confers poor prognosis in HCC patients.

Kaplan Meier curves of TCGA HCC patients with high or low expression of TRRAP-activated genes listed in Table 1. P-values were calculated using the log-rank Mantel-Cox test. The Kaplan Meier curve of BUB1B is shown in Figure 2.1C.

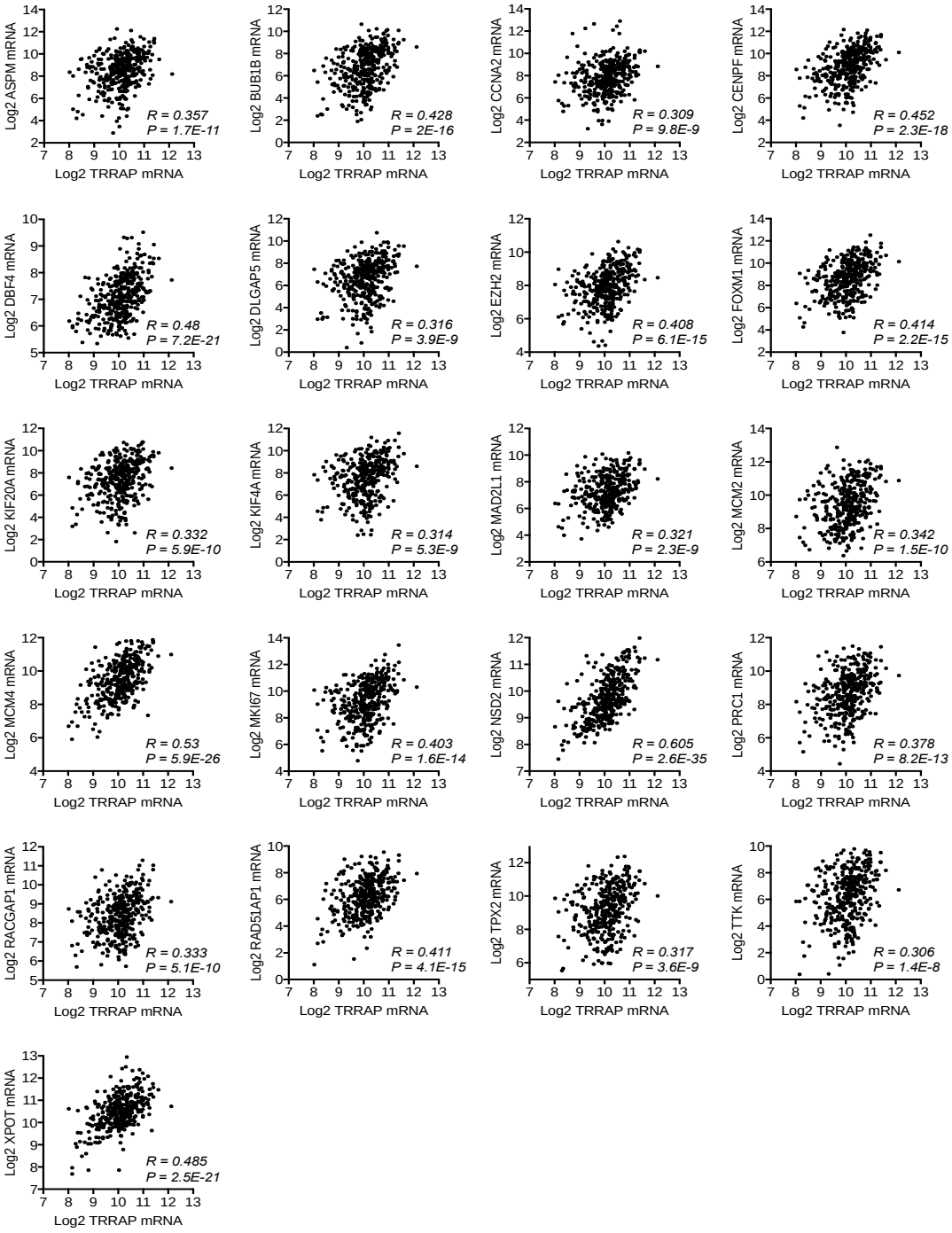

Figure 2.9. Positive correlation between mRNA expression of TRRAP and TRRAP-activated genes in HCC patient samples.

mRNA levels were downloaded from the TCGA HCC data set (n=360). Correlation was determined using Spearman's correlation analysis.

A

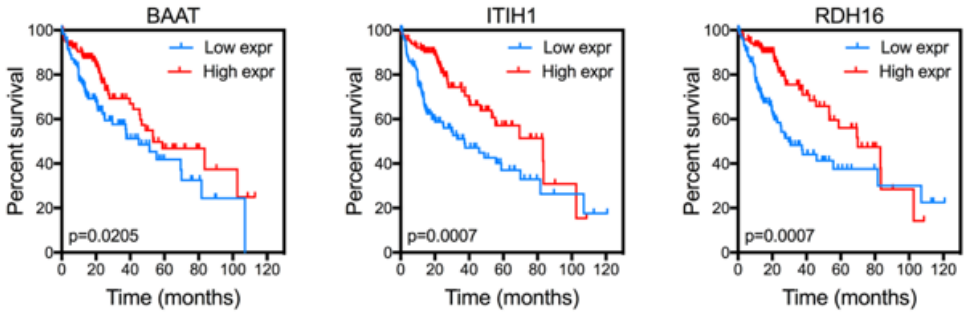

B

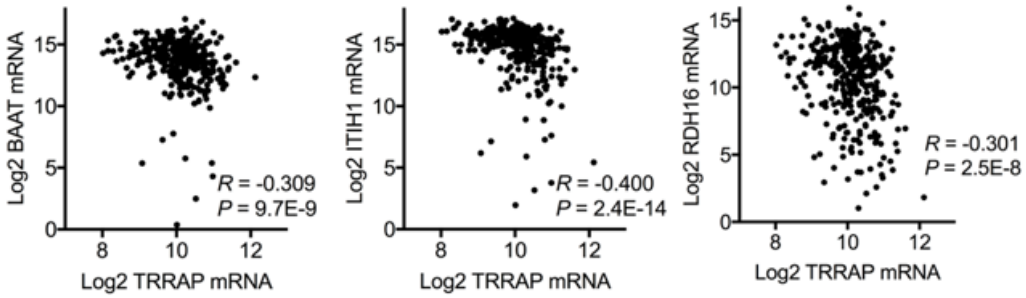

Figure 2.10. Identification of genes repressed by TRRAP.
A) Kaplan Meier curves of TCGA HCC patients with high or low expression of genes listed in Supplementary Table 3. **B)** Negative correlation between mRNA expression of TRRAP and TRRAP-inhibited genes in the TCGA HCC data set (n=360). Correlation was determined using Spearman's correlation analysis.

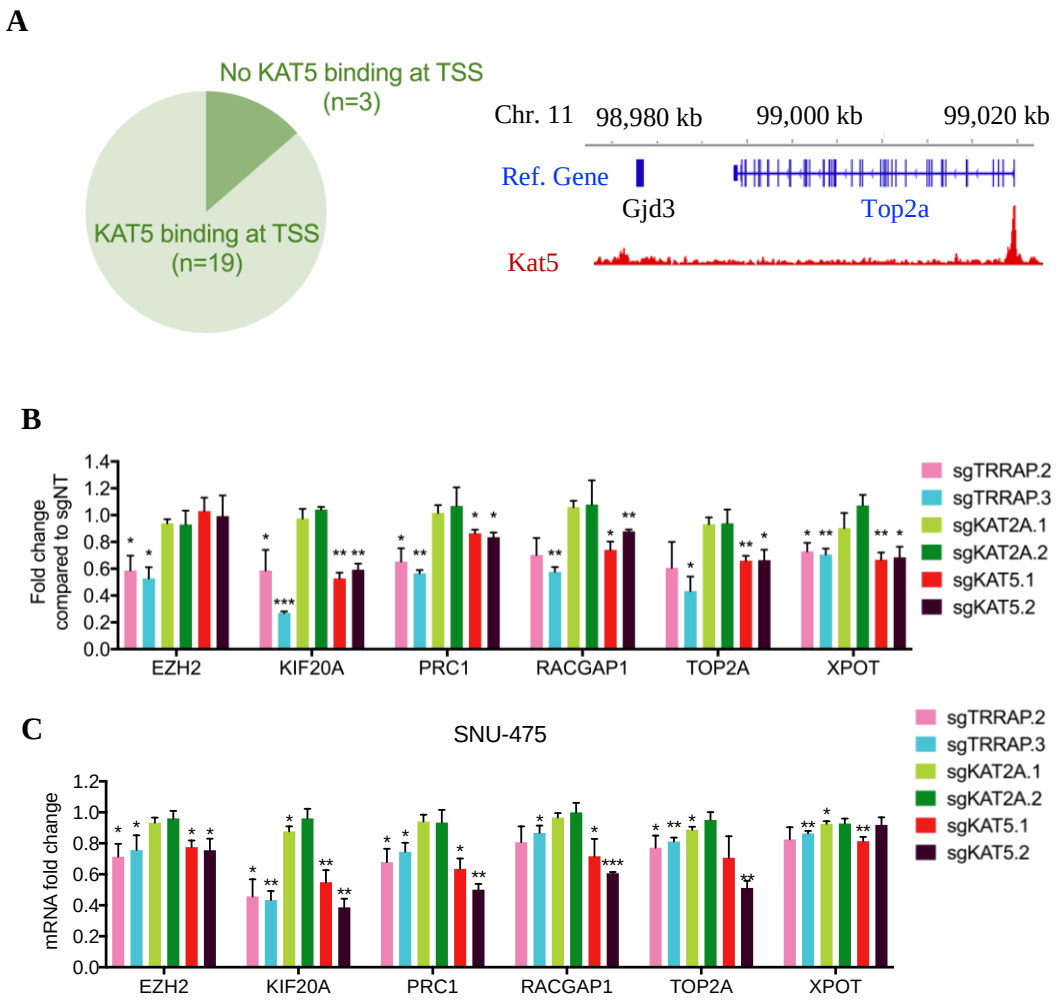

Figure 2.11. TRRAP/KAT5 activates transcription of mitotic genes.
A) KAT5 binding analysis at the transcriptional start sites (TSS) of the 22 TRRAP-activated genes using published ChIP-seq data (top). KAT5 binds to the TSS of TOP2A (bottom). **B)** mRNA levels of 6 TRRAP-activated genes in Huh7 cells infected with the indicated sgRNAs as measured by qRT-PCR. **C)** mRNA levels of 6 TRRAP-activated genes in SNU-475 cells infected with the indicated sgRNAs as measured by qRT-PCR.

Figure 2.12. KAT5 binds to the transcriptional start sites (TSS) of TRRAP-activated genes.

Analysis of published ChIP-sequencing data for KAT5 binding sites in mouse embryonic stem cells at TRRAP-activated genes (blue) identified in Table 1. Of note, no prominent peaks were observed at the TSS of Bub1b, Dlgap5 and Nsd2.

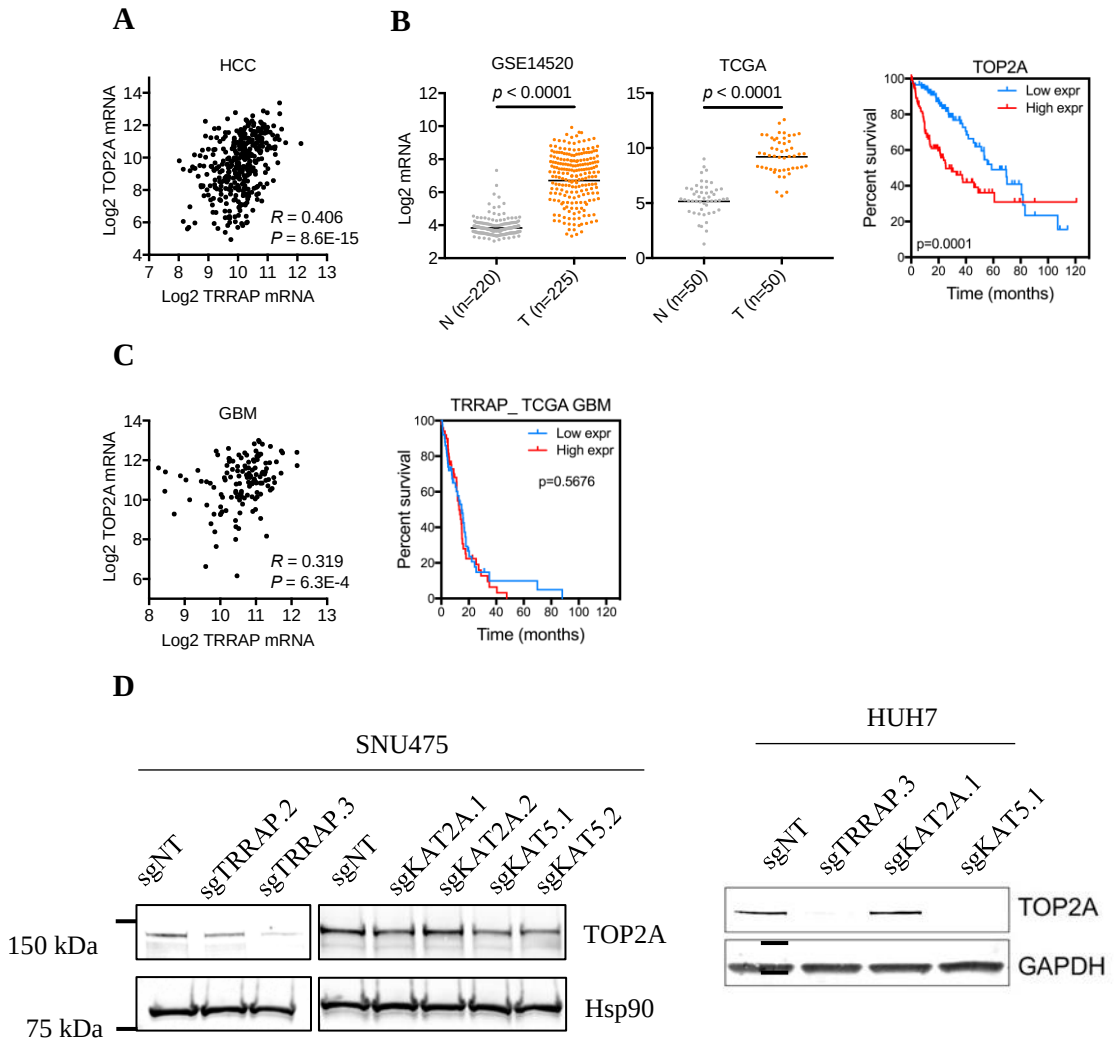

Figure 2.13. Loss of TRRAP and KAT5 reduces proliferation through down-regulation of TOP2A.

A) Correlation between TRRAP and TOP2A mRNA expression in the TCGA HCC data set (n=360) was determined using Spearman's correlation analysis (left). **B)** mRNA expression of TOP2A in non-tumor (N) and HCC (T) samples in the GSE14520 (left) and TCGA HCC (right) data sets, p-values were calculated using moderated t-test and the Wilcoxon signed-rank test respectively. Kaplan Meier curves of TCGA HCC patients with high or low TOP2A expression (right), p-value was calculated using the log-rank Mantel-Cox test. **C)** Correlation between TRRAP and TOP2A mRNA expression in the TCGA GBM data set (n=136) was determined using Spearman's correlation analysis (left). Kaplan Meier curve of TCGA GBM patients with high (n=50) or low (n=51) TRRAP expression

(right). P-value was calculated using the log-rank Mantel-Cox test. **D)** Protein levels of TOP2A after knockdown with indicated sgRNA in SNU-475 and HUH7 cell lines. GAPDH was used as a loading control.

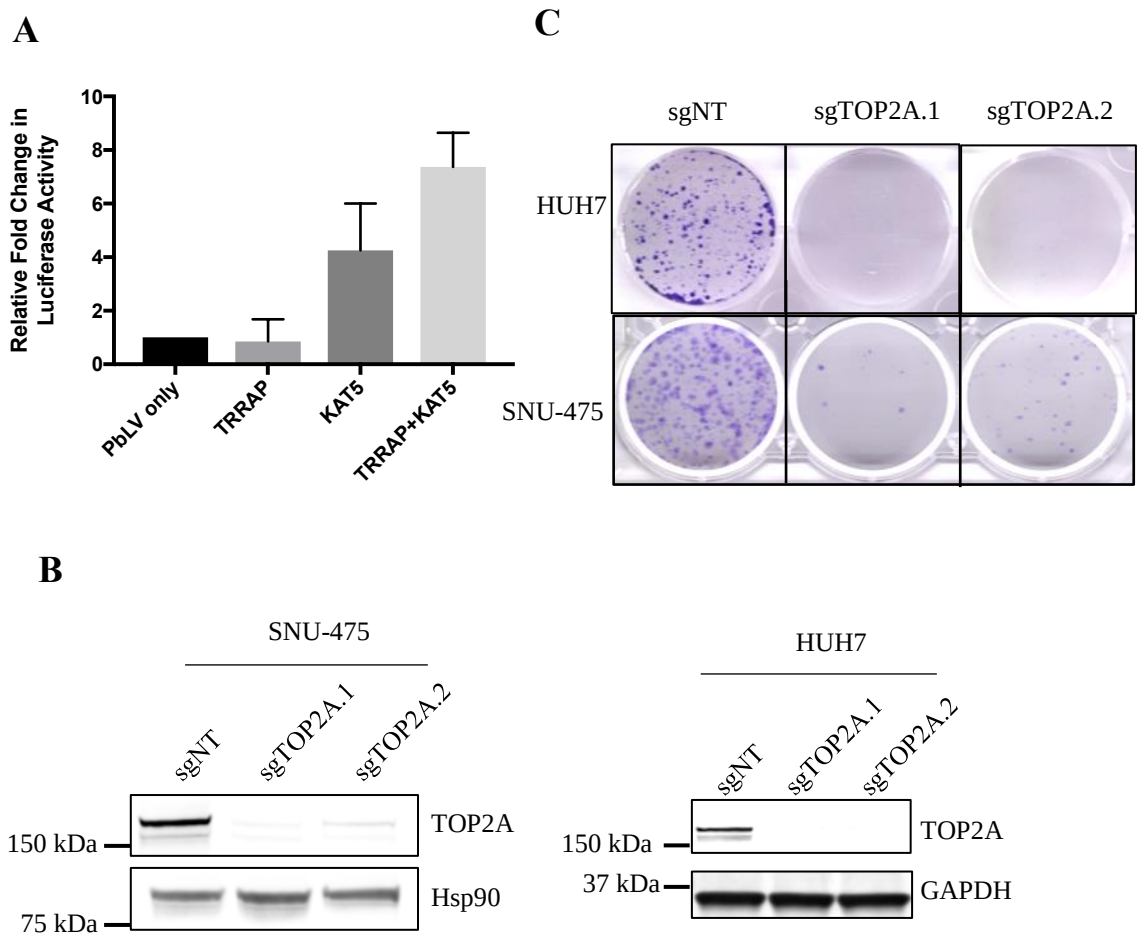

Figure 2.14. Loss of TOP2A Reduces Proliferation in HCC cells.
A) Top2A promoter luciferase assay in 293fs cells transfected with the indicated plasmids. Luciferase activity was normalized to the negative control pBV-luc. **B)** Protein levels of TOP2A in Huh7 and SNU-475 cells infected with the indicated sgRNAs. GAPDH was used as a loading control. **C)** Colony formation of Huh7 and SNU-475 cells infected with sgTOP2A.

Gene Symbol	Entrez gene name	RNA-seq sgTRRAP vs sgNT		GSE14520 HCC/ non-tumor tissue		TCGA HCC co-expressed with TRRAP	
		Fold change	P-value	Fold change	P-value	Spearman's coefficient	P-value
ASPM	Abnormal spindle microtubule assembly	0.46	1.8E-02	8.22	8.3E-112	0.357	1.7E-11
BUB1B	BUB1 mitotic checkpoint serine/threonine kinase B	0.42	2.6E-07	3.33	1.4E-73	0.428	2.0E-16
CCNA2	Cyclin A2	0.35	2.2E-03	2.45	1.7E-59	0.309	9.8E-09
CENPF	Centromere protein F	0.39	5.7E-03	5.25	3.9E-101	0.452	2.3E-18
DBF4	DBF4 zinc finger	0.46	8.4E-06	2.41	2.6E-71	0.48	7.2E-21
DLGAP5	DLG associated protein 5	0.42	2.9E-06	2.49	6.9E-60	0.316	3.9E-09
EZH2	Enhancer of zeste 2 polycomb repressive complex 2 subunit	0.38	5.5E-07	3.41	2.4E-78	0.408	6.1E-15
FOXM1	Forkhead box M1	0.38	4.5E-08	2.27	5.9E-67	0.414	2.2E-15
KIF20A	Kinesin family member 20A	0.23	1.2E-04	3.24	3.8E-80	0.332	5.9E-10
KIF4A	Kinesin family member 4A	0.41	5.5E-06	2.70	1.4E-69	0.314	5.3E-09
MAD2L1	Mitotic arrest deficient 2 like 1	0.45	1.2E-06	2.88	4.9E-62	0.321	2.3E-09
MCM2	Minichromosome maintenance complex component 2	0.38	1.9E-07	3.13	6.3E-69	0.342	1.5E-10
MCM4	Minichromosome maintenance complex component 4	0.46	1.0E-06	3.03	3.2E-72	0.53	5.9E-26
MKI67	Marker of proliferation ki-67	0.41	4.3E-02	2.38	9.5E-51	0.403	1.6E-14
NSD2	Nuclear receptor binding SET domain protein 2	0.46	3.5E-06	2.10	3.0E-61	0.605	2.6E-35
PRC1	Protein regulator of cytokinesis 1	0.40	4.9E-09	5.49	9.2E-106	0.378	8.2E-13
RACGAP1	Rac gtpase activating protein 1	0.39	1.2E-07	4.66	2.5E-108	0.333	5.1E-10
RAD51AP1	RAD51 associated protein 1	0.50	3.3E-04	2.59	2.0E-62	0.411	4.1E-15
TOP2A	DNA topoisomerase II alpha	0.34	5.2E-03	8.27	8.5E-98	0.406	8.6E-15
TPX2	TPX2, microtubule nucleation factor	0.37	5.6E-08	3.22	7.3E-71	0.317	3.6E-09
TTK	TTK protein kinase	0.47	2.0E-05	3.22	9.7E-69	0.306	1.4E-08
XPOT	Exportin for trna	0.47	1.5E-08	2.44	1.9E-62	0.485	2.5E-21

Table 2.1 List of genes that are down-regulated in the absence of TRRAP and identified from our bioinformatic analyses.

Gene Symbol	Entrez Gene Name	RNA-seq sgTRRAP vs sgNT		GSE14520 HCC/ non-tumor tissue		TCGA HCC co-expressed with TRRAP	
		Fold change	P-value	Fold change	P-value	Spearman's coefficient	P-value
BAAT	bile acid-CoA:amino acid N-acyltransferase	10.79	4.0E-40	0.41	5.4E-22	-0.309	9.7E-09
ITIH1	inter-alpha-trypsin inhibitor heavy chain 1	2.05	2.9E-03	0.41	1.1E-32	-0.4	2.4E-14
RDH16	retinol dehydrogenase 16	3.54	4.9E-02	0.14	1.3E-73	-0.301	2.5E-08

Table 3. List of genes that are up-regulated in the absence of TRRAP and identified from our bioinformatics analyses.

Gene symbol	Spearman's Correlation	p-Value
ASPM	**0.484**	**2.6E-08**
BUB1B	**0.315**	**7.6E-04**
CCNA2	0.117	2.8E-01
CENPF	**0.554**	**5.2E-11**
DBF4	0.139	1.9E-01
DLGAP5	0.211	3.3E-02
EZH2	**0.408**	**5.7E-06**
FOXM1	**0.437**	**8.5E-07**
KIF20A	**0.324**	**5.0E-04**
KIF4A	**0.418**	**2.9E-06**
MAD2L1	-0.084	4.5E-01
MCM2	**0.393**	**1.3E-05**
MCM4	**0.544**	**1.4E-10**
MKI67	**0.590**	**1.3E-12**
NSD2	**0.569**	**1.2E-11**
PRC1	**0.347**	**1.6E-04**
RACGAP1	0.136	2.0E-01
RAD51AP1	-0.036	7.7E-01
TOP2A	**0.319**	**6.3E-04**
TPX2	**0.375**	**3.8E-05**
TTK	0.177	8.2E-02
XPOT	0.205	3.9E-02

Table 4. TRRAP regulates a similar set of genes in HCC and GBM.

sgRNA name	Sequence (5'-3')
sgTRRAP.1	ACTCCTGATACAAGAGATCG
sgTRRAP.2	CTTGATCCGCCACTATACGA
sgTRRAP.3	CCACTGGGGATCGTTCAGTG
sgKAT2A.1	GCTGCTGGAAAAGTTCCGAG
sgKAT2A.2	TCACCATGCCACCCTCAGAG
sgKAT5.1	GATTGATGGACGTAAGAACA
sgKAT5.2	ACCAGGCTGCCAGTCATGCG
sgTOP2A.1	TGTACGCTTATCCTGACTGA
sgTOP2A.2	GATGCTGCTATCAGCCTGGT

Table 5. sgRNA sequences used in Chapter II

Primer name	Sequence (5'-3')
KAT2A-F	CAGGGTGTGCTGAACTTTGTG
KAT2A-R	TCCAGTAGTTAAGGCAGAGCAA
KAT5-F	GGGGAGATAATCGAGGGCTG
KAT5-R	TCCAGACGTTTGTTGAAGTCAAT
EZH2-F	AATCAGAGTACATGCGACTGAGA
EZH2-R	GCTGTATCCTTCGCTGTTTCC
GAPDH-F	CTGGGCTACACTGAGCACC
GAPDH-R	AAGTGGTCGTTGAGGGCAATG
KIF20A-F	GCCAACTTCATCCAACACCT
KIF20A-R	GTGGACAGCTCCTCCTCTTG
PRC1-F	ATCACCTTCGGGAAATATGGGA
PRC1-R	TCTTTCTGACAGACGGATATGCT
RACGAP1-F	CTATGATGCTGAATGTGCGG
RACGAP1-R	AATCCTCAAAGTCCTTCGCC
TOP2A-F	ACCATTGCAGCCTGTAAATGA
TOP2A-R	GGGCGGAGCAAAATATGTTCC
XPOT-F	AGGGAGACGCTCATATCATGG
XPOT-R	TTGGGCGGCTTTATTTCGTAT

Table 6 Primers used for qRT-PCR in Chapter II.

Primer name	Sequence (5'-3')
TOP2A 500bp F	CTTACGCGTGCTAGCCCTCTCTAGTCCCGC
TOP2A 500bp R	TATATACCCGAATTCTTCACTACTAGCACC
TOP2A neg control F	CTTACGCGTGCTAGCGCCTGTAAATGAAAA
TOP2A neg control R	TATATACCCGAATTCTCTTTATATTAAAGG

Table 7. Primers for cloning the TOP2A promoter

CHAPTER III

Loss of TRRAP and its cofactor KAT5 triggers senescence in HCC independent of P53 and P21

Introduction

In the previous chapter we identify TRRAP and its cofactor KAT5 as potential therapeutic targets in HCC. Loss of TRRAP and KAT5 reduces proliferation of HCC cell lines in vitro and in vivo. Furthermore, by cross referencing RNA-seq analysis of TRRAP depleted cells with data from HCC patients samples we identify that TRRAP and KAT5 reduce expression of a subset of genes responsible for mitotic progression including TOP2A.

Studies in mouse models have demonstrated that TRRAP loss is embryonic lethal as embryos do not survive past the blastocyst stage (126). However, inducible tissue specific models have provided some insight into the differential effects of TRRAP loss in normal tissue. Depletion of TRRAP in the CNS resulted in impaired differentiation of neuronal progenitor cells due to failure to induce expression of stemness regulator genes such as Nanog, Oct4 and Sox2 (133). Interestingly, TRRAP depletion in B cells does not impair immunoglobin class switching but instead results in apoptosis of the cells (236). Finally, TRRAP loss in the liver impaired regeneration after CCl4 induced damage due to failure to induce cyclin A expression (132).

The work in this thesis is not the first to implicate the role of TRRAP in malignancies. Studies in glioblastoma revealed that loss of TRRAP increased differentiation of cultured glioblastoma tumor-initiating cells and impaired cell cycle

progression (194). Another study identified TRRAP as an oncogene in melanomas. The authors of this study demonstrated, via Hoechst staining, that depletion of TRRAP in melanoma cell lines resulted in apoptosis (190). Studies in lymphoma models have demonstrated that TRRAP promotes cell growth by stabilizing mutant isoforms of P53. In line with this, loss of TRRAP results in decreased proliferation of lymphoma cell lines in vitro (195). However, the work in this thesis is the first to examine the role of TRRAP in HCC and investigate how TRRAP loss results in decreased cell proliferation and tumor growth.

KAT5, a TRRAP HAT cofactor, plays essential roles in development as well as the resolution of DNA damage via acetylation of both histone and non-histone targets. KAT5 histone acetylation activity is required for ATM mediated detection and resolution of DNA damage(147). Moreover, KAT5 mediated acetylation of P53 is required for apoptosis in response to DNA damage (237). The majority of studies investigating KAT5 in malignancies implicate it as a mediator of resistance to DNA damage therapies. Studies demonstrate that KAT5 is overexpressed in cisplatin resistant lung cancers, and that silencing of KAT5 sensitizes the cells to cisplatin treatment (238). Furthermore in androgen-resistant models of prostate cancer KAT5 is localized more in the nucleus compared to models of benign prostatic hyperplasia in which KAT5 is diffusely localized (239). In line with this, treatment with small molecule inhibitors of KAT5 such as NU9056 and TH1834 reduces proliferation of prostate and breast cancer cells in vitro (140). However, the consequences of KAT5 inhibition in HCC have not been studied.

In this chapter we demonstrate that loss of TRRAP/KAT5 and TOP2A induces senescence in HCC cells during. Moreover, the cells senescence during G2/M independent of DNA damage.

Results

Loss of TRRAP and KAT5 triggers senescence in HCC

After inducing TRRAP loss via CRISPR/Cas9 mediated genome editing HUH7 and SNU475 cells exhibit a distinct morphology—the cells became enlarged, flatter and resemble a fried egg (Figure 3.1A). These physical characteristics match those that are found in senescence cells (155). Indeed, loss of TRRAP in Huh7, Hep3B and SNU-475 cells resulted in positive senescence-associated-beta-galactosidase (SA-β-gal) staining (Figure 3.1B and 3.1C). Furthermore, the molecular markers of senescence—p15, p16, and p21were increased in sgTRRAP cells compared to non-targeting controls in HUH7 (Figure 3.2A), HEP3B (Figure 3.2B) and SNU-475 (Figure 3.3C) cell lines. Collectively, these data suggest that loss of TRRAP inhibits cell growth by inducing senescence.

To determine whether TRRAP depletion induces senescence due to loss of KAT2A or KAT5 expression, we depleted KAT2A and KAT5 using CRISPR (sgKAT2A and sgKAT5) in Huh7 and SNU-475 cells (Figure 2.5A and 2.5B). We found that depletion of KAT5, but not KAT2A induced senescence similarly to TRRAP-depleted cells (Figure 3.3A and 3.3B). We also found a higher increase in p15 and p21 expression in sgKAT5 cells compared to non-targeting control and sgKAT2A cells (Figure 3.3C and 3.3D).

TRRAP/KAT5 senescence is independent of canonical inducers of senescence

Senescence can be triggered by multiple stimuli, such as DNA damage, replicative stress, activation of oncogenes, and oxidative stress (240). A key molecular event in induction of senescence is p53 activation and Rb hypophosporylation (241). However, Huh7 and SNU-475 cells are p53-mutant, and Hep3B cells are p53-null and Rb-null, suggesting that induction of senescence due to TRRAP and KAT5 depletion is independent of p53. In line with this, western blot analysis of P53 and Phospho-Rb in TRRAP depleted HUH7 cells showed a decline in levels of P53 and no change in the levels of phospho-Rb (Figure 3.4A). Based on Hayflick's observations, low levels of telomerase expression (TERT) have also been demonstrated to induce senescence. However, TERT expression remained similar to controls in TRRAP and KAT5 depleted HUH7 cells (Figure 3.4B). Masashi Narita demonstrated that SAHF can also trigger senescence, however TRRAP depleted cells did not show increased DAPI foci compared to control HUH7 cells (Figure 3.4C). Since DNA damage can also induce senescence, we measured levels of the DNA damage mark γH2A.X via flow cytometry and found no changes in the level of γH2A.X compared to control cells (Figure 3.4D).

Since we observed an increase in the expression of p21, a p53 target that is also important in inducing senescence (241), we asked whether p21 is required to induce senescence in TRRAP- and KAT5-depleted cells. To this end, we co-depleted p21 and either TRRAP or KAT5 using CRISPR in Huh7 and SNU-475 cells via sequential infections (Figure 3.5A) and validated our knockouts via western blot (Figure 3.5B). We found that, even in the absence of p21, depletion of TRRAP and KAT5 inhibited colony

formation and induced senescence (Figure 3.5C and 3.5D). Using a similar sequential infection strategy, we also generated P53 and TRRAP/KAT5 double knockout HUH7 cells (Figure 3.6A) and found no difference in induction of senescence in the absence of P53 (Figure 3.6B). Taken together the data suggested that the canonical p53/p21 pathway is not required for senescence in this context.

Loss of TRRAP, KAT5 and TOP2A induces senescence during G2/M

Previous studies have found that cells undergoing oncogene-induced senescence are arrested at G1 phase (24), but more recent evidence suggests that G2 arrest can also induce senescence (39). Since we found that the majority of TRRAP target genes regulate mitosis, we reasoned that TRRAP depletion may cause alterations in cell cycle progression. We analyzed cell cycle profiles using BrdU and PI staining and found that sgTRRAP and sgKAT5 cells accumulated at the G2/M phase. As expected, sgKAT2A cells did not accumulate at G2/M phase and displayed a cell cycle profile similar to non-targeting controls (Figure 3.7A and Figure 3.7B).

In line with our observations with TRRAP and KAT5, cells depleted of TOP2A also displayed phenotypes resembling TRRAP and KAT5 depletion. TOP2A knockouts stained positive for SA-β-gal (Figure 3.8A), had elevated expression of the senescence markers p21, and p16 (Figure 3.8B and 3.8C). Furthermore, we found that γH2AX levels in sgTOP2A cells were similar to non-targeting controls, suggesting that DNA damage is not the cause senescence (Figure 3.9A). Finally, like TRRAP and KAT5 depleted cells, TOP2A depleted cells also arrested in G2/M (Figure 3.9B and 3.9C). Together, our

results suggest that TOP2A is a key mitotic target of TRRAP and KAT5 in regulating HCC cell growth.

Discussion

In this chapter we find that depletion of TRRAP, its cofactor KAT5 and its downstream target TOP2A reduces HCC proliferation by inducing senescence. In vitro, the cells stain positive for SA-β-gal and have elevated expression of the CDKIs p21 and p15. Furthermore, clearance of TRRAP depleted cells in vivo is correlated with the presence of $F480^{+}$ cells and not $CD4^{+}$ cells (Figure 2.6C). This is in line with previous observations that senescent cells are cleared by macrophages (182).

TOP2A is thought to be the primary topoisomerase required for the decatenation of chromosomes during mitosis. In line with this, loss of TOP2A is embryonic lethal as zygotes arrest at the four to eight cell stage of development (242). Furthermore depletion of TOP2A in the fibrosarcoma cell line HT1080, results in tangled chromosomes, aberrant mitoses, aneuploidy, and cells undergo cell cycle arrest followed by cell death via apoptosis (243). Classically, Topoisomerase poisons have been demonstrated to induce apoptosis in various cancer models (244), hence drugs like Etoposide and Doxorubicin have been core chemotherapies utilized for many cancer types. Surprisingly, the work in this thesis suggests that depletion of TOP2A results in senescence as opposed to apoptosis in HCC cells.

Several studies have demonstrated that the consequences of topoisomerase inhibition are dependent on p53. When p53 was inhibited in the HT1080 fibrosarcoma

cell line after TOP2A inhibition, cells did not arrest and instead immediately underwent apoptosis (243). MCF-7 breast cancer cells with functional p53 enter senescence following doxorubicin treatment, whereas those lacking functional p53 undergo apoptosis (245). Similarly glioblastoma cells with intact p53, senesce in response to inhibition of topoisomerase I, whereas cells with disrupted p53 undergo apoptosis (246). A later study demonstrated that this effect was mediated by PTEN as glioma cells with intact PTEN underwent senescence through the AKT/ROS/p53/p21 signaling pathway whereas glioma cells that were PTEN deficient underwent apoptosis in response to radiation induced DNA damage (247).

In addition to P53 status, a study in HCC revealed that treatment with Doxorubicin at high doses (10 uM) triggered apoptosis whereas treatment at low doses (40 nM) triggered senescence (248). This study demonstrated that treatment with low dose doxorubicin first triggered a “temporary senescence”, as marked by positive SA-β-gal staining, but cells underwent caspase positive cell death 48 hours after the appearance of SA-β-gal. The authors suggested that treatment with high dose doxorubicin triggered apoptosis due to a temporary activation of the JNK and NFκB pathways whereas NFκB activation was sustained in low dose doxorubicin treated cells (248). Senescence associated with sustained NFκB activation is in line with the autocrine effects of the SASP, however the factors that control the decision to senesce versus die in response to TOP2A inhibition in HCC remain unclear.

Interestingly, TRRAP and KAT5 depleted cells underwent senescence even in the absence of DNA damage as levels of γH2A.X remained similar to sgNT and sgKAT2A cells. Previous studies have demonstrated that the TRRAP-KAT5 complex mediates DNA repair by two mechanisms. First the TRRAP-KAT5 complex acetylates the chromatin surrounding the site of damage thereby increasing accessibility to other repair proteins (147). Second, the TRRAP-KAT5 complex acetylates ATM in order to activate signaling down this DNA damage pathway (147). Therefore, the lack of detectable DNA damage in TRRAP and KAT5 depleted cells is likely due to loss of γH2A.X deposition. However future experiments are required to determine if ATM signaling is attenuated in TRRAP and KAT5 depleted cells.

Paradoxically we found a *decline* in P53 protein levels and no change in Rb phosphorylation in cell lines with functional P53 and Rb, such as HUH7 and SNU475, after TRRAP and KAT5 depletion. Moreover, we found that the HEP3B cell line which had deletions in both P53 and Rb senesced after TRRAP loss which further emphasized that senescence was independent of this pathway. Interestingly while generating the TRRAP/P53 double knockout cells we also observed that, unlike with TRRAP loss, loss of KAT5 did not result in a decrease in P53 protein levels (Figure 3.6A). A previous study in lymphoma and colon cancer models identified that one of the HEAT repeat regions of TRRAP was crucial for mutp53 stabilization as TRRAP shielded it from degradation via the MDM2-proteasome axis (195). Perhaps TRRAP is performing a similar role in HCC containing mutant P53, however future studies are needed to elucidate this possible mechanism.

Generally, p53 activation is a key event in senescence, but we discovered that TRRAP depletion induces senescence independent of the p53/p21 pathway in HCC cells. This finding has clinical implications for HCC treatment as 30% of HCC patients have p53 mutations (14) and p53 is more frequently mutated in HCC patients with high TRRAP expression (Figure 2.2C). Multiple studies have established various mechanisms for P53 independent senescence. Loss of VHL, a tumor suppressor, in MEFs induces senescence independent of P53 but dependent on Rb activation and P400 reduction (249). Senescence induction via Cdk2 deficiency was independent of p53 activity but depended on induction of P21 and P16 (250). SKP2 inactivation in lymphoid cancer models induced senescence independent of P53 but dependent on P21 and P27 (251). Even in HCC, treatment of cells with TGF-β induced senescence independent of P53 but dependent on P21 and intracellular ROS accumulation (252). Overall, P53 independent senescence is a well-observed phenomenon but, as one would expect, the senescence inducing mechanisms were all dependent on Rb or CDKIs downstream of P53.

Our study identified that TRRAP and KAT5 depletion triggered senescence independent of p53 and its downstream molecules p21 and Rb. A p53- and p21-independent mechanism in immortalized human diploid fibroblasts has been described (253). In this previous study, loss of the histone acetyltransferase p300 induced senescence due to global H3 and H4 hypoacetylation resulting in SAHF and subsequent alterations in DNA replication timing and fork velocity (253). In the present study, we propose a different mechanism—TRRAP depletion leads to senescence due to downregulation of mitotic genes, such as TOP2A, and G2/M arrest that is also not

correlated with SAHF. This is distinct from cell cycle arrest as the cells are diploid, stain positive with SA-β-gal and have elevated expression of the CDKIs P16, P15 and P21. Our study is also the first to identify a p53, p21 independent mechanism of senescence in HCC.

To determine how perturbation of this network induced senescence, we examined whether previously known inducers of senescence were activated in our cells. One of the key roles of the TRRAP/KAT5 complex is to mediate repair of DNA DSBs via acetylating the sites of damage and aiding in activation of ATM(147). Given that DNA damage has been previously demonstrated to induce senescence in various models (151), we hypothesized that TRRAP depleted cells senesced due to increased DNA damage. However, there was no change in γH2A.X levels in TRRAP, KAT5 and TOP2A depleted HCC cell lines compared to non-target cells suggesting that our mechanism of senescence was independent of DNA damage. Furthermore, examination of telomerase levels and SAHF formation also showed no change upon TRRAP and KAT5 depletion.

Studies out of the Berger lab elegantly demonstrated that in senescent cells, DNA fragments pinch off from the nuclei and are ejected into the cytoplasm (254). Furthermore, these cytoplasmic DNA fragments bind and activate cGAS/sting in order to trigger the SASP (255). Interestingly, overexpression of the DNases, DNase2 and TREX1, in senescent cells reduces SASP activation and can attenuate the induction of senescence (256, 257). Future studies can aim to elucidate whether senescence in TRRAP depleted cells is due to SASP induction via the presence of these cytoplasmic DNA fragments.

Various models of OIS and replicative senescence triggers arrest during G1(258), however, we conclude that TRRAP and KAT5 depletion induced senescence arrested cells during G2/M. The arrest in G2/M provides our first clue into identifying how loss of TRRAP and KAT5 induces senescence. G2/M arrest can arise from failure to replicate DNA during S phase. The most common reason for this is ATM activation secondary to DNA damage (258) however other mechanisms also exist. Previous studies have shown that depletion of nucleotide pools and histone pools can induce arrest during G2 as the genome is not able to replicate completely (258-260). The study implicating p300 HAT and senescence discussed earlier demonstrated that G2/M senescence in their model was due to decreased velocity across the replication fork secondary to limited chromatin accessibility (253). Another group has implicated aberrant regulation of Cyclin B as a mediator of G2/M arrest. For normal cell cycle progression Cyclin B must be activated, associate with CDK1 and translocate into the nucleus in order to initiate mitosis. Interestingly, cells will senesce during G2 due to failure to activate Cyclin B (either via p53 or p21) (261) or if there is a delay in translocation of cyclin B into the nucleus (261, 262). Finally, studies have also demonstrated that formation of other secondary structures in DNA such as Anaphase Bridges, G-quadruplexes, and R-loops can trigger replication stress and subsequent cell cycle arrest during G2 (263). In Chapter II of this thesis, we demonstrate that TRRAP loss reduces expression of genes involved in mitotic progression however future studies need to examine the mechanism(s) that enforces G2/M arrest and subsequent senescence in TRRAP depleted cells.

Taken together, the work in this chapter demonstrates that depletion of TRRAP/KAT5 or TOP2A triggers senescence in HCC cells independent of p53, p21 and other canonical mediators of senescence. Overall targeting the TRRAP/KAT5 complex or its downstream mitotic genes may be a pro-senescent strategy for treating HCC patients.

Materials and Methods

Cell culture

Huh7 and SNU475 cells were provided by Dr. Scott Lowe. Huh7 cells were cultured in DMEM. SNU-475 cells were cultured in RPMI supplemented with 10 mM HEPES, 1 mM sodium pyruvate, and 4500 mg/L glucose. Hep3B cells were provided by Dr. Junwei Shi and cultured in MEM. All cell lines were grown in media supplemented with 10% FBS and 1% penicillin-streptomycin and maintained in a 37ºC incubator with 5% CO2. Huh7, Hep3B and SNU-475 cells were authenticated using ATCC's cell authentication service.

sgRNA design and lentivirus infection

sgRNAs were designed using https://portals.broadinstitute.org/gpp/public/analysis-tools/sgrna-design, cloned into the LentiCRISPRv2 backbone (Addgene #52961) and packaged into lentivirus using 293fs cells. HCC cells infected with lentivirus were selected with puromycin for 2-4 days. To generate double sgRNA-infected cells, sgNT and sgp21 were cloned into the LentiCRISPRv2 hygro backbone (Addgene #98291). SNU-475 and Huh7 cells infected with lentivirus were selected with 100 and 500 µg/mL hygromycin for 6 and 10 days respectively, then infected with sgNT, sgTRRAP, sgKAT5, and sgKAT2A, and selected with puromycin. Sequences of sgRNAs are listed in Table 3.1.

RNA extraction and RT-qPCR

RNA was extracted from cells using the RNeasy mini kit (Qiagen, Germantown, MD) and DNA was removed by on-column DNase digestion (Qiagen) according to the manufacturer's protocol. One microgram of RNA was used to synthesize cDNA using the high-capacity cDNA reverse transcription kit (Thermo Fisher Scientific) according to the manufacturer's protocol. RT-qPCR analyses were performed using SsoFast EvaGreen supermix (Bio-Rad, Hercules, CA) according to the manufacturer's protocol and GAPDH was used as a control. Primer sequences used for qRT-PCR are listed in Table 3.2.

SA-β-gal assay

Huh7, Hep3B, and SNU-475 cells were seeded onto 12-well plates, senescence-associated β-galactosidase (SA-β-gal) staining was performed at pH = 6.0 and positively stained cells were quantified as previously described (163).

Immunoblot Analysis

Cells were washed twice with ice-cold PBS and harvested in RIPA buffer (Boston Bioproducts, Ashland MA) supplemented with protease (Roche, Indianapolis, IN) and phosphatase inhibitor cocktails (Thermo Fisher Scientific). The concentration of protein was measured using the BCA assay (Thermo Fisher Scientific). For each sample, 25 µg of protein was loaded onto an SDS-PAGE gel. The following antibodies were used to probe against: TRRAP (#3967; Cell Signaling Technology, Danvers, MA), KAT2A

(#3305; Cell Signaling Technology), KAT5 (sc-166323; Santa-Cruz Biotechnology, Dallas, TX), GAPDH (MAB374; Millipore Sigma, Burlington, MA), Hsp90 (#610419; BD Bioscience, San Jose, CA), p21 (#2947; Cell Signaling Technology), and p53 (sc-126; Santa-Cruz Biotechnology). Bands were visualized with an immunofluorescent secondary antibody (LICOR) using the Odyssey Imaging system.

Flow cytometry analyses

For cell cycle analysis, Huh7 and SNU-475 cells were pulsed with 30 μg/mL 5-Bromo-2´-Deoxyuridine (BrdU, Thermo Fisher Scientific) for 1 hour at 37□C. Cells were then trypsinized and fixed with 70% ethanol, permeabilized with 0.3% Triton-X 100 and incubated with a BrdU-FITC conjugated antibody (Thermo Fisher Scientific). Cells were stained with 50 ng/mL propidium iodide (Thermo Fisher Scientific), 10 μg/mL RNase A (Thermo Fisher Scientific), and incubated for 30 minutes at 37ºC. For γH2AX analysis, cells were fixed in 70% ethanol, permeabilized with 0.3% Triton-X100 and blocked in 0.8% BSA. Cells were then incubated with an anti-γH2A.X antibody (#9718; Cell Signaling Technology), which was detected using a mouse-FITC IgG. Cells were also stained with propidium iodide as described above to identify 2N and >2N populations. For each sample, at least 40,000 cells were analyzed using the MACSQuant VYB Flow cytometer (MACS Miltenyi Biotec, Auburn, CA). All data were analyzed by FlowJo 10.0 software.

Statistics

Statistical analysis was performed using GraphPad Prism software and data were presented as means ± standard deviation. Student's t-test was used to determine P-values unless indicated otherwise. P-values of <0.05 were considered to be statistically significant.

Figures

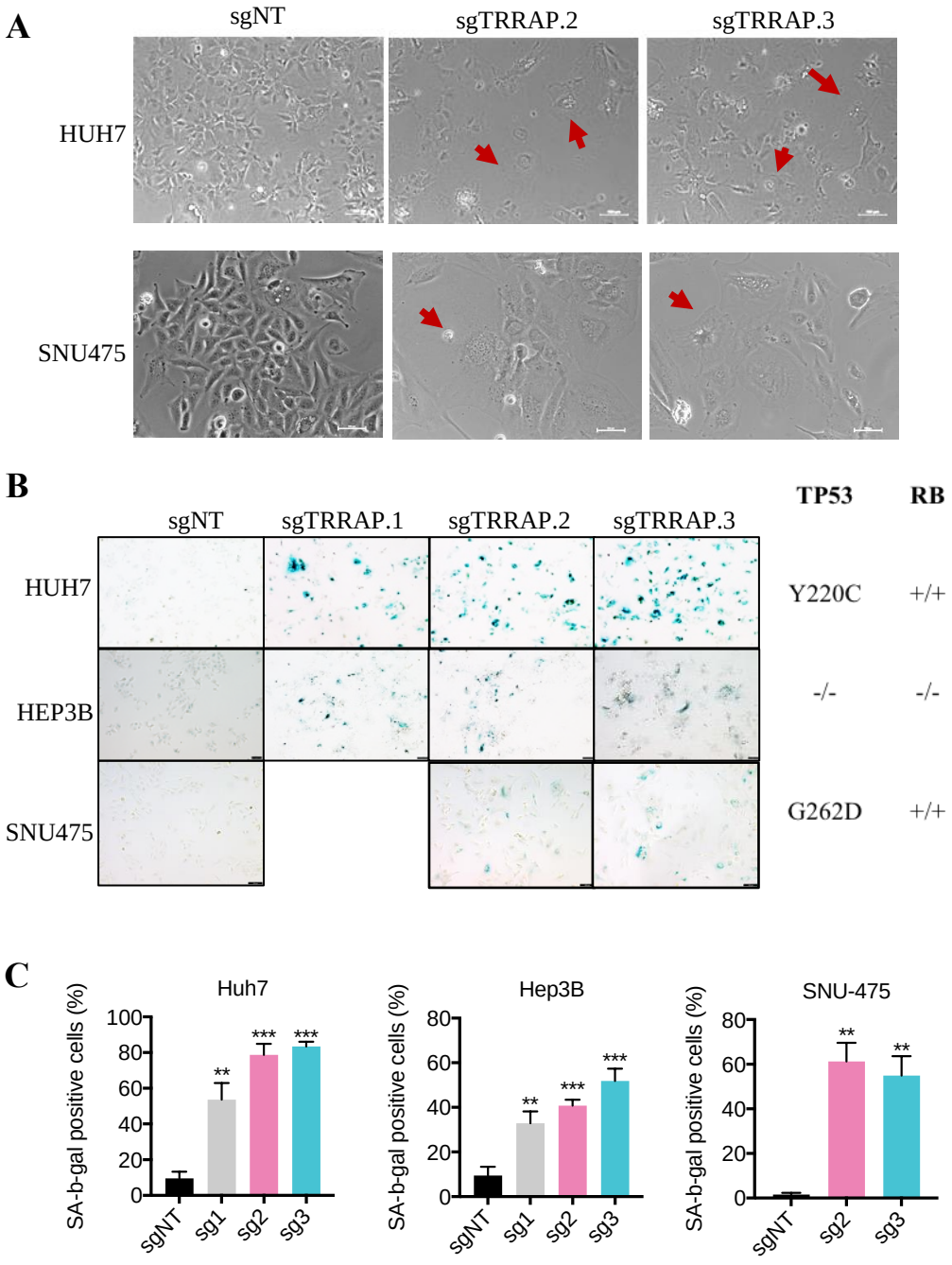

Figure 15. Loss of TRRAP induces senescence in HCC cells.
A) 10x Phase images of TRRAP depleted HUH7 and SNU-475 cells depicting senescent cells (red arrowhead). **B)** SA-β-gal staining of TRRAP depleted HUH7, SNU-475 and HEP3B cells with corresponding mutations in TP53 and RB. **C)** Quantification of SA-β-

gal shown in B. Data was presented as mean ± SD; p-values were calculated by comparing to sgNT, *p < 0.05, **p < 0.01, ***p < 0.001 (student's t test).

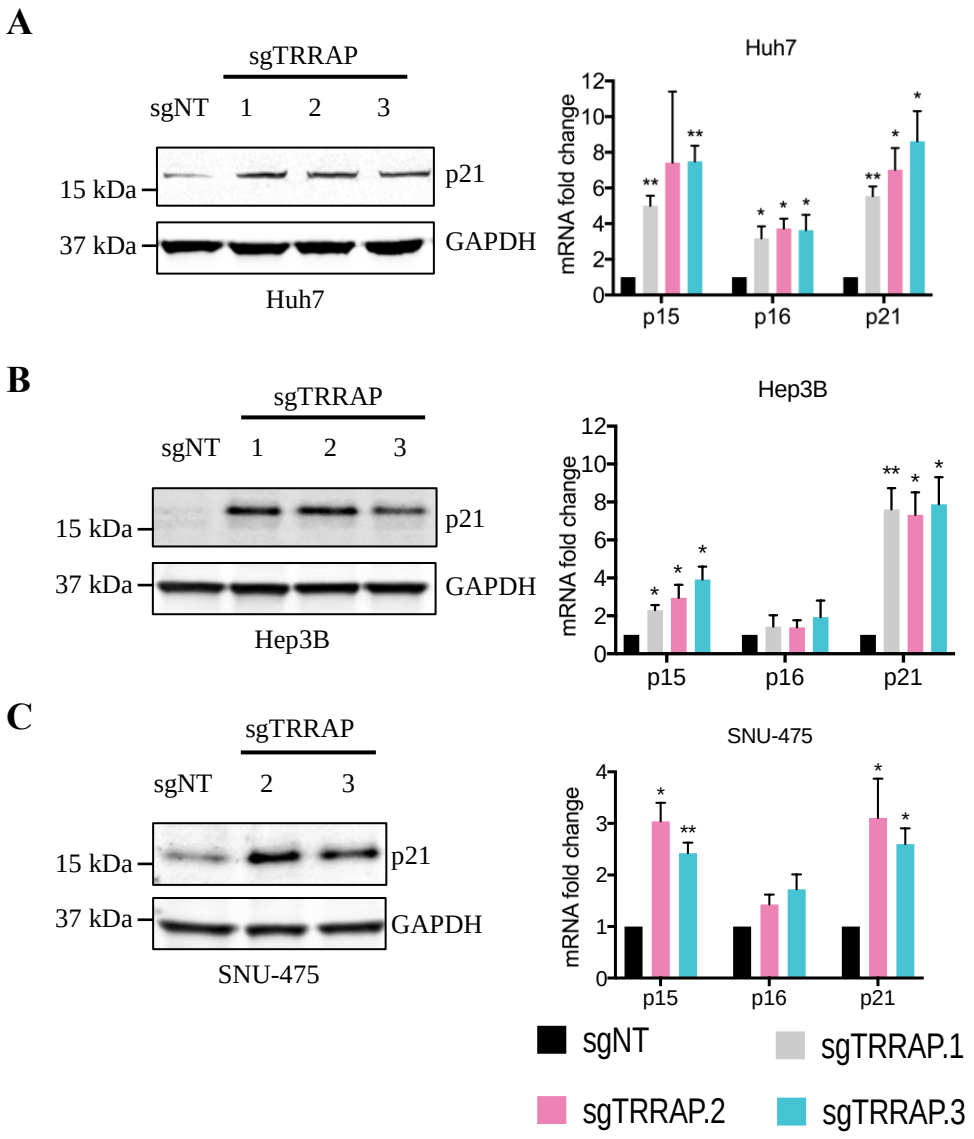

Figure 16. Loss of TRRAP results in elevation of senescence markers in HCC cells. P21 protein expression in **(A)** Huh7, **(B)** Hep3B, and **(C)** SNU-475 cells infected with non-target (sgNT) and 3 individual TRRAP sgRNAs (sgTRRAP) and mRNA levels of p15, p16, and p21 in the corresponding TRRAP depleted cells lines as measured by qRT-PCR and normalized to sgNT cells. GAPDH was used as a loading control for western blots. Data was presented as mean ± SD; p-values were calculated by comparing to sgNT, *$p < 0.05$, **$p < 0.01$, ***$p < 0.001$ (student's t test).

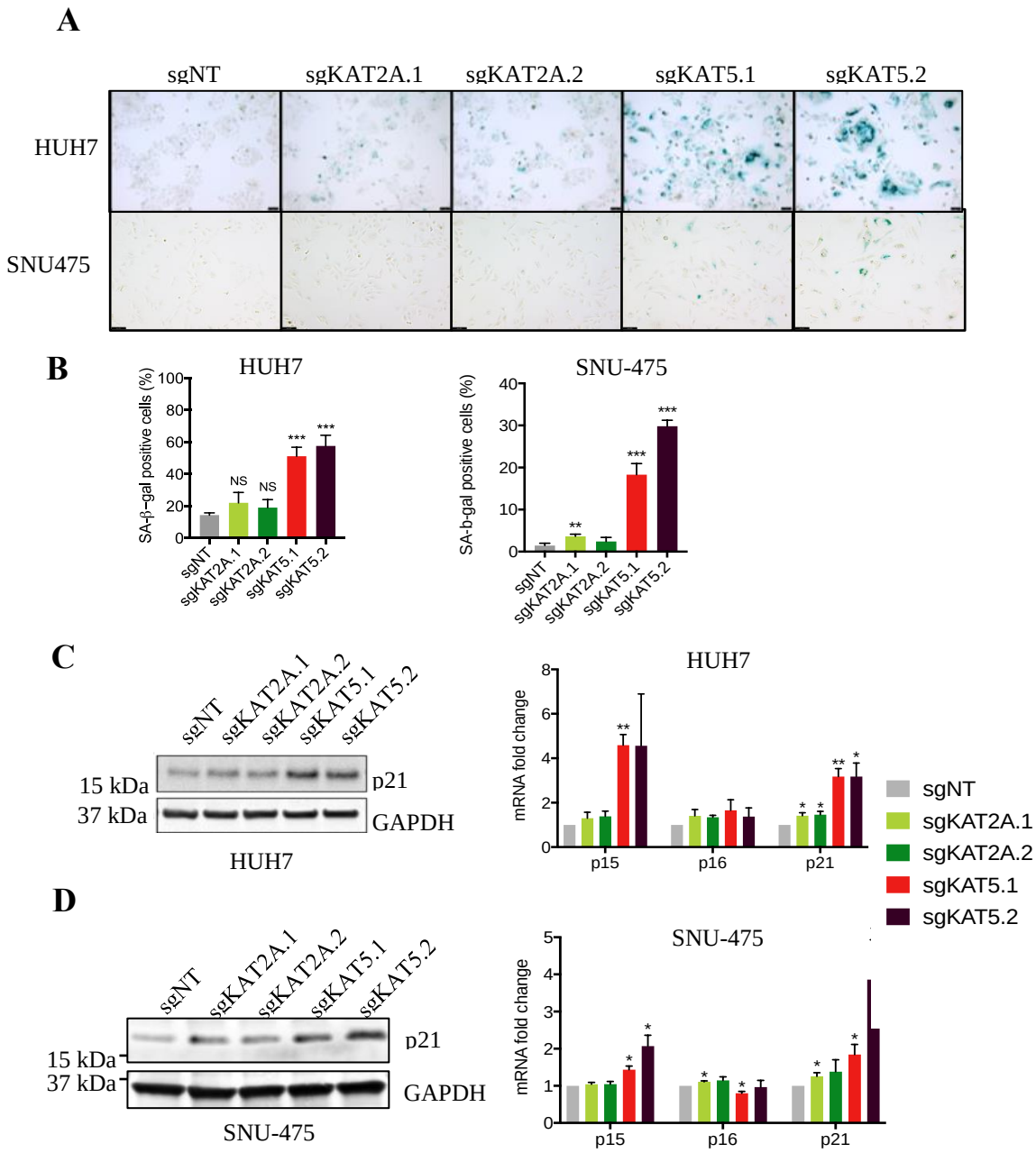

Figure 17. Loss of KAT5 and not KAT2A results in senescence in HCC cells. **A)** SA-β-gal staining of KAT2A and KAT5 depleted HUH7 and SNU-475 cells. **B)** Quantification of SA-β-gal shown in A. **C)** P21 protein expression in HUH7 and **D)** SNU-475 cells infected with sgNT and sgKAT2A and sgKAT5 and mRNA levels of p15, p16, and p21 in the corresponding cells lines as measured by qRT-PCR and normalized to sgNT cells. GAPDH was used as a loading control. Data was presented as mean ± SD;

p-values were calculated by comparing to sgNT, *p < 0.05, **p < 0.01, ***p < 0.001 (student's t test).

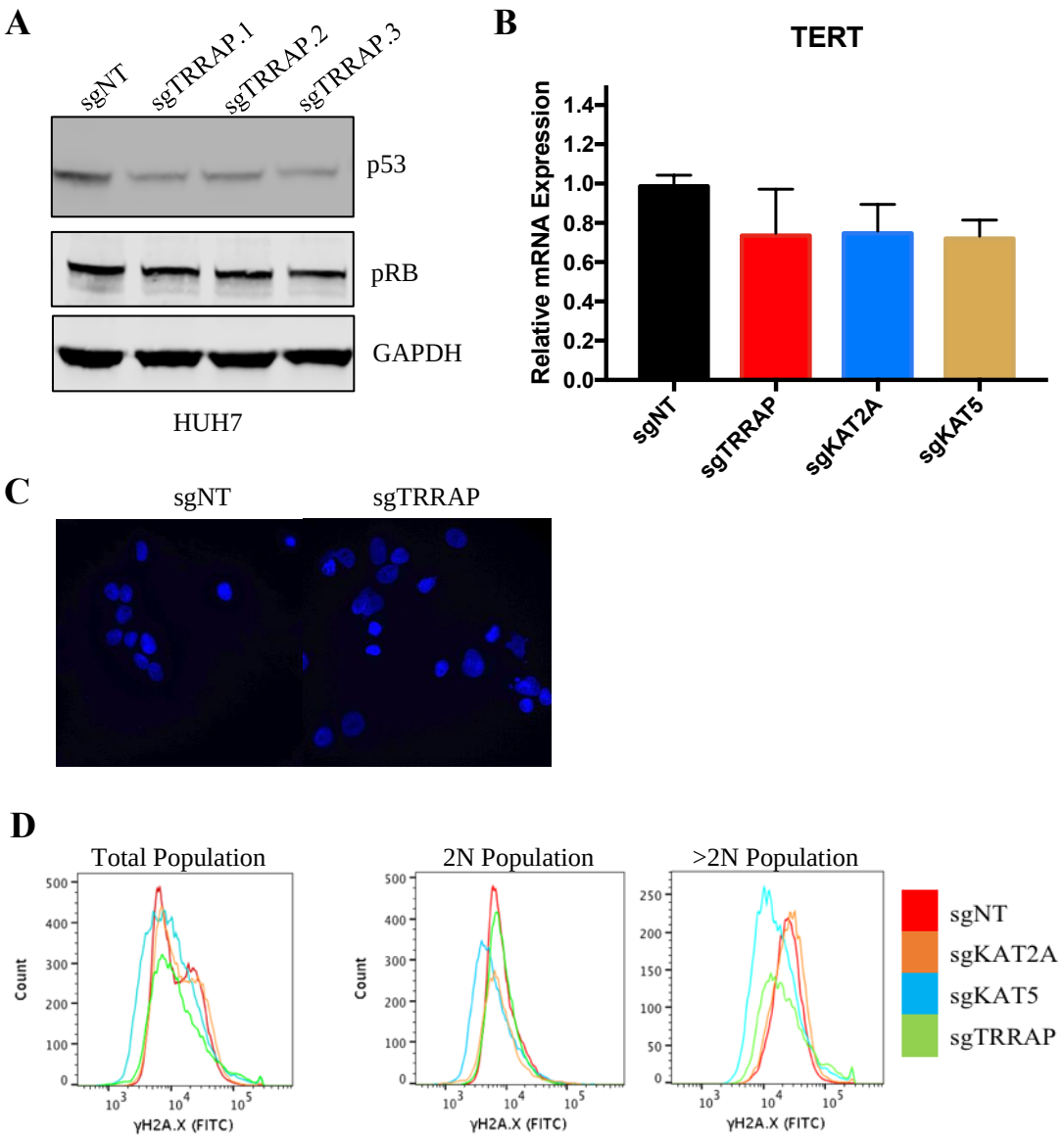

Figure 18. TRRAP/KAT5 loss induced senescence is independent of canonical mediators of senescence.
A) Protein expression of P21 and Phospho Rb in HUH7 cells infected with three individual TRRAP sgRNAs. GAPDH was used as a loading control. **B)** mRNA levels of TERT in HUH7 cells infected with sgNT, sgTRRAP, sgKAT2A and sgKAT5. **C)** DAPI staining of HUH7 cells infected with sgNT and sgTRRAP. **D)** Flow cytometry analysis of DNA damage in Huh7 cells using γH2A.X in the total cell population, 2N and >2N populations. DNA content was determined using PI staining.

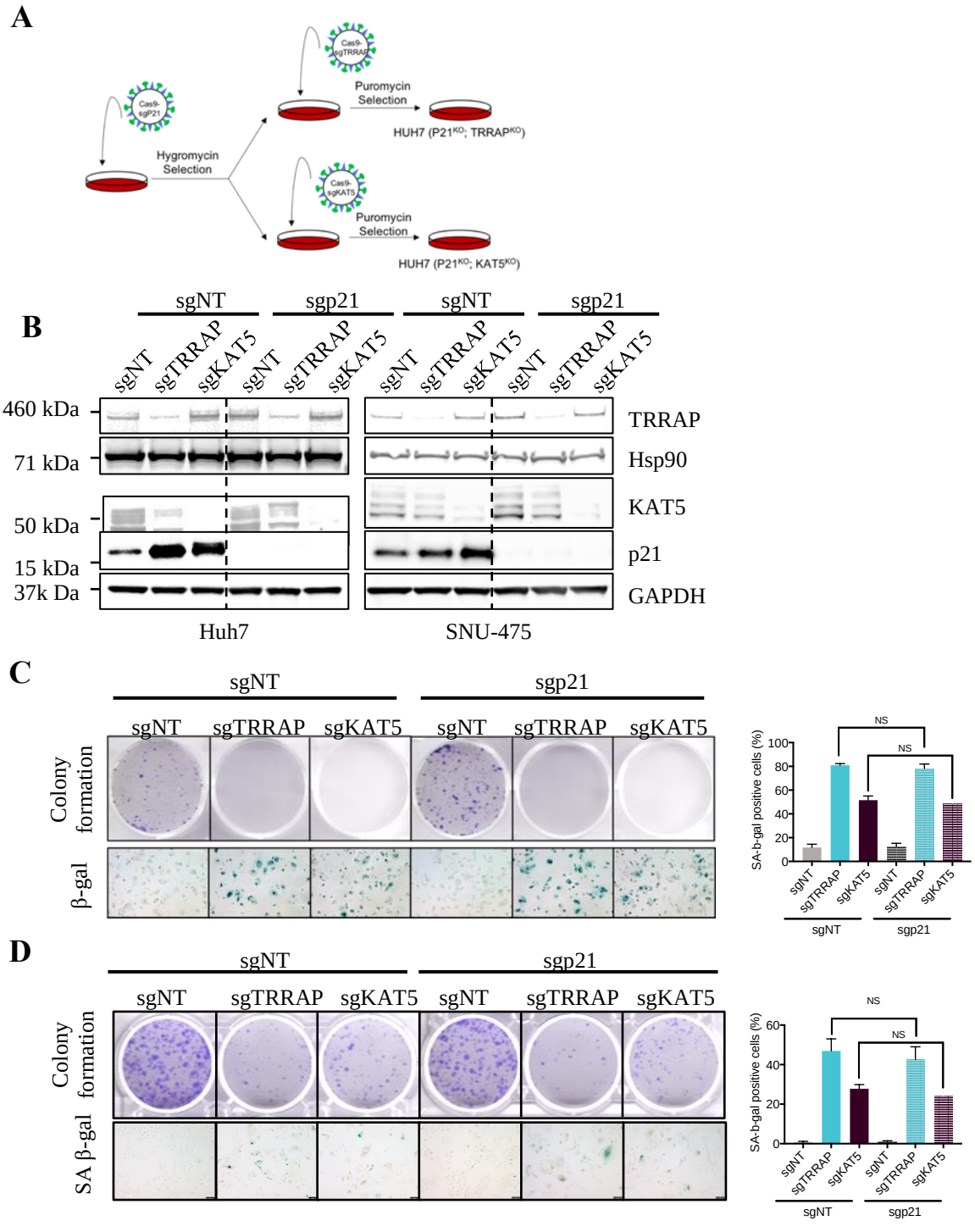

Figure 19. TRRAP and KAT5 depletion induced senescence is independent of P21.

A) Schematic illustrating generation of p21 and TRRAP/KAT5 double knockout cells using CRISPR. **B)** Western blot analysis of TRRAP, KAT5 and p21 levels in Huh7 and SNU-475 cells infected with the indicated sgRNAs. HSP90 and GAPDH were used as a loading control. **C)** Colony formation and SA-β-gal staining of Huh7 cells infected with the indicated sgRNAs. NS = not significant (student's t test). **D)** Colony formation and SA-β-gal staining of SNU-475 cells infected with the indicated sgRNAs. NS = not significant (student's t test).

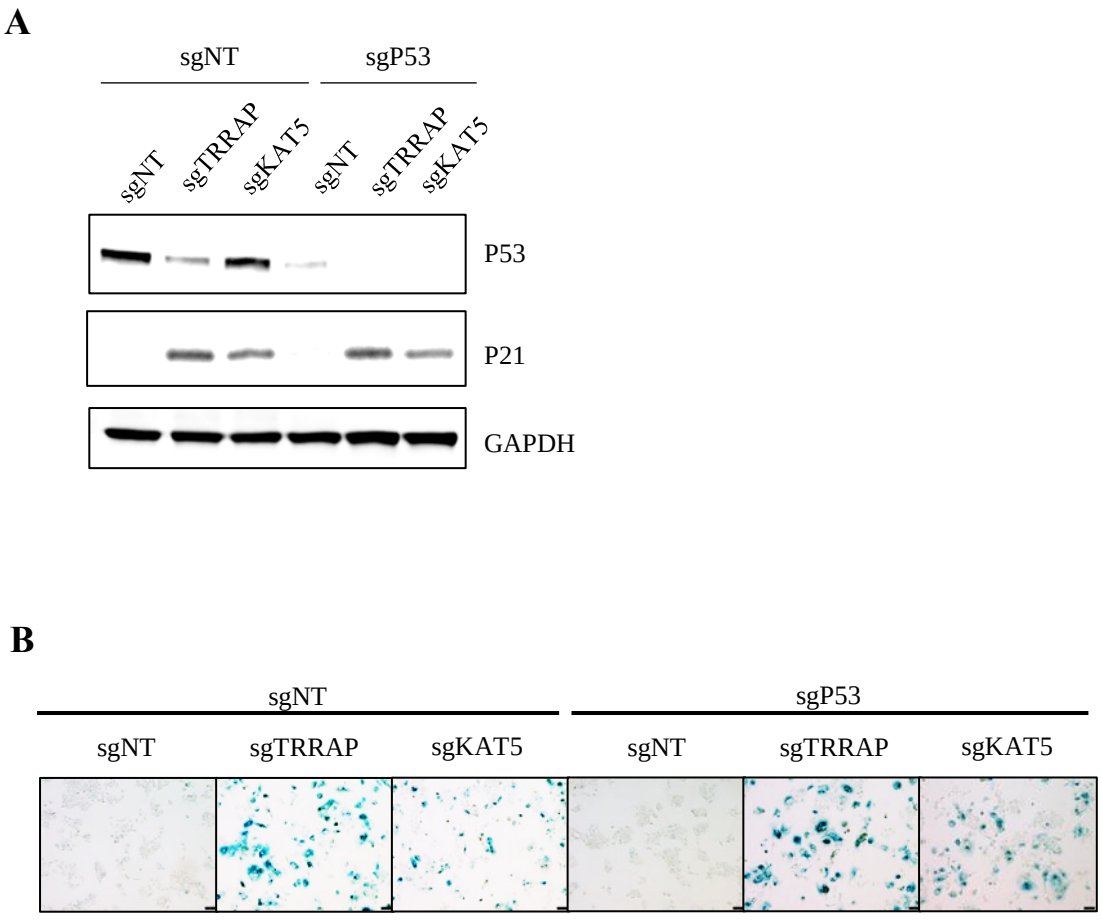

Figure 20. TRRAP and KAT5 depletion induced senescence is independent of P53. **A)** Western blot analysis of TRRAP, KAT5 and P53 levels in Huh7 cells infected with the indicated sgRNAs. GAPDH was used as a loading control.**B)** SA-β-gal staining of Huh7 cells infected with the indicated sgRNAs.

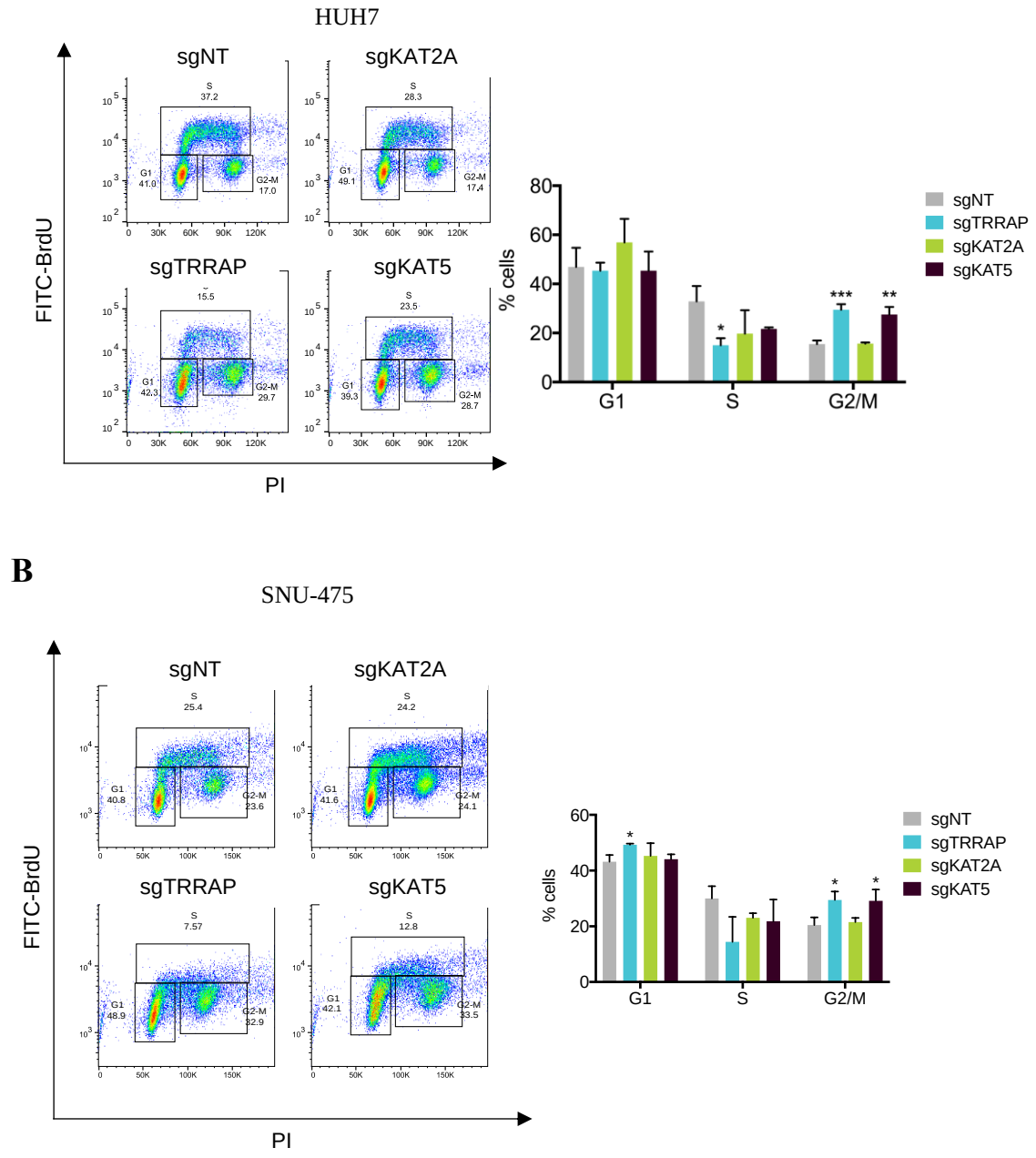

Figure 21. TRRAP and KAT5 depletion induces senescence during G2/M.
A) Cell cycle analysis of Huh7 cells and **B)** SNU-475 cells infected with the indicated sgRNAs by BrdU and PI staining. Representative data (left) and quantification (right) are

shown here. Data was presented as mean ± SD; p-values were calculated by comparing to non-targeting control, *$p < 0.05$, **$p < 0.01$, ***$p < 0.001$ (student's t test).

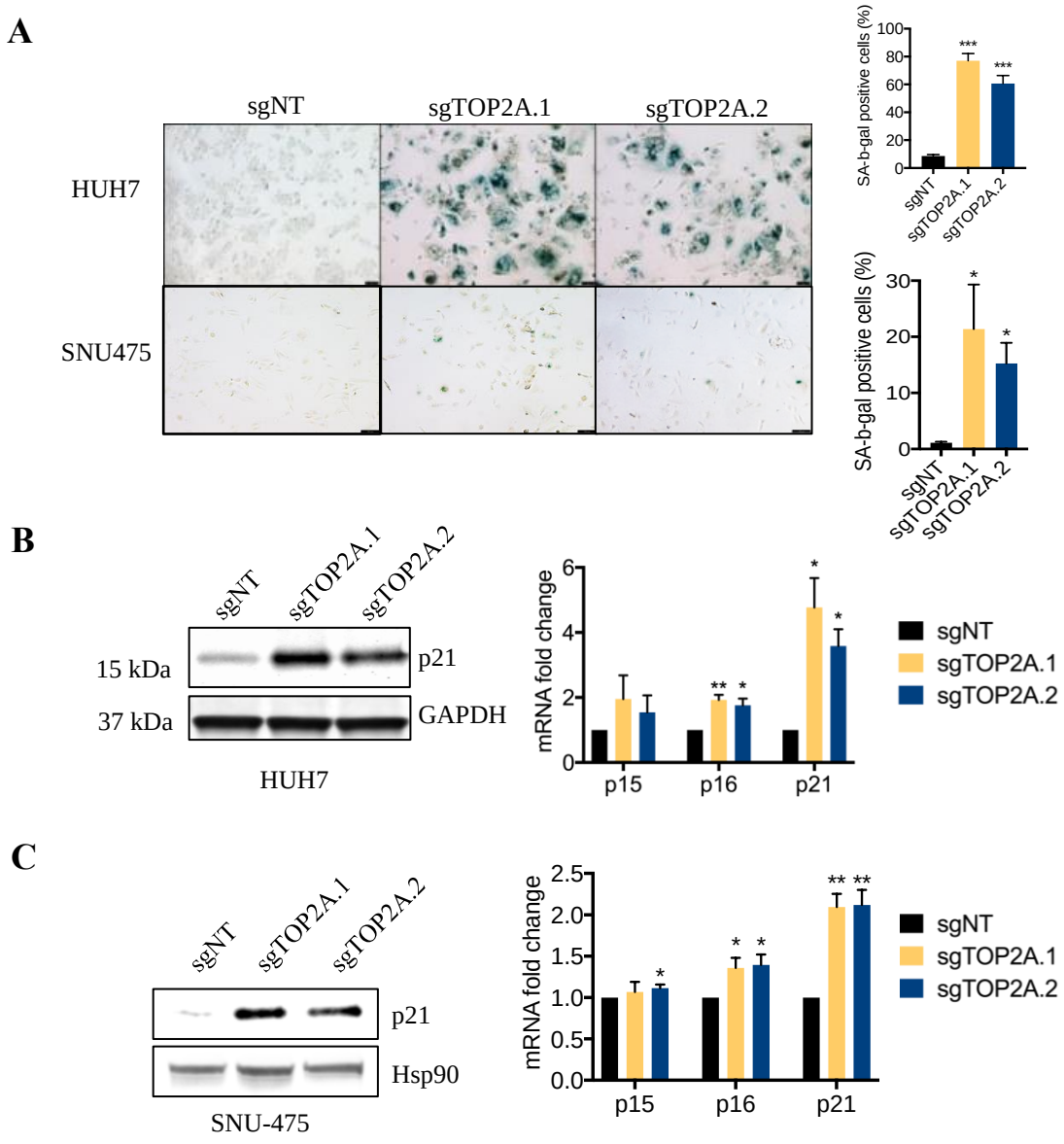

Figure 22. Loss of TOP2A induces senescence in HCC cells.
A) SA-β-gal staining of Huh7 and SNU-475 cells infected with sgTOP2A with quantification of positive cells. **B)** P21 protein expression in Huh7 cells infected with the indicated sgRNAs and mRNA levels of senescence markers p15, p16, and p21 in Huh7 cells infected with sgTOP2A. GAPDH was used as a loading control. **C)** P21 protein expression in SNU-475 cells infected with sgNT and sgKAT2A and sgKAT5 and mRNA levels of p15, p16, and p21 in the corresponding cells lines as measured by qRT-PCR and normalized to sgNT cells. HSP90 was used as a loading control. Data was presented as

mean ± SD; p-values were calculated by comparing to non-targeting control, *p < 0.05, **p < 0.01, ***p < 0.001 (student's t test).

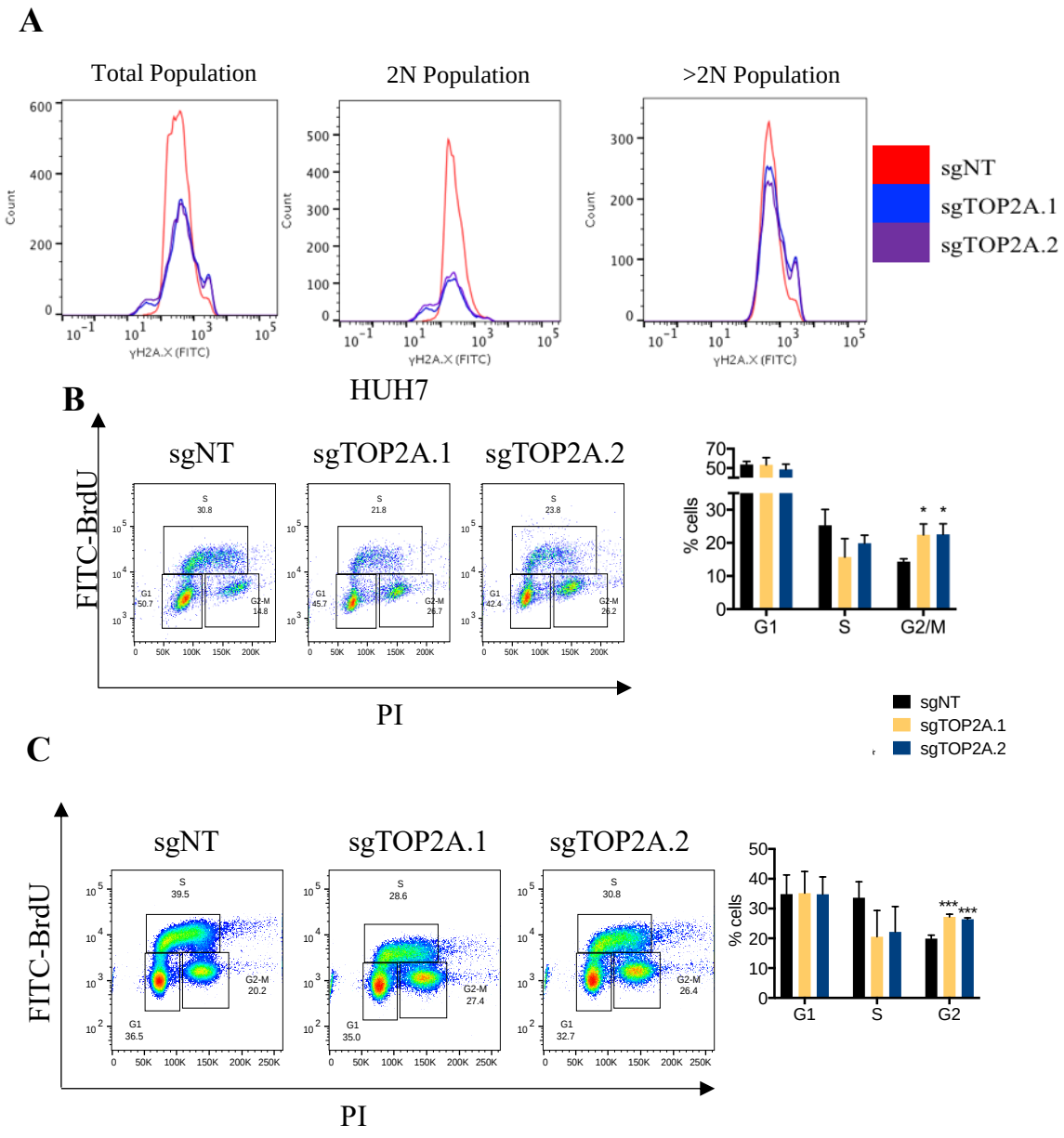

Figure 23. Loss of TOP2A arrests cells in G2/M independent of DNA damage. **A)** Flow cytometry analysis of DNA damage in Huh7 cells using γH2A.X in the total cell population, 2N and >2N populations after infection with the indicated sgRNAs. DNA content was determined using PI staining**. B)** Cell cycle analysis of Huh7 cells infected with the indicated sgRNAs. Representative data (left) and quantification (right) are

shown here. **C)** Cell cycle analysis of SNU-475 cells infected with the indicated sgRNAs. Representative data (left) and quantification (right) are shown here.

sgRNA name	Sequence (5'-3')
sgTRRAP.1	ACTCCTGATACAAGAGATCG
sgTRRAP.2	CTTGATCCGCCACTATACGA
sgTRRAP.3	CCACTGGGGATCGTTCAGTG
sgKAT2A.1	GCTGCTGGAAAAGTTCCGAG
sgKAT2A.2	TCACCATGCCACCCTCAGAG
sgKAT5.1	GATTGATGGACGTAAGAACA
sgKAT5.2	ACCAGGCTGCCAGTCATGCG
sgp21	GTCACCGAGACACCACTGGA
sgTOP2A.1	TGTACGCTTATCCTGACTGA
sgTOP2A.2	GATGCTGCTATCAGCCTGGT
sgP53	AGCGCTGCTCAGATAGCGA

Table 8 List of sgRNAs sequences used in Chapter III.

Primer name	**Sequence (5'-3')**
p15-F	AAGCTGAGCCCAGGTCTCCTA
p15-R	CCACCGTTGGCCGTAAACT
p16-F	CCCAACGCACCGAATAGTTA
p16-R	ACCAGCGTGTCCAGGAAG
p21-F	CAGCAGAGGAAGACCATGTG
p21-R	GAGGCACAAGGGTACAAGACA
GAPDH-F	CTGGGCTACACTGAGCACC
GAPDH-R	AAGTGGTCGTTGAGGGCAATG

Table 9 Primers used for qRT-PCR in Chapter III.

CHAPTER IV

Discussion

Overview of key findings and model

Hepatocellular carcinoma (HCC) is an aggressive subtype of liver cancer with few effective treatments as the underlying mechanisms that drive HCC pathogenesis remain poorly characterized. Identifying genes and pathways essential for HCC cell growth will aid the development of new targeted therapies for HCC. Using a kinome CRISPR screen in three human HCC cell lines, we identified transformation/transcription domain-associated protein (TRRAP) as an essential gene for HCC cell proliferation.

TRRAP has been implicated in oncogenic transformation, but how it functions in cancer cell proliferation is not established. Here, we show that depletion of TRRAP or its co-factor KAT5, inhibits HCC cell growth in vitro and in-vivo as tumor xenografts. Furthermore, using a genetically engineered mouse model, we demonstrated that TRRAP loss is correlated with loss of HCC tumor formation in vivo. Interestingly, we identify that loss of TRRAP results in loss of KAT5 protein while mRNA levels remain stable. Mechanistically we conclude that loss of KAT5 protein is not due to proteasome or lysosome mediated degradation suggesting that the KAT5 transcript is not being translated in the absence of TRRAP.

Integrating cancer genomics analyses using patient data and RNA-sequencing identified mitotic genes as key TRRAP/KAT5 targets in HCC. In line with this, cell cycle analyses revealed that TRRAP- and KAT5-depleted cells are arrested at G2/M phase. We

identify that TRRAP and KAT5 depletion results in induction of p53- and p21-independent senescence in the absence of DNA damage. Finally we identify TOP2A as a mitotic target gene of TRRAP/KAT5. Furthermore, depletion of TOP2A was sufficient to recapitulate the senescent phenotype of TRRAP/KAT5 knockdown.

Our results uncover a role for TRRAP/KAT5 in promoting HCC cell proliferation via activation of mitotic genes. Furthermore, the work in this thesis suggests that targeting the TRRAP/KAT5 complex is a potential therapeutic strategy for HCC (Figure 4.1).

The role of TRRAP in HCC development

The work in this thesis is one of the first to report a role for TRRAP in HCC. As an essential component of HAT cofactor complexes, TRRAP can exert its effects on the cell through transcriptional regulation of key programs. One of the first studies to characterize TRRAP driven transcriptional programs through microarrays demonstrated that *Trrap* loss in mouse embryonic fibroblasts (MEFs) resulted in decreased expression of programs related to transcription, protein turnover, cytoskeleton and cellular adhesion and cell cycle progression (130). ChIP based validation of some of these targets, like Cyclin A, attributed the decrease in expression to decreased histone acetylation. Interestingly after *Trrap* loss, MEFs had increased expression of programs related to protein turnover and metabolism suggesting that TRRAP binding to these loci may also play a repressive role. The authors did not directly address the significance of TRRAP

repressed genes in this study. Moreover, later studies also demonstrated that members of the MYST family, like KAT5, can also repress gene expression (146).

TRRAP's regulation of cell cycle genes warranted further investigation as this was the largest subset of genes that were depleted upon TRRAP depletion. A study demonstrated that *Trrap* loss led to chromosome missegregation and failure to induce expression of the checkpoint proteins Mad1 and Mad2 secondary to loss of Kat5 mediated epigenetic acetylation in MEFs (129). However, in that study, *Trrap*-deficient MEFs entered mitosis and initiated mitotic exit at similar kinetics as *Trrap*-containing MEFs and Kat5 protein levels were similar between *Trrap*-deficient and *Trrap*-containing cells suggesting that TRRAP targets in MEFs may differ from HCC.

Genome wide unbiased characterization of TRRAP programs in malignancies is currently lacking in the field. TRRAP has been implicated in multiple malignancies such as GBM and ovarian cancers in which it can drive differentiation of tumor initiating stem cells (194, 264). The work in this thesis is one of the first to characterize TRRAP regulated programs in HCC. Like the microarray study done by Herceg et al. (130), we identified similar transcriptional programs that were depleted upon TRRAP loss in HCC cells such as those responsible for cell cycle progression, chromosome segregation and cytokinesis. However, further transcriptome analysis of TRRAP depleted HCC cells also identified a subset of genes responsible for chromosomal instability. Previous studies have demonstrated that YAP1 and FOXM1 can drive expression of a chromosomal instability signature in HCC that correlates with survival in patients (206). Work in this

thesis suggests that TRRAP and KAT5 can also drive expression of a subset of the genes in this signature in both HCC cell lines and patient HCC samples.

Moreover, we also identified metabolism and extracellular matrix transcriptional signatures that were upregulated upon TRRAP loss. Studies investigating the direct relationship between TRRAP and cellular metabolism are limited. Furthermore given that TRRAP can bind and stabilize the transcription factor MYC, one of the major regulators of cellular metabolism (265), it would not be surprising that TRRAP can influence metabolic pathways. Interestingly, in this thesis we identify a subset of metabolism related genes normally inhibited by TRRAP that are liver specific. Furthermore, increased expression of these genes correlated with more favorable prognosis in patients. However future studies need to validate the consequences of TRRAP regulated metabolism genes in HCC models. Taken together, transcriptional programs regulated by TRRAP between MEFs and HCC is relatively conserved.

From the work in this thesis, we can begin to speculate the role of the TRRAP/KAT5 as an oncogene in HCC from its epigenetic functions. We demonstrate that TRRAP drives expression of a genetic signature responsible for mitotic progression. Overall aberrant mitotic activation and G2/M checkpoint dysregulation can result in chromosomal instability (37). Since chromosomal instability is a mediator of transformation in HCC (6) and hepatocytes suppress their normal functions as they transform into HCC (207), we can suggest that TRRAP overexpression can drive transformation of hepatocytes by inducing expression of this chromosomal instability signature thereby promoting aberrant mitosis and repressing genes required for normal

hepatocyte functions, such as those required for bile acid metabolism. However future studies examining the effect of TRRAP overexpression in hepatocytes are needed in order to test this hypothesis.

TRRAP is a large scaffold protein and serves as a binding partner for the HATs KAT5 and KAT2A. However TRRAP can also bind non HAT proteins such as MYC, ATM, E2F1 and P53 through its FATC and HEAT domains (118). Deletion of these domains in yeast does have deleterious effects on cell viability suggesting that TRRAP's interactions with non-HAT proteins and non-histone targets is also important for its function.

The MYC protein consists of six regions, termed MYC homology boxes (MB). Early studies demonstrated that TRRAP's interaction with MYC and E2F is required for transformation by both proteins (117, 144). Furthermore, a more recent study demonstrated that MBII, specifically, mediates interaction with TRRAP and is required for transformation (193). Moreover loss of TRRAP in hematopoietic stem cells led to a decrease in MYC protein levels indicating that TRRAP stabilized MYC in this cell population (266). In a mouse model of HCC, MYC depletion led to cellular differentiation (267). In this study the authors demonstrated that the surviving cells showed stem cell properties and had differentiated into normal hepatocytes. The potential MYC-TRRAP interaction is another avenue via which MYC can be drugged. However, future studies are required to validate, firstly, whether this interaction in HCC patient samples and HCC models exist and, secondly, the consequences of this interaction.

Studies in lymphoma models demonstrate that TRRAP can bind mutant P53 through its N-terminal HEAT domains. Silencing TRRAP in these models reduces protein pools of mutant P53 via MDM2 mediated degradation. This suggests that TRRAP binds p53 in order to shield it from degradation machinery (195). In this thesis we also identify that loss of TRRAP results in decreased expression of P53 in mutant P53 HCC cell lines. Taken together the data suggests that TRRAP is also protecting cellular pools of mutant P53 from degradation. However, this hypothesis would need to be tested in future studies comparing the effects of TRRAP loss on P53 protein levels in WT and mutant P53 HCC cell lines.

Overall, studies investigating TRRAP binding partners in liver biology and HCC are limited. One study showed in an HCC cell line that TRRAP can activate nuclear receptors such as liver X receptors (LXR), Farnesoid X receptor (FXR), and Peroxisome proliferator-activated receptors (PPARs) and regulate lipid metabolism, bile acid synthesis and glucose metabolism (268). However, identification of additional TRRAP binding partners and validation of previously identified binding partners such as MYC and P53 in HCC is required as such studies would identify additional potential therapeutic vulnerabilities.

Translational Implications in HCC

The purpose of the work in this thesis was to utilize a kinome wide CRISPR screen to identify therapeutic vulnerabilities in HCC that were independent of P53 status. Our screen identified TRRAP as a potential therapeutic target and our mechanism studies

elucidated that TRRAP's proliferative effect was mediated by KAT5. TRRAP is pseudokinase and member of the PI3K family of kinases. Like all PI3K family members, TRRAP contains a PI3K domain however, the specific residues mediating phosphate transfer are absent (117). Biochemical and functional assays demonstrate that TRRAP contains no catalytic activity of its own (125). However, studies have elucidated that TRRAP functions as a scaffold protein which binds and stabilizes other proteins. In line with this, sequence analyses have demonstrated that TRRAP contains multiple HEAT domains that mediate interactions with binding partners such as Myc and P53. TRRAP also contains a FATC domain which mediates its interaction with HAT cofactors as well as ATM. Due to the fact that TRRAP contains no catalytic activity of its own, there are currently no small molecule inhibitors available that can successfully target and inhibit TRRAP. However, given the essential functions of TRRAP in driving tumorigenesis identified in this thesis for HCC and in other cancers it is important to evaluate the potential therapeutic strategies that can be utilized to target this protein.

It is important to note that the crystal structure for Tra1, the yeast homolog of TRRAP, in both the SAGA complex and NuA4 complex has been solved within the last 3 years (226, 269, 270). Therefore, it may be possible to utilize this structural information to target and disrupt the interaction between TRRAP and KAT5 as a therapeutic strategy. Furthermore, advances in siRNA-based therapeutics now enables efficient silencing in vivo after one dose (271). In line with this, siRNA based therapies against the *MYC* oncogene and *Plk1* are currently in Phase 1 clinical trials for HCC (272). However it

would be imperative to assess the effects of TRRAP inhibition in normal hepatocytes to gain insight into the potential toxicities associated with “drugging” TRRAP.

In addition to identifying TRRAP as a therapeutic target, the work in this thesis also suggests that KAT5 depletion can phenocopy TRRAP loss. Moreover, small molecules that inhibit KAT5 are currently in development. Anacardic acid and its analogs have similar chemical structures to Acetyl CoA and therefore block the acetyl coA binding site of KAT5. Indeed, treatment with Anacardic acid inhibited KAT5 dependent acetylation and activation of ATM in HeLa cells and also sensitized the cells to radiation induced DNA damage (273). Moreover, treatment of HeLa cells with pentamidine, another Acetyl CoA mimic, also inhibited KAT5 activity and sensitized cells to radiation induced DNA damage (274). However, both these compounds were used at relatively high concentrations (>100μM) to elicit this response, suggesting that their in-vivo efficacies would be low. Furthermore, given that these compounds are Acetyl CoA mimics, it is possible they would bind to and inhibit the activity of other HATs such as KAT2A and P300 and lead to detrimental off target effects and toxicities.

Screening of small molecule inhibitors identified NU9056 as a drug that inhibited KAT5 function (275). In vitro studies demonstrated that NU9056 had an IC50 of 2.5μM and was 16.5, 29 and 50-fold more selective for KAT5 at this concentration than PCAF, P300 and KAT2A respectively. Treatment with NU9056 prevented acetylation of both histone and non-histone targets. Moreover, functionally, NU9056 treatment induced P21 expression and apoptosis in prostate cancer cell lines.

More recently, a group took advantage of the crystal structure of KAT5 and designed a small molecule, TH1834, which selectively bound the active site of KAT5 (227). In this study treatment with TH1834 induced apoptosis in MCF-7 cells, a HER2 negative breast cancer cell line, but did not affect viability of MCF-10 cells, a normal breast epithelial cell line. Furthermore, the authors demonstrated that the drug was selective for KAT5 as acetylation of the H4K16 residue, a target of the HAT MOF, was not impacted (227). However, the authors used a dose of 500uM in all of these studies suggesting that the drug may not show efficacy in vivo. Taken together, multiple attempts have been made to design small molecules that target the catalytic activity of KAT5. In vitro NU9056 and TH1834 demonstrate efficacy in prostate and HER2 negative breast cancer cell lines respectively however the efficacy of these compounds in HCCs remains to be tested.

Other HATs have also been successfully targeted using small molecule inhibitors. Of note Curcumin and Garcinol, both of which are p300 inhibitors demonstrated therapeutic efficacy in HCC cell lines in vitro (140). Furthermore inhibition of p300 with Curcumin induced senescence in SAOS-2 cells, an osteosarcoma cell line (253). KAT6 is often amplified in cancers (276) and functions to suppress senescence by repressing the p16 locus (277). In line with this, a group designed a small molecule inhibitor against KAT6A/B which decreased tumor progression by inducing senescence in a zebrafish model of HCC and in a mouse model of lymphoma (278).

The work in this thesis also identified that loss of TOP2A induces senescence in HCC models. Multiple attempts have been made in HCC patients to inhibit TOP2A using

drugs like doxorubicin and etoposide, however none have shown clinical efficacy through systemic delivery. However, delivery of Doxorubicin directly to tumors using transarterial chemoembolization has shown significant survival benefits in HCC with low toxicities (279) suggesting that failure of drugs like doxorubicin and etoposide is due to cytotoxicity secondary to off target effects. In line with this, studies have demonstrated that the cardiotoxicity commonly associated with Etoposide is due to inhibition of TOP2B, as TOP2A is not appreciably expressed in quiescent cells (280). Furthermore, in addition to inhibiting TOP2B (281), Doxorubicin has been demonstrated to dysregulate ceramide synthesis a mechanism potentially contributes to its toxicity (282).

Hence, there is a need to develop small molecule inhibitors that are selective for TOP2A. NK314 was one such compound that was developed that was highly selective against TOP2A (283). Moreover, in this study, the authors demonstrated that NK314 had greater anti-tumor activity and showed less toxicity towards cells that had low levels of expression of TOP2A compared to drugs like etoposide and doxorubicin. The antitumor effect of NK314 remains to be tested in HCC, however its development serves as evidence that designing inhibitors specific to TOP2A can revitalize TOP2A as a viable therapeutic target.

Study Caveats

Using CRISPR based screening and passaging cells for 10 passages we were able to identify kinases that were mediators of proliferations in HCC. However, our screen also identified key kinases that are responsible for proliferation in normal cells- these

include BUB1, AURKA, and PGK1. Thus, one caveat to this study was the fact that the screen also identified kinases that are responsible for proliferation in normal cells. Future studies can circumvent this and allow for stratification of kinases that are cancer specific by performing this screen in tandem with a normal immortalized hepatocyte cell line such as THLE-2. Furthermore, the hits of our screen are kinases that are implicated in proliferation, future studies can screen for kinases that can aid in other processes which can be therapeutically targeted including metabolism and autophagy.

Another caveat to the study arises from the nature of generating CRISPR knockouts. Due to the antiproliferative nature of the phenotype we were unable to generate knockouts that arise from a single clone. After the generation of a DSB at the desired genomic loci, the cells undergo NHEJ based DNA repair. The result is the generation of an indel that could be ±1, ±2 or ±3 nucleotides (89). Consequently, the knockouts generated in this study were comprised of a genetically polyclonal population with varying indels and, consequently, varying degrees of knockout at the single cell level. In line with this, we demonstrated via western blotting that the population as a whole had depleted levels of the target protein thereby providing credence to the conclusions made in this study. Furthermore, we were successfully able to validate the conclusions from our study using two different sgRNAs as well as sh- and siRNA-based knockdown therefore suggesting that our senescence phenotypes were due to gene specific knockdown.

The generation of a doxycycline inducible shRNA model of TRRAP loss would aid in circumventing this caveat as we could perform more mechanistic studies and

validate the conclusions from the current study using a monoclonal population. Alternatively, the relationship between TRRAP and KAT5 levels and TOP2A levels can be performed at the single cell level in our polyclonal population using immunofluorescence to further validate these relationships.

Additionally, the data suggesting that TRRAP loss induced senescence is mediated by KAT5 and TOP2A is correlative as we were unable to overexpress KAT5 and TOP2A in TRRAP depleted cells to determine if this would rescue TRRAP induced senescence. Given that TRRAP and KAT5 regulates a *network* of genes responsible for mitotic progression I would expect that overexpression of a single gene would not rescue the senescence phenotype, however this would need to be investigated by future experiments.

Outcomes of cell cycle arrest

As discussed earlier, cell cycle progression can be impeded due to a variety of toxic insults such as withdrawal of mitogenic factors, DNA damage, nucleotide deprivation and chemotherapeutics. However, the consequences after arrest are variable from cell to cell. The two major outcomes are senescence or cell death but how a cell decides to senesce or die remains relatively unknown. The emerging molecular pathways implicated in this fate decision are the P53-P21 axis, signaling through the PTEN-AKT-mTOR pathway and the degree of molecular damage (284).

The P53-P21 pathway is considered to control the balance between pro-apoptotic and pro-senescent pathways. p53 is a transcription factor and can activate hundreds of

genes in response to a large number of stress signals, including those that regulate cell cycle progression. An early study examined the balance of the p53 and p21 axis in regulating the decision to senesce or undergo apoptosis (285). In this previous study, the authors treated IMR-90 fibroblasts with H_2O_2 and noted a fraction of the cells had detached. Analysis of the detached cells revealed caspase-3 activation and typical morphological changes associated with apoptosis whereas the adherent cells were growth arrested during G1 and had elevated expression of p21. Interestingly, the authors observed greater induction of p53 in the detached cells compared to the adherent cells. Furthermore, depletion of p53 in this study decreased the activation of caspase-3 and decreased the proportion of apoptotic cells suggesting that expression levels of p53 can control the decision to undergo senescence or apoptosis (285). Recently, studies demonstrated that the temporal dynamics of P53 expression can influence cell fate decisions. IR induces P53 protein levels to appear in pulses and thereby allows for repair of damage without interruption in cell cycle progression. However, studies demonstrated that if this "pulse-like" expression pattern is pharmacologically altered such that P53 protein levels are sustained, the cells are unable to progress through the cell cycle and will senesce (286). Other studies examining cell fate at the single cell level demonstrate that the decision to die or arrest is not determined by a fixed threshold of p53 expression but rather depends on the time and levels of P53 as the threshold level of P53 to induce apoptosis increases with time due to induction of anti-apoptotic factors (287).

In addition to expression level, post translation acetylation can also control P53's ability to regulate cell fate decisions (284). P53 has two key residues that can be

acetylated, K120 and K164. Studies have shown that K120 is acetylated by KAT5 whereas K164 is acetylated by P300 (237, 288). K117 is the mouse analog of K120 in humans. Studies demonstrated that cells in mice with a K117R mutation in P53, could not initiate apoptosis in response to DNA damage as they were not able to induce expression of *puma* and initiate caspase activation (289). However, in this study, cells from these mutant mice were able to undergo senescence to the same extent as WT mice in response to doxorubicin suggesting that acetylation of K117 is required to initiate apoptosis. However MEFs isolated from mice harboring mutations in both acetylation residues were unable to senesce or undergo apoptosis in response to toxic stimuli (289) suggesting that acetylation of the K164 residue by P300, was responsible for activation of a senescence program.

Another study demonstrated that quaternary structure of P53 was important for the ability of P53 to activate apoptotic programs. Mutating a residue within P53 that was responsible for P53 multimerization and cooperativity of DNA binding resulted in failure to initiate pro-apoptotic programs. However, expression of other P53 target genes in these mutants, such as those responsible for senescence remained unchanged, and the cells retained their ability senesce in response to toxic stimuli (290).

p21 is a major target of p53 and is responsible for initiating a pro-senescence program. In vitro studies demonstrated that treatment with low dose doxorubicin triggered senescence associated with p21 induction whereas high dose doxorubicin triggered apoptosis in the absence of p21 induction in HCC, breast and colorectal cancer models (284). Furthermore, ectopic expression of p21 was sufficient to induce

senescence in cancer cell lines with WT p53 and those with mutations and deletions in P53 (291, 292). Mechanistically, p21 must be localized in the nucleus in order to mediate its cell cycle arrest functions. In line with this, studies have demonstrated that AKT mediated phosphorylation of p21 induces retention of p21 in the cytoplasm and allows for cellular proliferation (293).

Traditionally senescence studies involved analysis of polyclonal populations of cells. These studies established that p21 expression was induced during the process of senescence induction (i.e. 2-3 days before cells exhibited the classical flattened morphology and stained positive for SA-β-Gal) and that "high levels" of P21 were required for induction of senescence as p21 knockout cells were unable to undergo senescence (294). Longitudinal analysis of p21 expression at the single cell resolution however demonstrated that expression of p21 immediately after senescence inducing treatment influenced cell fate (295). In this recent study, the authors demonstrated that expression of p21 immediately after treatment withdrawal (within 5 hours) led to proliferation whereas p21 expression 23-36 hours after treatment withdrawal resulted in senescence. Furthermore the authors demonstrated that the cells fated for proliferation had a transient "pulse" of p21 expression during drug treatment (295). Interestingly, these studies were conducted in WT P53 cells. The mechanisms that regulate these unique dynamics of P21 expression remain unknown and require investigation in future studies.

The effects and targets of p53 have been well established in regulating the cells decision to undergo apoptosis or senescence. PTEN is a tumor suppressor gene that suppress activity of AKT and mTOR, two kinases implicated in cell cycle progression.

Studies have demonstrated that loss of PTEN induces senescence in certain mouse models of cancer and human cancer cell lines, including HCC (296). Interestingly, studies have demonstrated that PTEN can also regulate the cell's decision to undergo apoptosis or senescence. Radiation induced DNA damage of glioma cells that were WT PTEN resulted in cellular senescence that was mediated by the P53-P21 axis whereas DNA damage of PTEN null cells underwent apoptosis (247). In line with PTEN suppression of AKT, mTOR inhibition prevents senescence in response DNA damage (297).

Finally, studies have implicated DNA damage as a factor controlling the cells decision to undergo apoptosis or senescence. Although the exact mechanism of how DNA damage can result in senescence or apoptosis is unclear. Leaders in the field speculate that there is a "threshold" of DNA damage that once reached tips the balance between apoptosis and senescence (298). However experimental evidence of this threshold is lacking. Moreover, a recent study demonstrated that the decision to senesce is not due to the amount of DNA damage but rather the cell's ability to discern between repairable and irreparable damage (262). In this previous study, the authors demonstrated that "difficult to repair breaks" were marked by dual RPA and 53BP1 positive foci. Moreover cells that contained dual positive foci were the ones that senesced. This work was done in immortalized fibroblasts with functional WT P53 and a conserved P53-P21 axis. Whether the same decision-making criteria holds true in cancer cells with aberrations in P53 requires further investigation.

The work in this thesis demonstrates that loss of TRRAP/KAT5 induces senescence in HCC by downregulation of genes responsible for mitotic progression. Interestingly the work on this thesis was done in mutant and p53 null HCC cell lines suggesting that the decision to senesce after TRRAP/KAT5 depletion was independent of p53. p53 independent mechanisms of cell fate remain largely unknown. One study demonstrated that in response to DNA damage NF-κB, activated by ATM and NEMO, can drive cellular programs that either activate a pro-inflammatory signature containing IL-8 or activates FADD mediated caspase 8 activation (299). In this study the authors speculated that the IL-8 proinflammatory signature was similar to the SASP however they did not directly test this hypothesis. Furthermore other studies have demonstrated that p53 independent induction of p21 expression is mediated by ATM as ATM signaling can *directly* induce p21 expression (300). Taken together the data suggests that TRRAP/KAT5 induced senescence may be mediated via ATM and NF-κB, however future studies are required to test this hypothesis.

Senescence during G2/M

Cell cycle analysis revealed that classical inducers of senescence such as RAS and telomere erosion arrested cells during G1 (151). Mechanistically, this was attributed to increased expression of P16 and P21 which inhibited phosphorylation of Rb thus blocking progression into S phase. Almost 25 years ago studies first described that cells could arrest during G2/M in response to DNA damage. The prevailing mechanism in the

field suggests that ATM/ATR activates CHK1/2 kinase that inhibits CDC25 phosphatase activity thereby inhibiting activation of Cyclin B1 and arresting cells in G2 (258).

Initial work from the Vogelstein group demonstrated that p21 could maintain G2/M arrest. The group demonstrated DNA damage did not induce arrest in p21 knockout HCT116 cells. Instead the cells underwent aberrant mitosis resulting in polyploidy and cell death (301). Later studies elucidated multiple mechanisms for the role of p21 in G2/M arrest. One group demonstrated that p21 induced senescence during G2 by prematurely activating the APC/C complex which resulted in degradation of Cyclin B1 and other drivers of mitosis (302). Other groups suggested that E2F also has targets that allow progression through G2/M. In line with this they demonstrated that, in addition to during G1, p21 can bind and inhibit Rb phosphorylation during G2 and inhibit activation of G2/M related targets of E2F (258).

The initial studies utilized DNA damage to induce G2/M arrest. Several recent studies have confirmed the mechanistic findings from above but have also identified new triggers for G2/M senescence in addition to DNA damage. One group identified that a population of cells that undergo replicative senescence can also arrest during G2. Notably these cells had elevated levels of Cyclin E and Cyclin D, while Cyclin B was undetectable (303). In line with replicative senescence occurring during G2, another study found that telomerase negative cells with eroded telomeres senesced during G2 (304). Taken together the studies suggest that telomere attrition will activate the G2/M checkpoint and trigger senescence. Finally, another group demonstrated that loss of chromatin acetylation reduced accessibility to the chromatin during replication and

induced G2/M arrest (253). Additional studies have identified other inducers of G2/M arrest with drugs such as Curcumin and Naphthylamide derivatives. Furthermore arrest was correlated with activation of the ATM/ATR network (258).

In addition to activation of ATM/ATR studies have demonstrated that Cyclin B dynamics can influence G2 arrest. Work by the Medema group demonstrated that the decision to arrest during G2 is dictated by the timing of Cyclin B1 translocation into the nucleus (261). In this study, the authors fluorescently tagged Cyclin B1 at its native locus and visualized translocation dynamics after radiation induced DNA damaged. They concluded premature translocation into the nucleus of Cyclin B1 resulted in arrest and senescence. Interestingly depleting P53 and P21 via siRNAs reduced translocation of Cyclin B1 suggesting that the P53-P21 axis was required for Cyclin B1 translocation mediated cell cycle arrest. Furthermore, immunoprecipitation experiments in this study confirmed that P21 can bind to Cyclin B1.

In this thesis we demonstrate G2/M arrest that is not associated with increased levels of γH2A.X and DNA damage. The arrest and senescence during G2/M is most likely due to failure to activate genes required for mitotic progression by the TRRAP/KAT5 complex. In support of this, previous studies examining the effects of TRRAP depletion in MEFs demonstrate that re-expression of the mitotic assembly checkpoint genes, Mad1 and Mad2, rescues the cell cycle arrest induced after TRRAP depletion (129). Furthermore, the failure to induce expression of genes responsible for mitotic progression suggest that the cells are undergoing a form of replication stress. Previous studies have demonstrated that ATR activation can occur and induce senescence

without DSBs (305). Therefore, we predict that senescence induced after TRRAP/KAT5 depletion is mediated by ATR activation, however this hypothesis needs to be tested in future studies.

p21 Independent Senescence

The molecular pathways that are required for senescence are currently debated in the field. When they were first identified, studies suggested that senescence due to replication stress, SAHF, the SASP and introduction of oncogenes required components of the Rb pathway such as P53, P21 and P16 (155). However, as discussed earlier, studies are now demonstrating that signaling in other pathways such as AKT/mTOR, NFκB and ATM/ATR can converge on the targets of P53, P21 and P16 in order to mediate the senescence responses. Taken together with the data from this thesis, this suggests that the P53-P21 may not be required for some forms of senescence.

As discussed earlier, multiple groups have reported p53 independent senescence. However, there are few studies demonstrating p21 independent senescence. P300 HAT inhibition resulted in p53/p21 independent senescence (253). P300 HAT inhibition indeed resulted in induction of p21 however knockdown of p21 and p53 with shRNA did not rescue senescence. In order to explain this, the authors suggested that P21 was likely inactive. Analysis of P21 localization in this study via immunofluorescence and validation via fractionation of nuclear vs cytoplasmic components revealed that although P21 was increased after P300 inhibition it was localized in the cytoplasm as opposed to the nucleus (253). Similar to the findings with the previous study, in TRRAP/KAT5 depleted cells we observed induction of p21 expression, yet TRRAP/KAT5 depletion in

p21 knockout cells also resulted in senescence. This suggests that p21 is not active in TRRAP/KAT5 depleted cells. Therefore, future experiments are required to investigate localization of P21 in TRRAP/KAT5 knockout cells.

The major unanswered question that arises from the studies in this thesis is: What is the driving force of senescence in TRRAP/KAT5 depleted cells? There are many hypotheses that I have outlined in this thesis. I demonstrated that loss of TRRAP results in decreased expression of genes required for mitotic progression in HCC and others have demonstrated that re-expressing mitotic activator checkpoint genes in TRRAP depleted MEFs restores cell cycle progression (129). Therefore, G2/M arrest is likely due to ATR-induced replication stress incurred via failure to progress into/through mitosis. Studies examining localization of Cyclin B would also aid in validating this hypothesis. The next question is why cells are senescing independent of the p53-p21 axis and Rb. One group reported that OIS via RAS overexpression in human mammary epithelial cells was independent of the p53-p21 axis and DNA damage proteins (306). In this previous study they reported that senescence required the TGF-β receptor, however the authors did not speculate on the role of TGF-β in mediating their senescence response. As mentioned earlier, senescent cells also secrete a collection of pro-inflammatory cytokines and chemokines, referred to as the SASP. Given that part of the inflammatory cytokine milieu associated with the SASP is TGF- β, I would hypothesize that TRRAP/KAT5 depleted cells senesce due to activation of the SASP. Studies have previously demonstrated that pharmacological inhibition of ATR can attenuate the SASP in RAS induced senescence

(307). Therefore, I speculate that SASP genes are activated due to cross talk between ATR and NFκB. However future studies are required to test these hypotheses.

Senescence as a therapeutic strategy for cancer

Senescent cells remain viable, but their cellular state is distinct from their proliferating counterparts. The cells are characterized by the absence of proliferative markers, the presence of CDKIs, SA-β-gal staining and the presence of SAHF. More recently, the SASP has also been implicated as a characteristic of senescent cells. The SASP is one of the most profound features of senescence as it facilitates immune-surveillance and clearance of senescent cells by recruiting and activating distinct cells from the innate immune system such as macrophages and NK cells (183).

Consequently, multiple studies have demonstrated that inducing senescence can have an anti-tumor effect in vivo in multiple tumor models such as HCC, NSCLC, Colorectal Cancers, and multiple hematological malignancies (151). The cell cycle arrest associated with senescence can dramatically reduce cellular growth and proliferation. Furthermore, the paracrine effects of the SASP can not only induce senescence in surrounding cells but also recruit immune cells to clear the senescent cells.

The work in this thesis suggests that TRRAP/KAT5 loss induced senescence in HCC cells inhibits tumor growth in vivo as subcutaneous xenografts. Furthermore TRRAP loss in hepatocytes in vivo via CRISPR mediated editing inhibits tumor initiation. The failure to initiate tumorigenesis is correlated with the presence of immune

foci that stain negative for CD4 and positive for F480. Clinically, oncological therapeutics can result in stable disease, i.e. tumors no longer proliferate, or regression, i.e. tumors decrease in size. The in vivo studies data suggest that TRRAP loss induced senescence results in decreased proliferation of the cells but also induces the SASP in vivo to aid in *clearance* of the senescent cells. However further experiments are required to definitively conclude that can induce tumor *regression* in vivo. These experiments include generating a doxycycline inducible model of TRRAP loss in-vivo to monitor potential tumor regression in both WT mice and immunodeficient mice. Identifying tumor regression in this model would definitively conclude that loss of TRRAP can not only halt tumorigenesis but can also promote tumor regression and clearance.

However, there are studies that demonstrate situations in which senescent cells are not cleared as they have limited immune cell recruitment. Given that senescent cells themselves have altered physiology compared to their non-senescent counterparts, many of these changes can be targeted for therapeutic benefit especially in senescence models that do not elicit a strong SASP response. Work in Clemens Schmitt's group demonstrated that Adriamycin- or Doxorubicin-induced senescence in a Myc lymphoma model does not induce a strong SASP response (308). In this study, the authors demonstrated that senescent cells exhibited endoplasmic reticulum stress, an unfolded protein response (UPR), increased ubiquitination and a shift in glucose metabolism from glycolysis to oxidative phosphorylation. In line with this, treatment of Myc-driven lymphomas with a senescence inducing agent and an inhibitor of glucose utilization or autophagy, led to caspase-12 and caspase 3 mediated apoptosis. These findings unveiled

that the cellular changes associated with senescence can be targeted to induce a synthetic lethal phenotype.

Escape from Senescence

Although senescence is a desired therapeutic outcome, the presence of senescent cancer cells can have deleterious outcomes due to the fact that the cells remain viable. Analysis of single senescent cells via a fluorescence based SA-β-gal assay revealed a population of cells that remained at the boundary between "senescent" and "replicating" (154). These cellular populations were positive for SA-β-gal and the proliferation marker Ki67. The presence of both markers suggested that cells could spontaneously exit from senescence (154). Moreover, senescent cells exhibit increased plasticity, express a stem cell signature and stem cell phenotype secondary to WNT activation (172, 309). Taken together the studies suggested that these "stem-like" senescent cells have the capacity to escape however experimental validation of this phenomenon was lacking until recently.

Studies in Clemens Schmitt's lab demonstrated that senescent cells can "escape" their cell cycle arrest via reorganization of their chromatin. In line with this, when senescent cells were allowed to escape senescence via inactivation of Suv39h1, a histone methyltransferase that maintains the heterochromatic H3K9me3 residue, or p53 inactivation they exhibited a much greater tumor initiating capacity than their pre-senescent counterparts(172, 175, 309).

More long-term studies in TRRAP depleted HCC cells are required to elucidate the consequences of TRRAP loss induced senescence. Given that TRRAP can regulate

WNT signaling (118) and also regulate stem cell signatures in cancer models (194), it would be interesting to examine whether TRRAP depleted cells can indeed escape senescence and if this escape is mediated by stemness and WNT signaling. Furthermore, generation of such a model could serve as an endogenous model of escape from senescence whereas the work in the Schmitt lab utilized genetic means to induce senescence escape.

The Pro-tumorigenic effects of SASP

Senescence can also have deleterious effects due to the fact that senescent cells create a pro-inflammatory environment through the SASP. Initial studies demonstrated that when senescent fibroblasts expressing the SASP were co-injected with tumor cells into immunodeficient mice, tumor growth increased at a faster rate compared to when tumor cells were injected with control non-senescent fibroblasts (184). This study provided preliminary evidence that in the absence of immune mediated clearance, the SASP can have a pro-tumorigenic effect. Given that HCC arises from pro-inflammatory disease such as cirrhosis, obesity, alcoholism and infection with Hepatitis B virus or Hepatitis C virus (6) it is important to consider the effects of the pro-inflammatory SASP on HCC and overall hepatic health.

In line with this, mechanistic studies have demonstrated that the pro-inflammatory cytokines secreted from senescent cells can promote cell proliferation and lead to initiation of HCC in cirrhosis mouse models (310). In this study the authors demonstrated that IL-6, a key component of the SASP can activate STAT3, JNK and ERK signaling

and ultimately promote HCC tumorigenesis in an obesity mouse model. Similar studies have demonstrated that IL-6 secretion from senescent cells can promote breast and prostate tumorigenesis and metastasis (311). Furthermore, a more recent study demonstrated that IL-1β secretion from senescent hepatic stellate cells can promote HCC tumorigenesis in mice after treatment with a chemical carcinogen (312).

In addition to pro-inflammatory cytokines, SASP components also include growth factors like HGF and EGF, proteases like MMP1 and MMP3, and other components like collagen and fibronectin (183). All these factors have been demonstrated to promote cell proliferation and motility in normal fibroblasts along with cancer cells. Furthermore, treatment of cancer models with MMP3 and fibronectin has been demonstrated to promote epithelial-mesenchymal transition (EMT) and subsequent carcinogenesis along with treatment resistance (313).

Studies are now beginning to demonstrate that the exact components of the SASP vary from model to model and also vary between the reagent that is utilized to induce senescence (311). These differences in the SASP secretome can potentially explain this variability in response. An in-depth examination of the SASP components secreted in response to senescence inducers is integral to ensuring a long-term durable anti-tumor response.

Studies examining the long-term consequences of senescence in liver models and senescence in cancer models are lacking. Furthermore, studies demonstrating escape from senescence have only recently emerged, but they suggest that initiating senescence alone is insufficient for a long-term anti-tumor response. Taken together the studies suggest

that in addition to inducing senescence, the cells need to be cleared as this would limit escape and would, presumably, also attenuate the proinflammatory effect of the SASP. Preliminary data from this study suggests that TRRAP depleted cells can be cleared in vivo however the effect of TRRAP loss and clearance of TRRAP depleted cells on the tumor microenvironment needs to be studied more rigorously using inducible models of TRRAP loss. Furthermore, the consequences of inducing a SASP in the liver long term needs to be examined in order to validate senescence inducing agents as a therapeutic strategy in the liver.

Concluding Remarks

The goal of this thesis was to identify therapeutic targets in HCC that were independent of P53 mutations. In line with this we took advantage of advances in genome engineering techniques by utilizing the CRISPR Cas9 system to conduct a screen in three HCC cell lines with varying P53 mutations. The screen identified a number of potential oncogenes, some of which had been previously validated as therapeutic targets in HCC, including CDC7, AURKA and PGK1. However, our screen also identified TRRAP as a therapeutic target in HCC. Although TRRAP has been implicated in processes like cellular differentiation and DNA repair in glioblastoma and melanoma models, this study was the first to implicate TRRAP in HCC.

The work in this thesis demonstrates that TRRAP and its cofactor KAT5 can regulate expression of a genetic signature responsible for mitotic progression in HCC. Furthermore, genomic analyses revealed that TRRAP may also play a role in regulating

glucose and lipid metabolism in hepatocytes. Furthermore, loss of TRRAP results in decreased translation of the KAT5 mRNA thus reducing KAT5 protein levels. Indeed, loss of TRRAP and KAT5 results in decreased cell growth in vitro and cell proliferation in vivo. Furthermore, depletion of TRRAP in vivo in hepatocytes is correlated with decreased tumor initiation in-vivo and the presence of macrophage positive immune foci in the liver. TRRAP/KAT5 has been implicated in regulating cell cycle progression in various models. However, the work described here demonstrates that the anti-proliferative effect is due to the induction of senescence during G2/M. Finally, we identify TOP2A as a target of TRRAP/KAT5 which, when depleted, also induces senescence in HCC cell lines during G2/M.

Canonical mediators of senescence include the P53-P21 axis, phosphorylation of the Rb protein, SAHF and decreased TERT expression however the work in this thesis demonstrates that TRRAP/KAT5 loss is independent of these factors. DNA damage is a trigger of senescence and the TRRAP/KAT5 complex is implicated in playing an essential role in DNA repair. However, the work in this thesis demonstrates that TRRAP/KAT5 loss induced senescence is independent of DNA damage. The work in this thesis combined with the literature in the senescence field suggests that senescence may be mediated by replication stress induced ATR activation and subsequent SASP induction however future studies are required to confirm this. Overall, the work in this thesis identifies TRRAP, KAT5 and TOP2A as therapeutic targets in HCC and suggests that these targets warrants further drug design efforts.

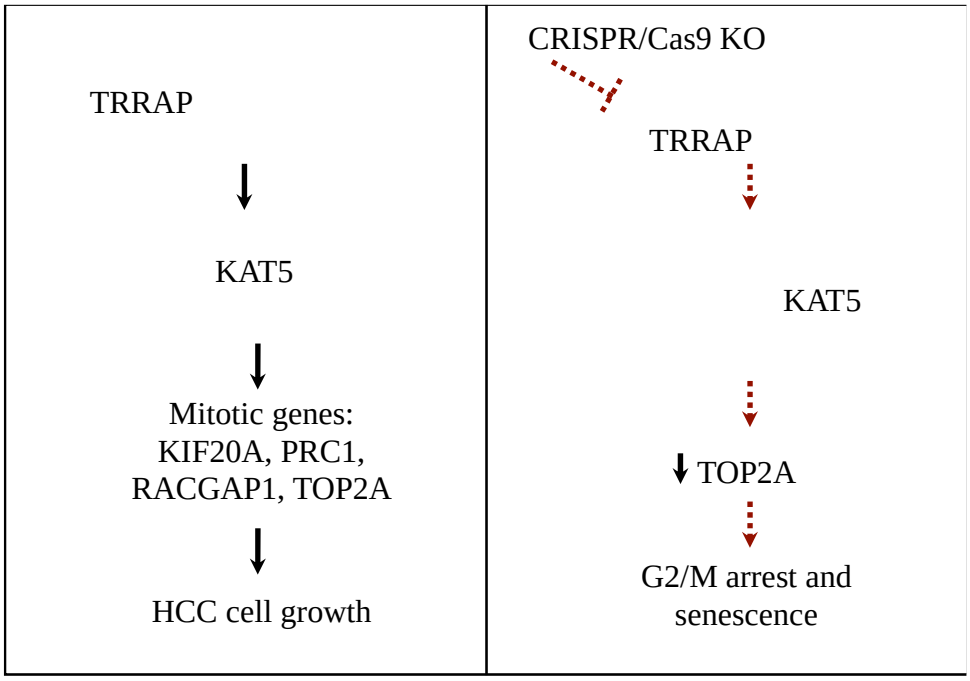

Figure 24. Overall model depicting key findings from this dissertation

APPENDIX I

TRRAP Loss Induces Formation of Micronuclei and DNA Bridges in HCC

Preface

The data presented in this appendix is unpublished preliminary data.

Background and Significant Results

Recently, the Senescence Associated Secretory Phenotype (SASP) has been described as a major component of senescent cells. Functionally, the SASP recruits immune cells to mediate clearance of senescent cells and also reinforces cell cycle arrest in neighboring cells. In line with the latter function, conditioned media of senescent cells can indeed induce senescence in dividing cells (314). Analysis of the secreted factors from senescent cells using antibody arrays revealed that the SASP included several families of factories that categorically were divided into: soluble signaling factors (interleukins, chemokines, and growth factors), secreted proteases, and secreted insoluble proteins/extracellular matrix (ECM) components (183).

Work from previous studies mechanistically established that the SASP transcriptional profile was activated by the cGAS-STING cytosolic DNA sensing pathway. One of the hallmarks of senescent cells is the presence of micronuclei. Senescent cells have fragile membranes due to decreased Lamin B expression (156). This nuclear frailty results in ejection of DNA that is bound by histones and often encased in Lamin, termed micronuclei (254). The micronuclei bind to and activate the cytosolic

receptor, cGAS, and induce expression of SASP genes via activation of the STING pathway (255).

In line with this, we sought to examine the nuclei of TRRAP, KAT5 and TOP2A depleted HUH7 senescent cells. DAPI staining revealed the presence of micronuclei and other secondary structures such as DNA bridges (Figure A1.1A) that were in greater abundance in TRRAP, KAT5 and TOP2A depleted cells compared to NT cells (Figure A1.1B and 1C). Furthermore, analysis of the RNA-seq data from Chapter II revealed that SASP genes (previous published in (179) were enriched in TRRAP depleted cells compared to NT cells (Figure A1.1D).

As seen in the original study by Dou et al (254), we also observe an increase in the presence of micronuclei in senescent cells. Furthermore, we also observe an increase in SASP gene expression via RNAseq analysis. Our in vivo studies suggest that TRRAP depletion is correlated with the presence of $F480^{+}$ macrophages (Figure 2.6C) suggesting that there is immune cell recruitment. Taken together the data suggests that TRRAP depleted cells also exhibit the SASP however this requires validation by further experiments. Specifically, future studies should validate the expression of SASP genes via qPCR or ELISA and should provide conclusive evidence for cGAS-STING activation via western blot. Furthermore, studies have demonstrated that overexpression of DNases can degrade cytoplasmic micronuclei and attenuate senescence (256). To test whether TRRAP loss induced senescence is driven by the presence of micronuclei, future studies can overexpress DNase IIa and TREX1 and examine if induction of senescence is decreased.

Studies in zebrafish demonstrated that loss of TOP2A impaired hepatocyte regeneration due to the failure to resolve DNA bridges during mitosis (315). Given that TRRAP/KAT5 can drive TOP2A expression, we also observed formation of DNA bridges in TRRAP, KAT5 and TOP2A depleted cells. The study by Dou et al demonstrated that micronuclei were ejected directly from nuclei (254). However live cell imaging studies of HeLa cells after replication stress demonstrated that an unresolved DNA bridge can also be ejected as micronuclei (316, 317). Future studies can utilize live cell imaging in H2B-GFP cells to identify the source of micronuclei in TRRAP/KAT5 depleted cells.

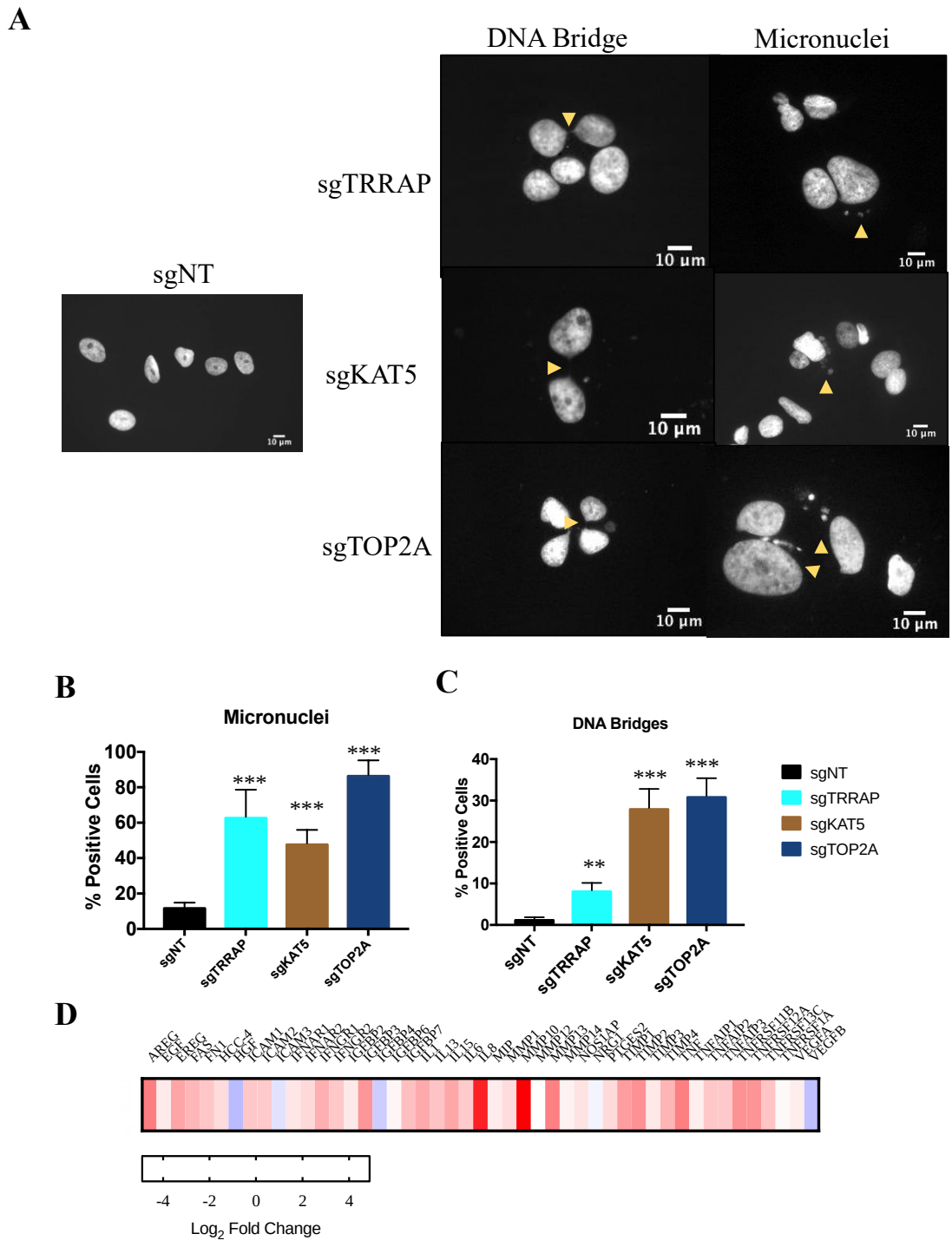

Figure 25. TRRAP/KAT5 depletion is associated with changes in nuclear structure and enrichment of SASP genes.

(**A)** DAPI staining of nuclei of HUH7 cells after infection with sgNT, sgTRRAP, sgKAT5 and sgTOP2A with yellow arrowheads identifying micronuclei and DNA bridges. **(B)** Quantification of micronuclei in TRRAP, KAT5 and TOP2A depleted HUH7 cells. **(C)** Quantification of DNA bridges in TRRAP, KAT5 and TOP2A depleted HUH7 cells. **(D)** Heatmap displaying log-2-fold changes in FPKM of SASP genes between TRRAP depleted and NT HUH7 cells. Data was presented as mean ± SD; p-values were calculated by comparing to sgNT, $^{**}p < 0.01$, $^{***}p < 0.001$ (student's t test).

APPENDIX II

Developing CRISPR tools for cancer research

Preface

The work described in this appendix describes two applications of CRISPR technology in cancer research. The first application was done in collaboration with Art Mercurio's lab in a study by Elaimy et al (Elaimy, A.L., **Sheel,A.**, Brown, C., Walker, M., Amante, J., Xue, W., Chan, A., Baer, C., Goel, H., & Mercurio, A. Real-time imaging of integrin β4 dynamics using a reporter cell line generated by Crispr/Cas9 genome editing) that describes generating a fusion protein to study its dynamics in breast cancers.

The second application is in a study by Mou et al (Mou, H., Ozata, D. M., Smith, J. L., **Sheel, A.,** Kwan, S. Y., Hough, S., Kucukural, A., Kennedy,Z., Cao, Y., & Xue, W. (2019). CRISPR-SONIC: targeted somatic oncogene knock-in enables rapid in vivo cancer modeling. Genome medicine, 11(1), 21.) that describes utilizing CRISPR to "knock-in" an oncogene in order to generate in vivo models of ICC.

Background and Significant Results

The advent of the CRISPR/Cas9 system has resulted in major advances in the field of genome engineering. CRISPR/Cas9 introduces site specific double-strand breaks (DSBs) using a programmable sgRNA. These DSB can be repaired via homology-independent repair, such as non-homologous end recombination (NHEJ), or homology-directed repair (HDR) with an exogenous homologous DNA template. NHEJ occurs more

frequently than HDR and can therefore be utilized to generate knockout cell lines, as demonstrated in Chapter II and Chapter III of this dissertation. Moreover, HDR can also be used to knock-in desired genes. This function has been utilized to generate models to study gene functions however due to the low efficacy of this system the use of CRISPR/Cas9 mediated HDR editing has been limited. However, in this appendix I will briefly describe two studies that utilize CRISPR to "knock-in" a casette in a cancer context.

In the first study by Elaimy et al. we utilize Comma D1 cells, a murine mammary epithelial cell line, to generate cell line that express a TdTomato tagged β4 Integrin from its native locus via HDR. In order to generate this cell line, we utilized Cas9 to generate a DSB at the end of the last exon in the endogenous β4 Integrin (*ITGB4*) gene and provided a donor plasmid to insert a cassette that containing a mutated stop codon followed by the TdTomato cassette (Figure A2.1A). This design allowed for integration of the TdTomato cassette at the end of the *ITGB4* ORF while simultaneously mutating the stop codon to allow for translation of the TdTomato tag. I validated successful integration via PCR using primer pairs that both bind inside the tdTomato cassette and flank the cassette at the 5' and 3' genomic locus (Figure A2.1B). Furthermore, I identify four genomic loci as predicted off target sites for the sgRNA utilized in this study and demonstrate that there is no TdTomato integration at predicted off target sites using the same PCR based approach as the expected band size for integration would be ~500bp (Figure A2.1.B). The band in OT4 at ~800bp is likely an artifact as integration is not seen in the reverse orientation. Alternatively, this band could also represent partial integration of the donor plasmid at

this site however this site is an intronic region therefore we would expected no aberrant TdTomato protein synthesized from this site.

While HDR is an invaluable tool that allows for the integration of exogenous cassettes, the efficiency of this process is low in vitro (~2%-5%) and cannot be detected in vivo without viral mediated delivery (318). Therefore, in the study by Mou et al.(319), we attempted to enhance integration of cassettes in vivo using a three-step process (Figure A2.2A). The first step utilized an sgRNA and Cas9 to induce a DSB at the target DNA locus, in this case *Actin*. The second step utilized another sgRNA to cut and linearize a Circular Donor plasmid which, in the third step, is then inserted into the DNA at the Actin locus. Using this system, termed CRISPR-based Somatic Oncogene kNock-In for Cancer Modeling (CRISPR-SONIC), we demonstrated GFP integration rates of ~17% in vitro (Figure A2.2B). However in some cell lines, integration of GFP was <1% (Figure A2.2C). We demonstrated that this was due to SNPs in the Actin locus near the sgRNA binding site (Figure A2.2D). These SNPs reduced the efficiency of cutting in step 1 of the CRISPR-SONIC process and therefore reduced GFP integration efficiency. Overall this data highlighted the importance of sequencing the target region prior to sgRNA design as mismatches between the genomic locus and sgRNA can dramatically reduce binding of Cas9 to the target locus and therefore reduce cutting efficiency. Furthermore, in this study we demonstrated that oncogenes like HRAS can also be inserted into this locus in hepatocytes, via hydrodynamic tail vein injection of the plasmids, to model ICC in vivo.

Overall these two studies highlighted two applications of CRISPR based HDR that can aid in the cancer research. Overexpressing fusion proteins in order to study their localization and binding partners can lead to false positives as expressing supra-physiological levels of proteins can alter cellular biology and the protein's functions/localizations/binding partners. By utilizing CRISPR based HDR, we are now able to easily tag proteins directly at their endogenous genomic locus and thereby bypass the deleterious effects of overexpression. Although HDR has low efficiency in vitro, techniques like CRISPR-SONIC can increase integration efficiency by ~15% and allow for integration. Furthermore CRISPR-SONIC can be utilized to integrate genes in-vivo without the use of transposases and Adeno-Associated viruses (AAVs).

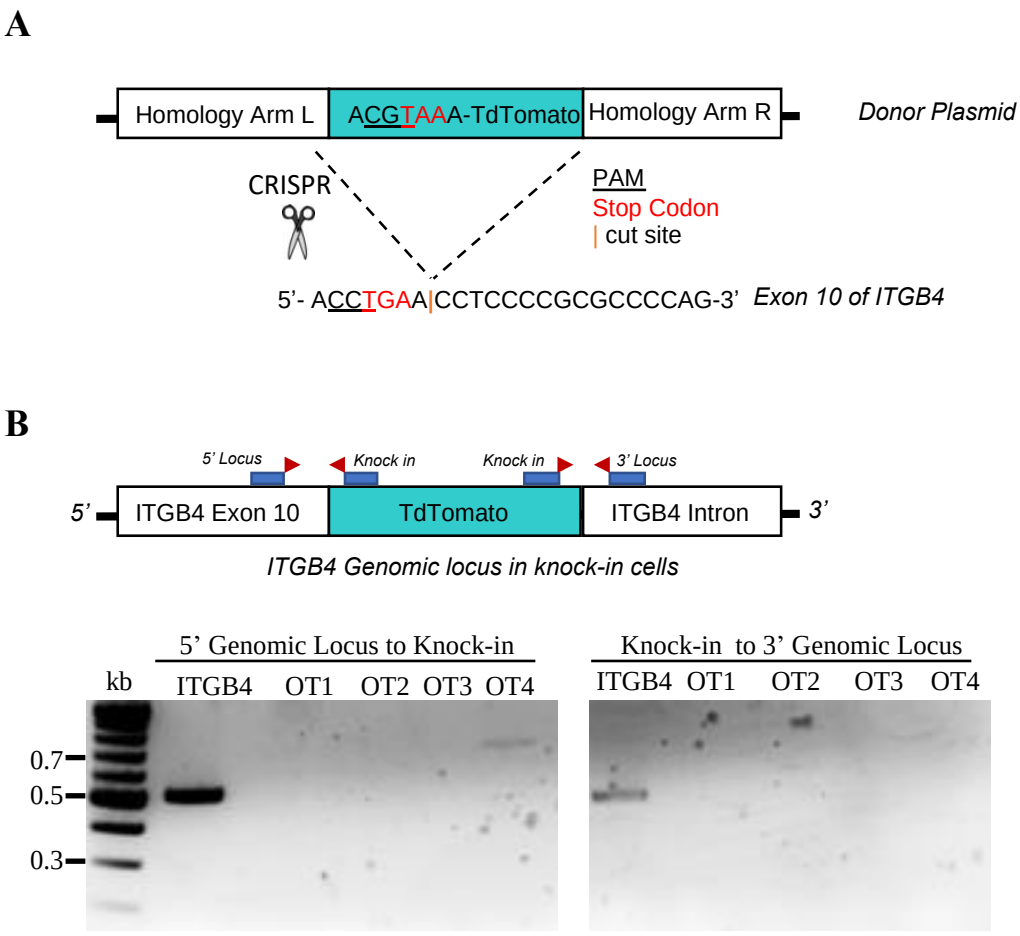

Figure 26. **HDR Mediated Integration of TdTomato in Comma D1 cell.**
(A) Diagram of the strategy utilized to generate insert a TdTomato cassette at the final exon of the ITGB4 genomic locus to generate a TD-Tomato-ITGB4 fusion protein TdTomato via CRISPR mediated HDR. **(B)** Strategy depicting PCR based approach to assay for integration at the ITGB4 site and at four off target sites (OT1-OT4). 2% agarose gel displaying PCR products at each site. The expected size for successful insertion was 500bp.

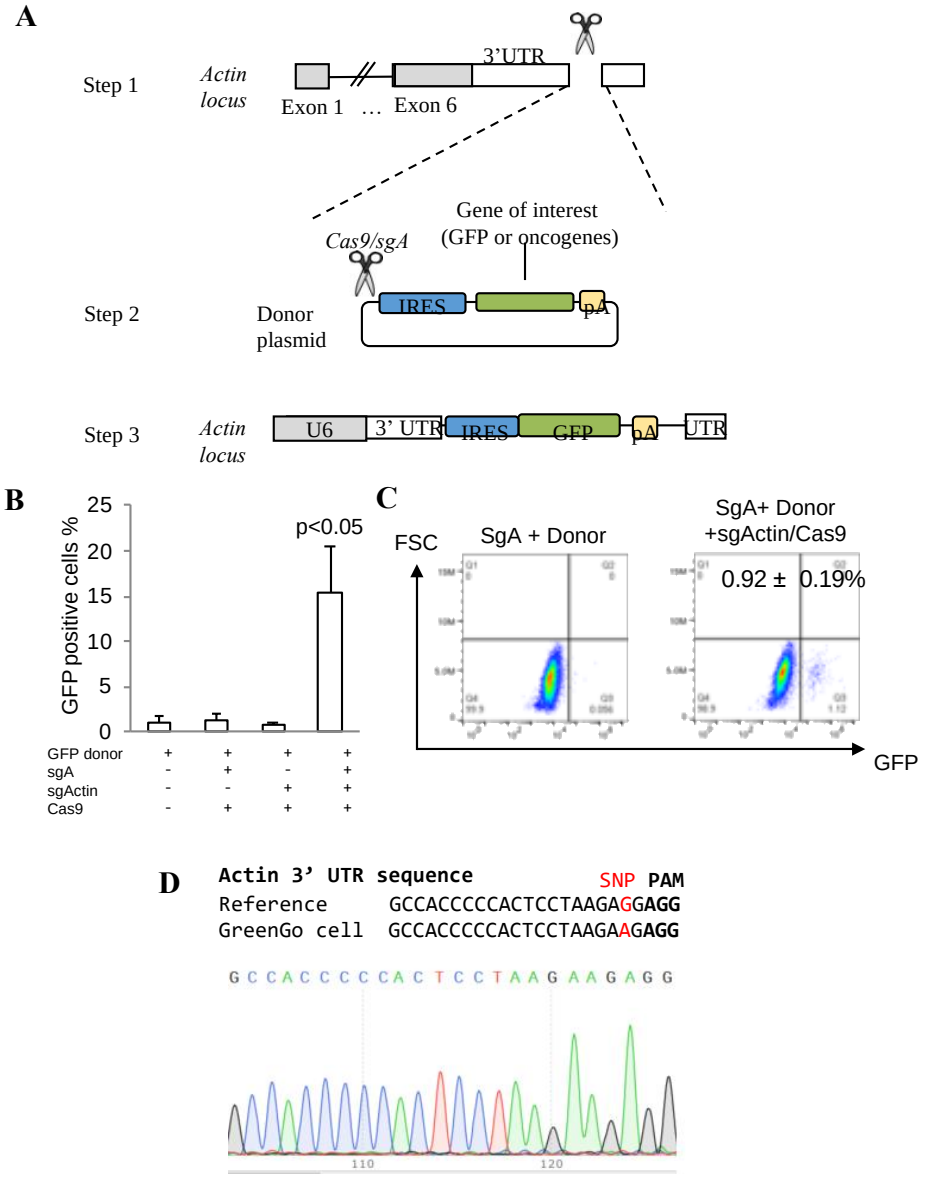

Figure 27. CRISPR-SONIC based approach for increased integration efficiency. **(A)** Schematic depicting three step strategy for CRISPR-SONIC based integration. **(B)** Quantification of insertion efficiency of GFP in vitro in Neuro2A cells **(C)** Flow Cytometric analysis of CRISPR-SONIC mediated GFP integration in GreenGo cells. **(D)** Sanger sequencing track of Actin 3'UTRin GreenGo cells highlighting the SNP (red) that is in the 3'UTR of this cell line.

REFERENCES

1. Ferlay J, Colombet M, Soerjomataram I, Mathers C, Parkin DM, Pineros M, Znaor A, Bray F. Estimating the global cancer incidence and mortality in 2018: GLOBOCAN sources and methods. Int J Cancer. 2019;144(8):1941-53. Epub 2018/10/24. doi: 10.1002/ijc.31937. PubMed PMID: 30350310.
2. Suriawinata A. Pathology of Malignant Liver Tumors. In: TW P, editor. UpToDate. Waltham, MA: UpToDate; 2017.
3. SEER, Surveillance, Epidemiology, and End Results Program. Bethesda, MD.: U.S. Dept. of Health and Human Services, National Institutes of Health, National Cancer Institute; 2005. 12 p. p.
4. Murphy SL, Xu J, Kochanek KD, Arias E. Mortality in the United States, 2017. NCHS Data Brief. 2018(328):1-8. Epub 2018/12/01. PubMed PMID: 30500322.
5. Jemal A, Ward EM, Johnson CJ, Cronin KA, Ma J, Ryerson B, Mariotto A, Lake AJ, Wilson R, Sherman RL, Anderson RN, Henley SJ, Kohler BA, Penberthy L, Feuer EJ, Weir HK. Annual Report to the Nation on the Status of Cancer, 1975-2014, Featuring Survival. J Natl Cancer Inst. 2017;109(9). Epub 2017/04/05. doi: 10.1093/jnci/djx030. PubMed PMID: 28376154; PMCID: PMC5409140.
6. Villanueva A. Hepatocellular Carcinoma. N Engl J Med. 2019;380(15):1450-62. Epub 2019/04/11. doi: 10.1056/NEJMra1713263. PubMed PMID: 30970190.
7. Schulze K, Nault JC, Villanueva A. Genetic profiling of hepatocellular carcinoma using next-generation sequencing. J Hepatol. 2016;65(5):1031-42. Epub 2016/10/19. doi: 10.1016/j.jhep.2016.05.035. PubMed PMID: 27262756.
8. Wilkens L, Flemming P, Gebel M, Bleck J, Terkamp C, Wingen L, Kreipe H, Schlegelberger B. Induction of aneuploidy by increasing chromosomal instability during dedifferentiation of hepatocellular carcinoma. Proc Natl Acad Sci U S A. 2004;101(5):1309-14. Epub 2004/01/28. doi: 10.1073/pnas.0305817101. PubMed PMID: 14745031; PMCID: PMC337049.
9. Roncalli M, Bianchi P, Bruni B, Laghi L, Destro A, Di Gioia S, Gennari L, Tommasini M, Malesci A, Coggi G. Methylation framework of cell cycle gene inhibitors in cirrhosis and associated hepatocellular carcinoma. Hepatology. 2002;36(2):427-32. Epub 2002/07/27. doi: 10.1053/jhep.2002.34852. PubMed PMID: 12143052.
10. Guichard C, Amaddeo G, Imbeaud S, Ladeiro Y, Pelletier L, Maad IB, Calderaro J, Bioulac-Sage P, Letexier M, Degos F, Clement B, Balabaud C, Chevet E, Laurent A, Couchy G, Letouze E, Calvo F, Zucman-Rossi J. Integrated analysis of somatic mutations and focal copy-number changes identifies key genes and pathways in hepatocellular carcinoma. Nat Genet. 2012;44(6):694-8. Epub 2012/05/09. doi: 10.1038/ng.2256. PubMed PMID: 22561517; PMCID: PMC3819251.
11. Schulze K, Imbeaud S, Letouze E, Alexandrov LB, Calderaro J, Rebouissou S, Couchy G, Meiller C, Shinde J, Soysouvanh F, Calatayud AL, Pinyol R, Pelletier L, Balabaud C, Laurent A, Blanc JF, Mazzaferro V, Calvo F, Villanueva A, Nault JC, Bioulac-Sage P, Stratton MR, Llovet JM, Zucman-Rossi J. Exome sequencing of hepatocellular carcinomas identifies new mutational signatures and potential therapeutic

targets. Nat Genet. 2015;47(5):505-11. Epub 2015/03/31. doi: 10.1038/ng.3252. PubMed PMID: 25822088; PMCID: PMC4587544.
12. Totoki Y, Tatsuno K, Covington KR, Ueda H, Creighton CJ, Kato M, Tsuji S, Donehower LA, Slagle BL, Nakamura H, Yamamoto S, Shinbrot E, Hama N, Lehmkuhl M, Hosoda F, Arai Y, Walker K, Dahdouli M, Gotoh K, Nagae G, Gingras MC, Muzny DM, Ojima H, Shimada K, Midorikawa Y, Goss JA, Cotton R, Hayashi A, Shibahara J, Ishikawa S, Guiteau J, Tanaka M, Urushidate T, Ohashi S, Okada N, Doddapaneni H, Wang M, Zhu Y, Dinh H, Okusaka T, Kokudo N, Kosuge T, Takayama T, Fukayama M, Gibbs RA, Wheeler DA, Aburatani H, Shibata T. Trans-ancestry mutational landscape of hepatocellular carcinoma genomes. Nat Genet. 2014;46(12):1267-73. Epub 2014/11/05. doi: 10.1038/ng.3126. PubMed PMID: 25362482.
13. Moore A, Wu L, Chuang JC, Sun X, Luo X, Gopal P, Li L, Celen C, Zimmer M, Zhu H. Arid1a Loss Drives Nonalcoholic Steatohepatitis in Mice Through Epigenetic Dysregulation of Hepatic Lipogenesis and Fatty Acid Oxidation. Hepatology. 2019;69(5):1931-45. Epub 2018/12/26. doi: 10.1002/hep.30487. PubMed PMID: 30584660; PMCID: PMC6461494.
14. Cancer Genome Atlas Research Network. Electronic address wbe, Cancer Genome Atlas Research N. Comprehensive and Integrative Genomic Characterization of Hepatocellular Carcinoma. Cell. 2017;169(7):1327-41 e23. Epub 2017/06/18. doi: 10.1016/j.cell.2017.05.046. PubMed PMID: 28622513; PMCID: PMC5680778.
15. Hoshida Y, Nijman SM, Kobayashi M, Chan JA, Brunet JP, Chiang DY, Villanueva A, Newell P, Ikeda K, Hashimoto M, Watanabe G, Gabriel S, Friedman SL, Kumada H, Llovet JM, Golub TR. Integrative transcriptome analysis reveals common molecular subclasses of human hepatocellular carcinoma. Cancer Res. 2009;69(18):7385-92. Epub 2009/09/03. doi: 10.1158/0008-5472.CAN-09-1089. PubMed PMID: 19723656; PMCID: PMC3549578.
16. Lee JS, Chu IS, Heo J, Calvisi DF, Sun Z, Roskams T, Durnez A, Demetris AJ, Thorgeirsson SS. Classification and prediction of survival in hepatocellular carcinoma by gene expression profiling. Hepatology. 2004;40(3):667-76. Epub 2004/09/07. doi: 10.1002/hep.20375. PubMed PMID: 15349906.
17. Zucman-Rossi J, Villanueva A, Nault JC, Llovet JM. Genetic Landscape and Biomarkers of Hepatocellular Carcinoma. Gastroenterology. 2015;149(5):1226-39 e4. Epub 2015/06/24. doi: 10.1053/j.gastro.2015.05.061. PubMed PMID: 26099527.
18. Hirschfield H, Bian CB, Higashi T, Nakagawa S, Zeleke TZ, Nair VD, Fuchs BC, Hoshida Y. In vitro modeling of hepatocellular carcinoma molecular subtypes for anti-cancer drug assessment. Exp Mol Med. 2018;50(1):e419. Epub 2018/01/06. doi: 10.1038/emm.2017.164. PubMed PMID: 29303513; PMCID: PMC5992986.
19. Schmidt B, Wei L, DePeralta DK, Hoshida Y, Tan PS, Sun X, Sventek JP, Lanuti M, Tanabe KK, Fuchs BC. Molecular subclasses of hepatocellular carcinoma predict sensitivity to fibroblast growth factor receptor inhibition. Int J Cancer. 2016;138(6):1494-505. Epub 2015/10/21. doi: 10.1002/ijc.29893. PubMed PMID: 26481559; PMCID: PMC5297453.

20. Bruix J, Sherman M, American Association for the Study of Liver D. Management of hepatocellular carcinoma: an update. Hepatology. 2011;53(3):1020-2. Epub 2011/03/05. doi: 10.1002/hep.24199. PubMed PMID: 21374666; PMCID: PMC3084991.
21. Bismuth H, Chiche L, Adam R, Castaing D, Diamond T, Dennison A. Liver resection versus transplantation for hepatocellular carcinoma in cirrhotic patients. Ann Surg. 1993;218(2):145-51. Epub 1993/08/01. doi: 10.1097/00000658-199308000-00005. PubMed PMID: 8393649; PMCID: PMC1242923.
22. Marrero JA, Kulik LM, Sirlin CB, Zhu AX, Finn RS, Abecassis MM, Roberts LR, Heimbach JK. Diagnosis, Staging, and Management of Hepatocellular Carcinoma: 2018 Practice Guidance by the American Association for the Study of Liver Diseases. Hepatology. 2018;68(2):723-50. Epub 2018/04/07. doi: 10.1002/hep.29913. PubMed PMID: 29624699.
23. Llovet JM, Burroughs A, Bruix J. Hepatocellular carcinoma. Lancet. 2003;362(9399):1907-17. Epub 2003/12/12. doi: 10.1016/S0140-6736(03)14964-1. PubMed PMID: 14667750.
24. Lencioni R, de Baere T, Soulen MC, Rilling WS, Geschwind JF. Lipiodol transarterial chemoembolization for hepatocellular carcinoma: A systematic review of efficacy and safety data. Hepatology. 2016;64(1):106-16. Epub 2016/01/15. doi: 10.1002/hep.28453. PubMed PMID: 26765068.
25. Llovet JM, Ricci S, Mazzaferro V, Hilgard P, Gane E, Blanc JF, de Oliveira AC, Santoro A, Raoul JL, Forner A, Schwartz M, Porta C, Zeuzem S, Bolondi L, Greten TF, Galle PR, Seitz JF, Borbath I, Haussinger D, Giannaris T, Shan M, Moscovici M, Voliotis D, Bruix J, Group SIS. Sorafenib in advanced hepatocellular carcinoma. N Engl J Med. 2008;359(4):378-90. Epub 2008/07/25. doi: 10.1056/NEJMoa0708857. PubMed PMID: 18650514.
26. Kudo M, Finn RS, Qin S, Han KH, Ikeda K, Piscaglia F, Baron A, Park JW, Han G, Jassem J, Blanc JF, Vogel A, Komov D, Evans TRJ, Lopez C, Dutcus C, Guo M, Saito K, Kraljevic S, Tamai T, Ren M, Cheng AL. Lenvatinib versus sorafenib in first-line treatment of patients with unresectable hepatocellular carcinoma: a randomised phase 3 non-inferiority trial. Lancet. 2018;391(10126):1163-73. Epub 2018/02/13. doi: 10.1016/S0140-6736(18)30207-1. PubMed PMID: 29433850.
27. Bruix J, Qin S, Merle P, Granito A, Huang YH, Bodoky G, Pracht M, Yokosuka O, Rosmorduc O, Breder V, Gerolami R, Masi G, Ross PJ, Song T, Bronowicki JP, Ollivier-Hourmand I, Kudo M, Cheng AL, Llovet JM, Finn RS, LeBerre MA, Baumhauer A, Meinhardt G, Han G, Investigators R. Regorafenib for patients with hepatocellular carcinoma who progressed on sorafenib treatment (RESORCE): a randomised, double-blind, placebo-controlled, phase 3 trial. Lancet. 2017;389(10064):56-66. Epub 2016/12/10. doi: 10.1016/S0140-6736(16)32453-9. PubMed PMID: 27932229.
28. Zhu AX, Finn RS, Edeline J, Cattan S, Ogasawara S, Palmer D, Verslype C, Zagonel V, Fartoux L, Vogel A, Sarker D, Verset G, Chan SL, Knox J, Daniele B, Webber AL, Ebbinghaus SW, Ma J, Siegel AB, Cheng AL, Kudo M, investigators K-. Pembrolizumab in patients with advanced hepatocellular carcinoma previously treated

with sorafenib (KEYNOTE-224): a non-randomised, open-label phase 2 trial. Lancet Oncol. 2018;19(7):940-52. Epub 2018/06/08. doi: 10.1016/S1470-2045(18)30351-6. PubMed PMID: 29875066.
29. El-Khoueiry AB, Sangro B, Yau T, Crocenzi TS, Kudo M, Hsu C, Kim TY, Choo SP, Trojan J, Welling THR, Meyer T, Kang YK, Yeo W, Chopra A, Anderson J, Dela Cruz C, Lang L, Neely J, Tang H, Dastani HB, Melero I. Nivolumab in patients with advanced hepatocellular carcinoma (CheckMate 040): an open-label, non-comparative, phase 1/2 dose escalation and expansion trial. Lancet. 2017;389(10088):2492-502. Epub 2017/04/25. doi: 10.1016/S0140-6736(17)31046-2. PubMed PMID: 28434648.
30. Malumbres M, Barbacid M. Cell cycle, CDKs and cancer: a changing paradigm. Nat Rev Cancer. 2009;9(3):153-66. Epub 2009/02/25. doi: 10.1038/nrc2602. PubMed PMID: 19238148.
31. Ezhevsky SA, Ho A, Becker-Hapak M, Davis PK, Dowdy SF. Differential regulation of retinoblastoma tumor suppressor protein by G(1) cyclin-dependent kinase complexes in vivo. Mol Cell Biol. 2001;21(14):4773-84. Epub 2001/06/21. doi: 10.1128/MCB.21.14.4773-4784.2001. PubMed PMID: 11416152; PMCID: PMC87164.
32. Sherr CJ, Roberts JM. CDK inhibitors: positive and negative regulators of G1-phase progression. Genes Dev. 1999;13(12):1501-12. Epub 1999/07/01. doi: 10.1101/gad.13.12.1501. PubMed PMID: 10385618.
33. Otto T, Sicinski P. Cell cycle proteins as promising targets in cancer therapy. Nat Rev Cancer. 2017;17(2):93-115. Epub 2017/01/28. doi: 10.1038/nrc.2016.138. PubMed PMID: 28127048; PMCID: PMC5345933.
34. Koepp DM, Schaefer LK, Ye X, Keyomarsi K, Chu C, Harper JW, Elledge SJ. Phosphorylation-dependent ubiquitination of cyclin E by the SCFFbw7 ubiquitin ligase. Science. 2001;294(5540):173-7. Epub 2001/09/05. doi: 10.1126/science.1065203. PubMed PMID: 11533444.
35. Liao H, Ji F, Helleday T, Ying S. Mechanisms for stalled replication fork stabilization: new targets for synthetic lethality strategies in cancer treatments. EMBO Rep. 2018;19(9). Epub 2018/08/16. doi: 10.15252/embr.201846263. PubMed PMID: 30108055; PMCID: PMC6123652.
36. Bartek J, Lukas C, Lukas J. Checking on DNA damage in S phase. Nat Rev Mol Cell Biol. 2004;5(10):792-804. Epub 2004/10/02. doi: 10.1038/nrm1493. PubMed PMID: 15459660.
37. Lobrich M, Jeggo PA. The impact of a negligent G2/M checkpoint on genomic instability and cancer induction. Nat Rev Cancer. 2007;7(11):861-9. Epub 2007/10/19. doi: 10.1038/nrc2248. PubMed PMID: 17943134.
38. Seki A, Coppinger JA, Jang CY, Yates JR, Fang G. Bora and the kinase Aurora a cooperatively activate the kinase Plk1 and control mitotic entry. Science. 2008;320(5883):1655-8. Epub 2008/06/21. doi: 10.1126/science.1157425. PubMed PMID: 18566290; PMCID: PMC2834883.
39. Goldenson B, Crispino JD. The aurora kinases in cell cycle and leukemia. Oncogene. 2015;34(5):537-45. Epub 2014/03/19. doi: 10.1038/onc.2014.14. PubMed PMID: 24632603; PMCID: PMC4167158.

40. Gavet O, Pines J. Progressive activation of CyclinB1-Cdk1 coordinates entry to mitosis. Dev Cell. 2010;18(4):533-43. Epub 2010/04/24. doi: 10.1016/j.devcel.2010.02.013. PubMed PMID: 20412769; PMCID: PMC3325599.
41. Dominguez-Brauer C, Thu KL, Mason JM, Blaser H, Bray MR, Mak TW. Targeting Mitosis in Cancer: Emerging Strategies. Mol Cell. 2015;60(4):524-36. Epub 2015/11/23. doi: 10.1016/j.molcel.2015.11.006. PubMed PMID: 26590712.
42. Carr BI. Hepatocellular carcinoma: current management and future trends. Gastroenterology. 2004;127(5 Suppl 1):S218-24. Epub 2004/10/28. PubMed PMID: 15508087.
43. Song MJ, Chun HJ, Song DS, Kim HY, Yoo SH, Park CH, Bae SH, Choi JY, Chang UI, Yang JM, Lee HG, Yoon SK. Comparative study between doxorubicin-eluting beads and conventional transarterial chemoembolization for treatment of hepatocellular carcinoma. J Hepatol. 2012;57(6):1244-50. Epub 2012/07/25. doi: 10.1016/j.jhep.2012.07.017. PubMed PMID: 22824821.
44. Huang K, Zhou Q, Wang R, Cheng D, Ma Y. Doxorubicin-eluting beads versus conventional transarterial chemoembolization for the treatment of hepatocellular carcinoma. J Gastroenterol Hepatol. 2014;29(5):920-5. Epub 2013/11/15. doi: 10.1111/jgh.12439. PubMed PMID: 24224722.
45. Xia Y, Qiu Y, Li J, Shi L, Wang K, Xi T, Shen F, Yan Z, Wu M. Adjuvant therapy with capecitabine postpones recurrence of hepatocellular carcinoma after curative resection: a randomized controlled trial. Ann Surg Oncol. 2010;17(12):3137-44. Epub 2010/07/06. doi: 10.1245/s10434-010-1148-3. PubMed PMID: 20602260.
46. Loong HH, Yeo W. Microtubule-targeting agents in oncology and therapeutic potential in hepatocellular carcinoma. Onco Targets Ther. 2014;7:575-85. Epub 2014/05/03. doi: 10.2147/OTT.S46019. PubMed PMID: 24790457; PMCID: PMC3999274.
47. Falkson G, Burger W. A phase II trial of vindesine in hepatocellular cancer. Oncology. 1995;52(1):86-7. Epub 1995/01/01. doi: 10.1159/000227434. PubMed PMID: 7800350.
48. Gagandeep S, Novikoff PM, Ott M, Gupta S. Paclitaxel shows cytotoxic activity in human hepatocellular carcinoma cell lines. Cancer Lett. 1999;136(1):109-18. Epub 1999/04/22. PubMed PMID: 10211948.
49. Geng CX, Zeng ZC, Wang JY. Docetaxel inhibits SMMC-7721 human hepatocellular carcinoma cells growth and induces apoptosis. World J Gastroenterol. 2003;9(4):696-700. Epub 2003/04/08. doi: 10.3748/wjg.v9.i4.696. PubMed PMID: 12679913; PMCID: PMC4611431.
50. Chao Y, Chan WK, Birkhofer MJ, Hu OY, Wang SS, Huang YS, Liu M, Whang-Peng J, Chi KH, Lui WY, Lee SD. Phase II and pharmacokinetic study of paclitaxel therapy for unresectable hepatocellular carcinoma patients. Br J Cancer. 1998;78(1):34-9. Epub 1998/07/14. doi: 10.1038/bjc.1998.438. PubMed PMID: 9662247; PMCID: PMC2062942.

51. Mukhtar E, Adhami VM, Mukhtar H. Targeting microtubules by natural agents for cancer therapy. Mol Cancer Ther. 2014;13(2):275-84. Epub 2014/01/18. doi: 10.1158/1535-7163.MCT-13-0791. PubMed PMID: 24435445; PMCID: PMC3946048.
52. Luke JJ, D'Adamo DR, Dickson MA, Keohan ML, Carvajal RD, Maki RG, de Stanchina E, Musi E, Singer S, Schwartz GK. The cyclin-dependent kinase inhibitor flavopiridol potentiates doxorubicin efficacy in advanced sarcomas: preclinical investigations and results of a phase I dose-escalation clinical trial. Clin Cancer Res. 2012;18(9):2638-47. Epub 2012/03/01. doi: 10.1158/1078-0432.CCR-11-3203. PubMed PMID: 22374332; PMCID: PMC3343204.
53. George S, Kasimis BS, Cogswell J, Schwarzenberger P, Shapiro GI, Fidias P, Bukowski RM. Phase I study of flavopiridol in combination with Paclitaxel and Carboplatin in patients with non-small-cell lung cancer. Clin Lung Cancer. 2008;9(3):160-5. Epub 2008/07/16. doi: 10.3816/CLC.2008.n.024. PubMed PMID: 18621626.
54. Ang C, O'Reilly EM, Carvajal RD, Capanu M, Gonen M, Doyle L, Ghossein R, Schwartz L, Jacobs G, Ma J, Schwartz GK, Abou-Alfa GK. A Nonrandomized, Phase II Study of Sequential Irinotecan and Flavopiridol in Patients With Advanced Hepatocellular Carcinoma. Gastrointest Cancer Res. 2012;5(6):185-9. Epub 2013/01/08. PubMed PMID: 23293699; PMCID: PMC3533846.
55. Parry D, Guzi T, Shanahan F, Davis N, Prabhavalkar D, Wiswell D, Seghezzi W, Paruch K, Dwyer MP, Doll R, Nomeir A, Windsor W, Fischmann T, Wang Y, Oft M, Chen T, Kirschmeier P, Lees EM. Dinaciclib (SCH 727965), a novel and potent cyclin-dependent kinase inhibitor. Mol Cancer Ther. 2010;9(8):2344-53. Epub 2010/07/29. doi: 10.1158/1535-7163.MCT-10-0324. PubMed PMID: 20663931.
56. Kumar SK, LaPlant B, Chng WJ, Zonder J, Callander N, Fonseca R, Fruth B, Roy V, Erlichman C, Stewart AK, Mayo Phase C. Dinaciclib, a novel CDK inhibitor, demonstrates encouraging single-agent activity in patients with relapsed multiple myeloma. Blood. 2015;125(3):443-8. Epub 2014/11/15. doi: 10.1182/blood-2014-05-573741. PubMed PMID: 25395429; PMCID: PMC4296007.
57. Flynn J, Jones J, Johnson AJ, Andritsos L, Maddocks K, Jaglowski S, Hessler J, Grever MR, Im E, Zhou H, Zhu Y, Zhang D, Small K, Bannerji R, Byrd JC. Dinaciclib is a novel cyclin-dependent kinase inhibitor with significant clinical activity in relapsed and refractory chronic lymphocytic leukemia. Leukemia. 2015;29(7):1524-9. Epub 2015/02/25. doi: 10.1038/leu.2015.31. PubMed PMID: 25708835; PMCID: PMC4551390.
58. Mita MM, Joy AA, Mita A, Sankhala K, Jou YM, Zhang D, Statkevich P, Zhu Y, Yao SL, Small K, Bannerji R, Shapiro CL. Randomized phase II trial of the cyclin-dependent kinase inhibitor dinaciclib (MK-7965) versus capecitabine in patients with advanced breast cancer. Clin Breast Cancer. 2014;14(3):169-76. Epub 2014/01/08. doi: 10.1016/j.clbc.2013.10.016. PubMed PMID: 24393852.
59. Stephenson JJ, Nemunaitis J, Joy AA, Martin JC, Jou YM, Zhang D, Statkevich P, Yao SL, Zhu Y, Zhou H, Small K, Bannerji R, Edelman MJ. Randomized phase 2 study of the cyclin-dependent kinase inhibitor dinaciclib (MK-7965) versus erlotinib in

patients with non-small cell lung cancer. Lung Cancer. 2014;83(2):219-23. Epub 2014/01/07. doi: 10.1016/j.lungcan.2013.11.020. PubMed PMID: 24388167.
60. Nemunaitis JJ, Small KA, Kirschmeier P, Zhang D, Zhu Y, Jou YM, Statkevich P, Yao SL, Bannerji R. A first-in-human, phase 1, dose-escalation study of dinaciclib, a novel cyclin-dependent kinase inhibitor, administered weekly in subjects with advanced malignancies. J Transl Med. 2013;11:259. Epub 2013/10/18. doi: 10.1186/1479-5876-11-259. PubMed PMID: 24131779; PMCID: PMC3853718.
61. Horiuchi D, Kusdra L, Huskey NE, Chandriani S, Lenburg ME, Gonzalez-Angulo AM, Creasman KJ, Bazarov AV, Smyth JW, Davis SE, Yaswen P, Mills GB, Esserman LJ, Goga A. MYC pathway activation in triple-negative breast cancer is synthetic lethal with CDK inhibition. J Exp Med. 2012;209(4):679-96. Epub 2012/03/21. doi: 10.1084/jem.20111512. PubMed PMID: 22430491; PMCID: PMC3328367.
62. Gregory GP, Hogg SJ, Kats LM, Vidacs E, Baker AJ, Gilan O, Lefebure M, Martin BP, Dawson MA, Johnstone RW, Shortt J. CDK9 inhibition by dinaciclib potently suppresses Mcl-1 to induce durable apoptotic responses in aggressive MYC-driven B-cell lymphoma in vivo. Leukemia. 2015;29(6):1437-41. Epub 2015/01/13. doi: 10.1038/leu.2015.10. PubMed PMID: 25578475; PMCID: PMC4498453.
63. Huang CH, Lujambio A, Zuber J, Tschaharganeh DF, Doran MG, Evans MJ, Kitzing T, Zhu N, de Stanchina E, Sawyers CL, Armstrong SA, Lewis JS, Sherr CJ, Lowe SW. CDK9-mediated transcription elongation is required for MYC addiction in hepatocellular carcinoma. Genes Dev. 2014;28(16):1800-14. Epub 2014/08/17. doi: 10.1101/gad.244368.114. PubMed PMID: 25128497; PMCID: PMC4197965.
64. Wang L, Wang J, Blaser BW, Duchemin AM, Kusewitt DF, Liu T, Caligiuri MA, Briesewitz R. Pharmacologic inhibition of CDK4/6: mechanistic evidence for selective activity or acquired resistance in acute myeloid leukemia. Blood. 2007;110(6):2075-83. Epub 2007/06/01. doi: 10.1182/blood-2007-02-071266. PubMed PMID: 17537993.
65. Baughn LB, Di Liberto M, Wu K, Toogood PL, Louie T, Gottschalk R, Niesvizky R, Cho H, Ely S, Moore MA, Chen-Kiang S. A novel orally active small molecule potently induces G1 arrest in primary myeloma cells and prevents tumor growth by specific inhibition of cyclin-dependent kinase 4/6. Cancer Res. 2006;66(15):7661-7. Epub 2006/08/04. doi: 10.1158/0008-5472.CAN-06-1098. PubMed PMID: 16885367.
66. Nemoto A, Saida S, Kato I, Kikuchi J, Furukawa Y, Maeda Y, Akahane K, Honna-Oshiro H, Goi K, Kagami K, Kimura S, Sato Y, Okabe S, Niwa A, Watanabe K, Nakahata T, Heike T, Sugita K, Inukai T. Specific Antileukemic Activity of PD0332991, a CDK4/6 Inhibitor, against Philadelphia Chromosome-Positive Lymphoid Leukemia. Mol Cancer Ther. 2016;15(1):94-105. Epub 2015/12/08. doi: 10.1158/1535-7163.MCT-14-1065. PubMed PMID: 26637365.
67. Sherr CJ, Beach D, Shapiro GI. Targeting CDK4 and CDK6: From Discovery to Therapy. Cancer Discov. 2016;6(4):353-67. Epub 2015/12/15. doi: 10.1158/2159-8290.CD-15-0894. PubMed PMID: 26658964; PMCID: PMC4821753.
68. Michaud K, Solomon DA, Oermann E, Kim JS, Zhong WZ, Prados MD, Ozawa T, James CD, Waldman T. Pharmacologic inhibition of cyclin-dependent kinases 4 and 6 arrests the growth of glioblastoma multiforme intracranial xenografts. Cancer Res.

2010;70(8):3228-38. Epub 2010/04/01. doi: 10.1158/0008-5472.CAN-09-4559. PubMed PMID: 20354191; PMCID: PMC2855904.
69. Bollard J, Miguela V, Ruiz de Galarreta M, Venkatesh A, Bian CB, Roberto MP, Tovar V, Sia D, Molina-Sanchez P, Nguyen CB, Nakagawa S, Llovet JM, Hoshida Y, Lujambio A. Palbociclib (PD-0332991), a selective CDK4/6 inhibitor, restricts tumour growth in preclinical models of hepatocellular carcinoma. Gut. 2017;66(7):1286-96. Epub 2016/11/17. doi: 10.1136/gutjnl-2016-312268. PubMed PMID: 27849562; PMCID: PMC5512174.
70. Dean JL, Thangavel C, McClendon AK, Reed CA, Knudsen ES. Therapeutic CDK4/6 inhibition in breast cancer: key mechanisms of response and failure. Oncogene. 2010;29(28):4018-32. Epub 2010/05/18. doi: 10.1038/onc.2010.154. PubMed PMID: 20473330.
71. Dhillon S. Palbociclib: first global approval. Drugs. 2015;75(5):543-51. Epub 2015/03/21. doi: 10.1007/s40265-015-0379-9. PubMed PMID: 25792301.
72. Melichar B, Adenis A, Lockhart AC, Bennouna J, Dees EC, Kayaleh O, Obermannova R, DeMichele A, Zatloukal P, Zhang B, Ullmann CD, Schusterbauer C. Safety and activity of alisertib, an investigational aurora kinase A inhibitor, in patients with breast cancer, small-cell lung cancer, non-small-cell lung cancer, head and neck squamous-cell carcinoma, and gastro-oesophageal adenocarcinoma: a five-arm phase 2 study. Lancet Oncol. 2015;16(4):395-405. Epub 2015/03/03. doi: 10.1016/S1470-2045(15)70051-3. PubMed PMID: 25728526.
73. Qi W, Cooke LS, Liu X, Rimsza L, Roe DJ, Manziolli A, Persky DO, Miller TP, Mahadevan D. Aurora inhibitor MLN8237 in combination with docetaxel enhances apoptosis and anti-tumor activity in mantle cell lymphoma. Biochem Pharmacol. 2011;81(7):881-90. Epub 2011/02/05. doi: 10.1016/j.bcp.2011.01.017. PubMed PMID: 21291867; PMCID: PMC3792566.
74. Brockmann M, Poon E, Berry T, Carstensen A, Deubzer HE, Rycak L, Jamin Y, Thway K, Robinson SP, Roels F, Witt O, Fischer M, Chesler L, Eilers M. Small Molecule Inhibitors of Aurora-A Induce Proteasomal Degradation of N-Myc in Childhood Neuroblastoma. Cancer Cell. 2016;30(2):357-8. Epub 2016/08/10. doi: 10.1016/j.ccell.2016.07.002. PubMed PMID: 27505677.
75. Dauch D, Rudalska R, Cossa G, Nault JC, Kang TW, Wuestefeld T, Hohmeyer A, Imbeaud S, Yevsa T, Hoenicke L, Pantsar T, Bozko P, Malek NP, Longerich T, Laufer S, Poso A, Zucman-Rossi J, Eilers M, Zender L. A MYC-aurora kinase A protein complex represents an actionable drug target in p53-altered liver cancer. Nat Med. 2016;22(7):744-53. Epub 2016/05/24. doi: 10.1038/nm.4107. PubMed PMID: 27213815.
76. Aihara A, Tanaka S, Yasen M, Matsumura S, Mitsunori Y, Murakata A, Noguchi N, Kudo A, Nakamura N, Ito K, Arii S. The selective Aurora B kinase inhibitor AZD1152 as a novel treatment for hepatocellular carcinoma. J Hepatol. 2010;52(1):63-71. Epub 2009/11/17. doi: 10.1016/j.jhep.2009.10.013. PubMed PMID: 19913935.
77. Foran J, Ravandi F, Wierda W, Garcia-Manero G, Verstovsek S, Kadia T, Burger J, Yule M, Langford G, Lyons J, Ayrton J, Lock V, Borthakur G, Cortes J, Kantarjian H. A phase I and pharmacodynamic study of AT9283, a small-molecule inhibitor of aurora

kinases in patients with relapsed/refractory leukemia or myelofibrosis. Clin Lymphoma Myeloma Leuk. 2014;14(3):223-30. Epub 2013/12/21. doi: 10.1016/j.clml.2013.11.001. PubMed PMID: 24355079; PMCID: PMC4096861.
78. Mita M, Gordon M, Rejeb N, Gianella-Borradori A, Jego V, Mita A, Sarantopoulos J, Sankhala K, Mendelson D. A phase l study of three different dosing schedules of the oral aurora kinase inhibitor MSC1992371A in patients with solid tumors. Target Oncol. 2014;9(3):215-24. Epub 2013/07/09. doi: 10.1007/s11523-013-0288-3. PubMed PMID: 23832397.
79. Fletcher GC, Brokx RD, Denny TA, Hembrough TA, Plum SM, Fogler WE, Sidor CF, Bray MR. ENMD-2076 is an orally active kinase inhibitor with antiangiogenic and antiproliferative mechanisms of action. Mol Cancer Ther. 2011;10(1):126-37. Epub 2010/12/24. doi: 10.1158/1535-7163.MCT-10-0574. PubMed PMID: 21177375.
80. Diamond JR, Bastos BR, Hansen RJ, Gustafson DL, Eckhardt SG, Kwak EL, Pandya SS, Fletcher GC, Pitts TM, Kulikowski GN, Morrow M, Arnott J, Bray MR, Sidor C, Messersmith W, Shapiro GI. Phase I safety, pharmacokinetic, and pharmacodynamic study of ENMD-2076, a novel angiogenic and Aurora kinase inhibitor, in patients with advanced solid tumors. Clin Cancer Res. 2011;17(4):849-60. Epub 2010/12/07. doi: 10.1158/1078-0432.CCR-10-2144. PubMed PMID: 21131552; PMCID: PMC3867298.
81. Boehm JS, Hahn WC. Towards systematic functional characterization of cancer genomes. Nat Rev Genet. 2011;12(7):487-98. Epub 2011/06/18. doi: 10.1038/nrg3013. PubMed PMID: 21681210.
82. Rad R, Rad L, Wang W, Cadinanos J, Vassiliou G, Rice S, Campos LS, Yusa K, Banerjee R, Li MA, de la Rosa J, Strong A, Lu D, Ellis P, Conte N, Yang FT, Liu P, Bradley A. PiggyBac transposon mutagenesis: a tool for cancer gene discovery in mice. Science. 2010;330(6007):1104-7. Epub 2010/10/16. doi: 10.1126/science.1193004. PubMed PMID: 20947725; PMCID: PMC3719098.
83. Starr TK, Allaei R, Silverstein KA, Staggs RA, Sarver AL, Bergemann TL, Gupta M, O'Sullivan MG, Matise I, Dupuy AJ, Collier LS, Powers S, Oberg AL, Asmann YW, Thibodeau SN, Tessarollo L, Copeland NG, Jenkins NA, Cormier RT, Largaespada DA. A transposon-based genetic screen in mice identifies genes altered in colorectal cancer. Science. 2009;323(5922):1747-50. Epub 2009/03/03. doi: 10.1126/science.1163040. PubMed PMID: 19251594; PMCID: PMC2743559.
84. Moriarity BS, Otto GM, Rahrmann EP, Rathe SK, Wolf NK, Weg MT, Manlove LA, LaRue RS, Temiz NA, Molyneux SD, Choi K, Holly KJ, Sarver AL, Scott MC, Forster CL, Modiano JF, Khanna C, Hewitt SM, Khokha R, Yang Y, Gorlick R, Dyer MA, Largaespada DA. A Sleeping Beauty forward genetic screen identifies new genes and pathways driving osteosarcoma development and metastasis. Nat Genet. 2015;47(6):615-24. Epub 2015/05/12. doi: 10.1038/ng.3293. PubMed PMID: 25961939; PMCID: PMC4767150.
85. Kodama T, Yi J, Newberg JY, Tien JC, Wu H, Finegold MJ, Kodama M, Wei Z, Tamura T, Takehara T, Johnson RL, Jenkins NA, Copeland NG. Molecular profiling of nonalcoholic fatty liver disease-associated hepatocellular carcinoma using SB transposon

mutagenesis. Proc Natl Acad Sci U S A. 2018;115(44):E10417-E26. Epub 2018/10/18. doi: 10.1073/pnas.1808968115. PubMed PMID: 30327349; PMCID: PMC6217425.
86. Kaelin WG, Jr. Molecular biology. Use and abuse of RNAi to study mammalian gene function. Science. 2012;337(6093):421-2. Epub 2012/07/28. doi: 10.1126/science.1225787. PubMed PMID: 22837515; PMCID: PMC3705935.
87. Jiang F, Doudna JA. CRISPR-Cas9 Structures and Mechanisms. Annu Rev Biophys. 2017;46:505-29. Epub 2017/04/05. doi: 10.1146/annurev-biophys-062215-010822. PubMed PMID: 28375731.
88. Lieber MR. The mechanism of double-strand DNA break repair by the nonhomologous DNA end-joining pathway. Annu Rev Biochem. 2010;79:181-211. Epub 2010/03/03. doi: 10.1146/annurev.biochem.052308.093131. PubMed PMID: 20192759; PMCID: PMC3079308.
89. Wang H, La Russa M, Qi LS. CRISPR/Cas9 in Genome Editing and Beyond. Annu Rev Biochem. 2016;85:227-64. Epub 2016/05/06. doi: 10.1146/annurev-biochem-060815-014607. PubMed PMID: 27145843.
90. Kweon J, Kim Y. High-throughput genetic screens using CRISPR-Cas9 system. Arch Pharm Res. 2018;41(9):875-84. Epub 2018/04/11. doi: 10.1007/s12272-018-1029-z. PubMed PMID: 29637495.
91. Shalem O, Sanjana NE, Zhang F. High-throughput functional genomics using CRISPR-Cas9. Nat Rev Genet. 2015;16(5):299-311. Epub 2015/04/10. doi: 10.1038/nrg3899. PubMed PMID: 25854182; PMCID: PMC4503232.
92. Shalem O, Sanjana NE, Hartenian E, Shi X, Scott DA, Mikkelson T, Heckl D, Ebert BL, Root DE, Doench JG, Zhang F. Genome-scale CRISPR-Cas9 knockout screening in human cells. Science. 2014;343(6166):84-7. Epub 2013/12/18. doi: 10.1126/science.1247005. PubMed PMID: 24336571; PMCID: PMC4089965.
93. Wang T, Wei JJ, Sabatini DM, Lander ES. Genetic screens in human cells using the CRISPR-Cas9 system. Science. 2014;343(6166):80-4. Epub 2013/12/18. doi: 10.1126/science.1246981. PubMed PMID: 24336569; PMCID: PMC3972032.
94. Hess GT, Fresard L, Han K, Lee CH, Li A, Cimprich KA, Montgomery SB, Bassik MC. Directed evolution using dCas9-targeted somatic hypermutation in mammalian cells. Nat Methods. 2016;13(12):1036-42. Epub 2016/11/01. doi: 10.1038/nmeth.4038. PubMed PMID: 27798611; PMCID: PMC5557288.
95. Li Q, Li Y, Yang S, Huang S, Yan M, Ding Y, Tang W, Lou X, Yin Q, Sun Z, Lu L, Shi H, Wang H, Chen Y, Li J. CRISPR-Cas9-mediated base-editing screening in mice identifies DND1 amino acids that are critical for primordial germ cell development. Nat Cell Biol. 2018;20(11):1315-25. Epub 2018/10/03. doi: 10.1038/s41556-018-0202-4. PubMed PMID: 30275529.
96. Konermann S, Brigham MD, Trevino AE, Joung J, Abudayyeh OO, Barcena C, Hsu PD, Habib N, Gootenberg JS, Nishimasu H, Nureki O, Zhang F. Genome-scale transcriptional activation by an engineered CRISPR-Cas9 complex. Nature. 2015;517(7536):583-8. Epub 2014/12/11. doi: 10.1038/nature14136. PubMed PMID: 25494202; PMCID: PMC4420636.

97. Klann TS, Black JB, Chellappan M, Safi A, Song L, Hilton IB, Crawford GE, Reddy TE, Gersbach CA. CRISPR-Cas9 epigenome editing enables high-throughput screening for functional regulatory elements in the human genome. Nat Biotechnol. 2017;35(6):561-8. Epub 2017/04/04. doi: 10.1038/nbt.3853. PubMed PMID: 28369033; PMCID: PMC5462860.
98. Liu Y, Cao Z, Wang Y, Guo Y, Xu P, Yuan P, Liu Z, He Y, Wei W. Genome-wide screening for functional long noncoding RNAs in human cells by Cas9 targeting of splice sites. Nat Biotechnol. 2018. Epub 2018/11/06. doi: 10.1038/nbt.4283. PubMed PMID: 30395134.
99. Wang T, Birsoy K, Hughes NW, Krupczak KM, Post Y, Wei JJ, Lander ES, Sabatini DM. Identification and characterization of essential genes in the human genome. Science. 2015;350(6264):1096-101. Epub 2015/10/17. doi: 10.1126/science.aac7041. PubMed PMID: 26472758; PMCID: PMC4662922.
100. Doench JG, Fusi N, Sullender M, Hegde M, Vaimberg EW, Donovan KF, Smith I, Tothova Z, Wilen C, Orchard R, Virgin HW, Listgarten J, Root DE. Optimized sgRNA design to maximize activity and minimize off-target effects of CRISPR-Cas9. Nat Biotechnol. 2016;34(2):184-91. Epub 2016/01/19. doi: 10.1038/nbt.3437. PubMed PMID: 26780180; PMCID: PMC4744125.
101. Cowley GS, Weir BA, Vazquez F, Tamayo P, Scott JA, Rusin S, East-Seletsky A, Ali LD, Gerath WF, Pantel SE, Lizotte PH, Jiang G, Hsiao J, Tsherniak A, Dwinell E, Aoyama S, Okamoto M, Harrington W, Gelfand E, Green TM, Tomko MJ, Gopal S, Wong TC, Li H, Howell S, Stransky N, Liefeld T, Jang D, Bistline J, Hill Meyers B, Armstrong SA, Anderson KC, Stegmaier K, Reich M, Pellman D, Boehm JS, Mesirov JP, Golub TR, Root DE, Hahn WC. Parallel genome-scale loss of function screens in 216 cancer cell lines for the identification of context-specific genetic dependencies. Sci Data. 2014;1:140035. Epub 2014/01/01. doi: 10.1038/sdata.2014.35. PubMed PMID: 25984343; PMCID: PMC4432652.
102. Tsherniak A, Vazquez F, Montgomery PG, Weir BA, Kryukov G, Cowley GS, Gill S, Harrington WF, Pantel S, Krill-Burger JM, Meyers RM, Ali L, Goodale A, Lee Y, Jiang G, Hsiao J, Gerath WFJ, Howell S, Merkel E, Ghandi M, Garraway LA, Root DE, Golub TR, Boehm JS, Hahn WC. Defining a Cancer Dependency Map. Cell. 2017;170(3):564-76 e16. Epub 2017/07/29. doi: 10.1016/j.cell.2017.06.010. PubMed PMID: 28753430; PMCID: PMC5667678.
103. Manguso RT, Pope HW, Zimmer MD, Brown FD, Yates KB, Miller BC, Collins NB, Bi K, LaFleur MW, Juneja VR, Weiss SA, Lo J, Fisher DE, Miao D, Van Allen E, Root DE, Sharpe AH, Doench JG, Haining WN. In vivo CRISPR screening identifies Ptpn2 as a cancer immunotherapy target. Nature. 2017;547(7664):413-8. Epub 2017/07/21. doi: 10.1038/nature23270. PubMed PMID: 28723893; PMCID: PMC5924693.
104. Song CQ, Li Y, Mou H, Moore J, Park A, Pomyen Y, Hough S, Kennedy Z, Fischer A, Yin H, Anderson DG, Conte D, Jr., Zender L, Wang XW, Thorgeirsson S, Weng Z, Xue W. Genome-Wide CRISPR Screen Identifies Regulators of Mitogen-Activated Protein Kinase as Suppressors of Liver Tumors in Mice. Gastroenterology.

2017;152(5):1161-73 e1. Epub 2016/12/14. doi: 10.1053/j.gastro.2016.12.002. PubMed PMID: 27956228; PMCID: PMC6204228.
105. Zhu M, Lu T, Jia Y, Luo X, Gopal P, Li L, Odewole M, Renteria V, Singal AG, Jang Y, Ge K, Wang SC, Sorouri M, Parekh JR, MacConmara MP, Yopp AC, Wang T, Zhu H. Somatic Mutations Increase Hepatic Clonal Fitness and Regeneration in Chronic Liver Disease. Cell. 2019;177(3):608-21 e12. Epub 2019/04/09. doi: 10.1016/j.cell.2019.03.026. PubMed PMID: 30955891; PMCID: PMC6519461.
106. Housden BE, Perrimon N. Comparing CRISPR and RNAi-based screening technologies. Nat Biotechnol. 2016;34(6):621-3. Epub 2016/06/10. doi: 10.1038/nbt.3599. PubMed PMID: 27281421.
107. DuPage M, Chopra G, Quiros J, Rosenthal WL, Morar MM, Holohan D, Zhang R, Turka L, Marson A, Bluestone JA. The chromatin-modifying enzyme Ezh2 is critical for the maintenance of regulatory T cell identity after activation. Immunity. 2015;42(2):227-38. doi: 10.1016/j.immuni.2015.01.007. PubMed PMID: 25680271; PMCID: PMC4347854.
108. Munoz DM, Cassiani PJ, Li L, Billy E, Korn JM, Jones MD, Golji J, Ruddy DA, Yu K, McAllister G, DeWeck A, Abramowski D, Wan J, Shirley MD, Neshat SY, Rakiec D, de Beaumont R, Weber O, Kauffmann A, McDonald ER, 3rd, Keen N, Hofmann F, Sellers WR, Schmelzle T, Stegmeier F, Schlabach MR. CRISPR Screens Provide a Comprehensive Assessment of Cancer Vulnerabilities but Generate False-Positive Hits for Highly Amplified Genomic Regions. Cancer Discov. 2016;6(8):900-13. Epub 2016/06/05. doi: 10.1158/2159-8290.CD-16-0178. PubMed PMID: 27260157.
109. Aguirre AJ, Meyers RM, Weir BA, Vazquez F, Zhang CZ, Ben-David U, Cook A, Ha G, Harrington WF, Doshi MB, Kost-Alimova M, Gill S, Xu H, Ali LD, Jiang G, Pantel S, Lee Y, Goodale A, Cherniack AD, Oh C, Kryukov G, Cowley GS, Garraway LA, Stegmaier K, Roberts CW, Golub TR, Meyerson M, Root DE, Tsherniak A, Hahn WC. Genomic Copy Number Dictates a Gene-Independent Cell Response to CRISPR/Cas9 Targeting. Cancer Discov. 2016;6(8):914-29. Epub 2016/06/05. doi: 10.1158/2159-8290.CD-16-0154. PubMed PMID: 27260156; PMCID: PMC4972686.
110. Haapaniemi E, Botla S, Persson J, Schmierer B, Taipale J. CRISPR-Cas9 genome editing induces a p53-mediated DNA damage response. Nat Med. 2018;24(7):927-30. Epub 2018/06/13. doi: 10.1038/s41591-018-0049-z. PubMed PMID: 29892067.
111. Kuscu C, Arslan S, Singh R, Thorpe J, Adli M. Genome-wide analysis reveals characteristics of off-target sites bound by the Cas9 endonuclease. Nat Biotechnol. 2014;32(7):677-83. Epub 2014/05/20. doi: 10.1038/nbt.2916. PubMed PMID: 24837660.
112. Schuster A, Erasimus H, Fritah S, Nazarov PV, van Dyck E, Niclou SP, Golebiewska A. RNAi/CRISPR Screens: from a Pool to a Valid Hit. Trends Biotechnol. 2019;37(1):38-55. Epub 2018/09/05. doi: 10.1016/j.tibtech.2018.08.002. PubMed PMID: 30177380.
113. Zender L, Xue W, Zuber J, Semighini CP, Krasnitz A, Ma B, Zender P, Kubicka S, Luk JM, Schirmacher P, McCombie WR, Wigler M, Hicks J, Hannon GJ, Powers S, Lowe SW. An oncogenomics-based in vivo RNAi screen identifies tumor suppressors in

liver cancer. Cell. 2008;135(5):852-64. Epub 2008/11/18. doi: 10.1016/j.cell.2008.09.061. PubMed PMID: 19012953; PMCID: PMC2990916.
114. Rudalska R, Dauch D, Longerich T, McJunkin K, Wuestefeld T, Kang TW, Hohmeyer A, Pesic M, Leibold J, von Thun A, Schirmacher P, Zuber J, Weiss KH, Powers S, Malek NP, Eilers M, Sipos B, Lowe SW, Geffers R, Laufer S, Zender L. In vivo RNAi screening identifies a mechanism of sorafenib resistance in liver cancer. Nat Med. 2014;20(10):1138-46. Epub 2014/09/14. doi: 10.1038/nm.3679. PubMed PMID: 25216638; PMCID: PMC4587571.
115. Takai A, Dang H, Oishi N, Khatib S, Martin SP, Dominguez DA, Luo J, Bagni R, Wu X, Powell K, Ye QH, Jia HL, Qin LX, Chen J, Mitchell GA, Luo X, Thorgeirsson SS, Wang XW. Genome-Wide RNAi Screen Identifies PMPCB as a Therapeutic Vulnerability in EpCAM(+) Hepatocellular Carcinoma. Cancer Res. 2019;79(9):2379-91. Epub 2019/03/14. doi: 10.1158/0008-5472.CAN-18-3015. PubMed PMID: 30862714; PMCID: PMC6497533.
116. Wang C, Jin H, Gao D, Wang L, Evers B, Xue Z, Jin G, Lieftink C, Beijersbergen RL, Qin W, Bernards R. A CRISPR screen identifies CDK7 as a therapeutic target in hepatocellular carcinoma. Cell Res. 2018;28(6):690-2. Epub 2018/03/07. doi: 10.1038/s41422-018-0020-z. PubMed PMID: 29507396; PMCID: PMC5993748.
117. McMahon SB, Van Buskirk HA, Dugan KA, Copeland TD, Cole MD. The novel ATM-related protein TRRAP is an essential cofactor for the c-Myc and E2F oncoproteins. Cell. 1998;94(3):363-74. Epub 1998/08/26. PubMed PMID: 9708738.
118. Murr R, Vaissiere T, Sawan C, Shukla V, Herceg Z. Orchestration of chromatin-based processes: mind the TRRAP. Oncogene. 2007;26(37):5358-72. Epub 2007/08/19. doi: 10.1038/sj.onc.1210605. PubMed PMID: 17694078.
119. Sikorski RS, Boguski MS, Goebl M, Hieter P. A repeating amino acid motif in CDC23 defines a family of proteins and a new relationship among genes required for mitosis and RNA synthesis. Cell. 1990;60(2):307-17. Epub 1990/01/26. PubMed PMID: 2404612.
120. Knutson BA, Hahn S. Domains of Tra1 important for activator recruitment and transcription coactivator functions of SAGA and NuA4 complexes. Mol Cell Biol. 2011;31(4):818-31. Epub 2010/12/15. doi: 10.1128/MCB.00687-10. PubMed PMID: 21149579; PMCID: PMC3028633.
121. Park J, Kunjibettu S, McMahon SB, Cole MD. The ATM-related domain of TRRAP is required for histone acetyltransferase recruitment and Myc-dependent oncogenesis. Genes Dev. 2001;15(13):1619-24. Epub 2001/07/11. doi: 10.1101/gad.900101. PubMed PMID: 11445536; PMCID: PMC312730.
122. Ard PG, Chatterjee C, Kunjibettu S, Adside LR, Gralinski LE, McMahon SB. Transcriptional regulation of the mdm2 oncogene by p53 requires TRRAP acetyltransferase complexes. Mol Cell Biol. 2002;22(16):5650-61. Epub 2002/07/26. doi: 10.1128/mcb.22.16.5650-5661.2002. PubMed PMID: 12138177; PMCID: PMC133988.
123. Jiang X, Sun Y, Chen S, Roy K, Price BD. The FATC domains of PIKK proteins are functionally equivalent and participate in the Tip60-dependent activation of DNA-

PKcs and ATM. J Biol Chem. 2006;281(23):15741-6. Epub 2006/04/11. doi: 10.1074/jbc.M513172200. PubMed PMID: 16603769.
124. Berg MD, Genereaux J, Karagiannis J, Brandl CJ. The Pseudokinase Domain of Saccharomyces cerevisiae Tra1 Is Required for Nuclear Localization and Incorporation into the SAGA and NuA4 Complexes. G3 (Bethesda). 2018;8(6):1943-57. Epub 2018/04/08. doi: 10.1534/g3.118.200288. PubMed PMID: 29626083; PMCID: PMC5982823.
125. Saleh A, Schieltz D, Ting N, McMahon SB, Litchfield DW, Yates JR, 3rd, Lees-Miller SP, Cole MD, Brandl CJ. Tra1p is a component of the yeast Ada.Spt transcriptional regulatory complexes. J Biol Chem. 1998;273(41):26559-65. Epub 1998/10/03. doi: 10.1074/jbc.273.41.26559. PubMed PMID: 9756893.
126. Herceg Z, Hulla W, Gell D, Cuenin C, Lleonart M, Jackson S, Wang ZQ. Disruption of Trrap causes early embryonic lethality and defects in cell cycle progression. Nat Genet. 2001;29(2):206-11. Epub 2001/09/07. doi: 10.1038/ng725. PubMed PMID: 11544477.
127. Ceol CJ, Horvitz HR. A new class of C. elegans synMuv genes implicates a Tip60/NuA4-like HAT complex as a negative regulator of Ras signaling. Dev Cell. 2004;6(4):563-76. Epub 2004/04/08. PubMed PMID: 15068795.
128. Myster SH, Wang F, Cavallo R, Christian W, Bhotika S, Anderson CT, Peifer M. Genetic and bioinformatic analysis of 41C and the 2R heterochromatin of Drosophila melanogaster: a window on the heterochromatin-euchromatin junction. Genetics. 2004;166(2):807-22. Epub 2004/03/17. PubMed PMID: 15020470; PMCID: PMC1470754.
129. Li H, Cuenin C, Murr R, Wang ZQ, Herceg Z. HAT cofactor Trrap regulates the mitotic checkpoint by modulation of Mad1 and Mad2 expression. EMBO J. 2004;23(24):4824-34. Epub 2004/11/19. doi: 10.1038/sj.emboj.7600479. PubMed PMID: 15549134; PMCID: PMC535091.
130. Herceg Z, Li H, Cuenin C, Shukla V, Radolf M, Steinlein P, Wang ZQ. Genome-wide analysis of gene expression regulated by the HAT cofactor Trrap in conditional knockout cells. Nucleic Acids Res. 2003;31(23):7011-23. Epub 2003/11/25. doi: 10.1093/nar/gkg902. PubMed PMID: 14627834; PMCID: PMC290270.
131. Sawan C, Hernandez-Vargas H, Murr R, Lopez F, Vaissiere T, Ghantous AY, Cuenin C, Imbert J, Wang ZQ, Ren B, Herceg Z. Histone acetyltransferase cofactor Trrap maintains self-renewal and restricts differentiation of embryonic stem cells. Stem Cells. 2013;31(5):979-91. Epub 2013/01/31. doi: 10.1002/stem.1341. PubMed PMID: 23362228.
132. Shukla V, Cuenin C, Dubey N, Herceg Z. Loss of histone acetyltransferase cofactor transformation/transcription domain-associated protein impairs liver regeneration after toxic injury. Hepatology. 2011;53(3):954-63. Epub 2011/02/15. doi: 10.1002/hep.24120. PubMed PMID: 21319192.
133. Tapias A, Zhou ZW, Shi Y, Chong Z, Wang P, Groth M, Platzer M, Huttner W, Herceg Z, Yang YG, Wang ZQ. Trrap-dependent histone acetylation specifically regulates cell-cycle gene transcription to control neural progenitor fate decisions. Cell

Stem Cell. 2014;14(5):632-43. Epub 2014/05/06. doi: 10.1016/j.stem.2014.04.001. PubMed PMID: 24792116.
134. Grant PA, Schieltz D, Pray-Grant MG, Yates JR, 3rd, Workman JL. The ATM-related cofactor Tra1 is a component of the purified SAGA complex. Mol Cell. 1998;2(6):863-7. Epub 1999/01/14. PubMed PMID: 9885573.
135. Brown CE, Howe L, Sousa K, Alley SC, Carrozza MJ, Tan S, Workman JL. Recruitment of HAT complexes by direct activator interactions with the ATM-related Tra1 subunit. Science. 2001;292(5525):2333-7. Epub 2001/06/26. doi: 10.1126/science.1060214. PubMed PMID: 11423663.
136. Bhaumik SR, Raha T, Aiello DP, Green MR. In vivo target of a transcriptional activator revealed by fluorescence resonance energy transfer. Genes Dev. 2004;18(3):333-43. Epub 2004/02/12. doi: 10.1101/gad.1148404. PubMed PMID: 14871930; PMCID: PMC338285.
137. Park J, Wood MA, Cole MD. BAF53 forms distinct nuclear complexes and functions as a critical c-Myc-interacting nuclear cofactor for oncogenic transformation. Mol Cell Biol. 2002;22(5):1307-16. Epub 2002/02/13. doi: 10.1128/mcb.22.5.1307-1316.2002. PubMed PMID: 11839798; PMCID: PMC134713.
138. Xu W, Edmondson DG, Evrard YA, Wakamiya M, Behringer RR, Roth SY. Loss of Gcn5l2 leads to increased apoptosis and mesodermal defects during mouse development. Nat Genet. 2000;26(2):229-32. Epub 2000/10/04. doi: 10.1038/79973. PubMed PMID: 11017084.
139. Yamauchi T, Yamauchi J, Kuwata T, Tamura T, Yamashita T, Bae N, Westphal H, Ozato K, Nakatani Y. Distinct but overlapping roles of histone acetylase PCAF and of the closely related PCAF-B/GCN5 in mouse embryogenesis. Proc Natl Acad Sci U S A. 2000;97(21):11303-6. Epub 2000/10/12. doi: 10.1073/pnas.97.21.11303. PubMed PMID: 11027331; PMCID: PMC17195.
140. Farria A, Li W, Dent SY. KATs in cancer: functions and therapies. Oncogene. 2015;34(38):4901-13. Epub 2015/02/11. doi: 10.1038/onc.2014.453. PubMed PMID: 25659580; PMCID: PMC4530097.
141. Cheung ACM, Diaz-Santin LM. Share and share alike: the role of Tra1 from the SAGA and NuA4 coactivator complexes. Transcription. 2019;10(1):37-43. Epub 2018/10/31. doi: 10.1080/21541264.2018.1530936. PubMed PMID: 30375921; PMCID: PMC6351133.
142. Atanassov BS, Evrard YA, Multani AS, Zhang Z, Tora L, Devys D, Chang S, Dent SY. Gcn5 and SAGA regulate shelterin protein turnover and telomere maintenance. Mol Cell. 2009;35(3):352-64. Epub 2009/08/18. doi: 10.1016/j.molcel.2009.06.015. PubMed PMID: 19683498; PMCID: PMC2749492.
143. Bondy-Chorney E, Denoncourt A, Sai Y, Downey M. Nonhistone targets of KAT2A and KAT2B implicated in cancer biology (1). Biochem Cell Biol. 2019;97(1):30-45. Epub 2018/04/20. doi: 10.1139/bcb-2017-0297. PubMed PMID: 29671337.
144. McMahon SB, Wood MA, Cole MD. The essential cofactor TRRAP recruits the histone acetyltransferase hGCN5 to c-Myc. Mol Cell Biol. 2000;20(2):556-62. Epub

1999/12/28. doi: 10.1128/mcb.20.2.556-562.2000. PubMed PMID: 10611234; PMCID: PMC85131.
145. Chen J, Luo Q, Yuan Y, Huang X, Cai W, Li C, Wei T, Zhang L, Yang M, Liu Q, Ye G, Dai X, Li B. Pygo2 associates with MLL2 histone methyltransferase and GCN5 histone acetyltransferase complexes to augment Wnt target gene expression and breast cancer stem-like cell expansion. Mol Cell Biol. 2010;30(24):5621-35. Epub 2010/10/13. doi: 10.1128/MCB.00465-10. PubMed PMID: 20937768; PMCID: PMC3004275.
146. Fazzio TG, Huff JT, Panning B. An RNAi screen of chromatin proteins identifies Tip60-p400 as a regulator of embryonic stem cell identity. Cell. 2008;134(1):162-74. Epub 2008/07/11. doi: 10.1016/j.cell.2008.05.031. PubMed PMID: 18614019; PMCID: PMC4308735.
147. Murr R, Loizou JI, Yang YG, Cuenin C, Li H, Wang ZQ, Herceg Z. Histone acetylation by Trrap-Tip60 modulates loading of repair proteins and repair of DNA double-strand breaks. Nat Cell Biol. 2006;8(1):91-9. Epub 2005/12/13. doi: 10.1038/ncb1343. PubMed PMID: 16341205.
148. Sapountzi V, Logan IR, Robson CN. Cellular functions of TIP60. Int J Biochem Cell Biol. 2006;38(9):1496-509. Epub 2006/05/16. doi: 10.1016/j.biocel.2006.03.003. PubMed PMID: 16698308.
149. Hayflick L, Moorhead PS. The serial cultivation of human diploid cell strains. Exp Cell Res. 1961;25:585-621. Epub 1961/12/01. PubMed PMID: 13905658.
150. Hayflick L. The Limited in Vitro Lifetime of Human Diploid Cell Strains. Exp Cell Res. 1965;37:614-36. Epub 1965/03/01. PubMed PMID: 14315085.
151. Kuilman T, Michaloglou C, Mooi WJ, Peeper DS. The essence of senescence. Genes Dev. 2010;24(22):2463-79. Epub 2010/11/17. doi: 10.1101/gad.1971610. PubMed PMID: 21078816; PMCID: PMC2975923.
152. Dimri GP, Lee X, Basile G, Acosta M, Scott G, Roskelley C, Medrano EE, Linskens M, Rubelj I, Pereira-Smith O, et al. A biomarker that identifies senescent human cells in culture and in aging skin in vivo. Proc Natl Acad Sci U S A. 1995;92(20):9363-7. Epub 1995/09/26. doi: 10.1073/pnas.92.20.9363. PubMed PMID: 7568133; PMCID: PMC40985.
153. Lee BY, Han JA, Im JS, Morrone A, Johung K, Goodwin EC, Kleijer WJ, DiMaio D, Hwang ES. Senescence-associated beta-galactosidase is lysosomal beta-galactosidase. Aging Cell. 2006;5(2):187-95. Epub 2006/04/22. doi: 10.1111/j.1474-9726.2006.00199.x. PubMed PMID: 16626397.
154. Debacq-Chainiaux F, Erusalimsky JD, Campisi J, Toussaint O. Protocols to detect senescence-associated beta-galactosidase (SA-betagal) activity, a biomarker of senescent cells in culture and in vivo. Nat Protoc. 2009;4(12):1798-806. Epub 2009/12/17. doi: 10.1038/nprot.2009.191. PubMed PMID: 20010931.
155. Narita M, Nunez S, Heard E, Narita M, Lin AW, Hearn SA, Spector DL, Hannon GJ, Lowe SW. Rb-mediated heterochromatin formation and silencing of E2F target genes during cellular senescence. Cell. 2003;113(6):703-16. Epub 2003/06/18. PubMed PMID: 12809602.

156. Freund A, Laberge RM, Demaria M, Campisi J. Lamin B1 loss is a senescence-associated biomarker. Mol Biol Cell. 2012;23(11):2066-75. Epub 2012/04/13. doi: 10.1091/mbc.E11-10-0884. PubMed PMID: 22496421; PMCID: PMC3364172.
157. Harley CB, Futcher AB, Greider CW. Telomeres shorten during ageing of human fibroblasts. Nature. 1990;345(6274):458-60. Epub 1990/05/31. doi: 10.1038/345458a0. PubMed PMID: 2342578.
158. d'Adda di Fagagna F, Reaper PM, Clay-Farrace L, Fiegler H, Carr P, Von Zglinicki T, Saretzki G, Carter NP, Jackson SP. A DNA damage checkpoint response in telomere-initiated senescence. Nature. 2003;426(6963):194-8. Epub 2003/11/11. doi: 10.1038/nature02118. PubMed PMID: 14608368.
159. Campisi J. Aging, cellular senescence, and cancer. Annu Rev Physiol. 2013;75:685-705. Epub 2012/11/13. doi: 10.1146/annurev-physiol-030212-183653. PubMed PMID: 23140366; PMCID: PMC4166529.
160. Beausejour CM, Krtolica A, Galimi F, Narita M, Lowe SW, Yaswen P, Campisi J. Reversal of human cellular senescence: roles of the p53 and p16 pathways. EMBO J. 2003;22(16):4212-22. Epub 2003/08/13. doi: 10.1093/emboj/cdg417. PubMed PMID: 12912919; PMCID: PMC175806.
161. Shih C, Padhy LC, Murray M, Weinberg RA. Transforming genes of carcinomas and neuroblastomas introduced into mouse fibroblasts. Nature. 1981;290(5803):261-4. Epub 1981/03/19. PubMed PMID: 7207618.
162. Land H, Parada LF, Weinberg RA. Tumorigenic conversion of primary embryo fibroblasts requires at least two cooperating oncogenes. Nature. 1983;304(5927):596-602. Epub 1983/08/18. PubMed PMID: 6308472.
163. Serrano M, Lin AW, McCurrach ME, Beach D, Lowe SW. Oncogenic ras provokes premature cell senescence associated with accumulation of p53 and p16INK4a. Cell. 1997;88(5):593-602. Epub 1997/03/07. PubMed PMID: 9054499.
164. Mallette FA, Ferbeyre G. The DNA damage signaling pathway connects oncogenic stress to cellular senescence. Cell Cycle. 2007;6(15):1831-6. Epub 2007/08/03. doi: 10.4161/cc.6.15.4516. PubMed PMID: 17671427.
165. Jones CJ, Kipling D, Morris M, Hepburn P, Skinner J, Bounacer A, Wyllie FS, Ivan M, Bartek J, Wynford-Thomas D, Bond JA. Evidence for a telomere-independent "clock" limiting RAS oncogene-driven proliferation of human thyroid epithelial cells. Mol Cell Biol. 2000;20(15):5690-9. Epub 2000/07/13. doi: 10.1128/mcb.20.15.5690-5699.2000. PubMed PMID: 10891505; PMCID: PMC86042.
166. Davies H, Bignell GR, Cox C, Stephens P, Edkins S, Clegg S, Teague J, Woffendin H, Garnett MJ, Bottomley W, Davis N, Dicks E, Ewing R, Floyd Y, Gray K, Hall S, Hawes R, Hughes J, Kosmidou V, Menzies A, Mould C, Parker A, Stevens C, Watt S, Hooper S, Wilson R, Jayatilake H, Gusterson BA, Cooper C, Shipley J, Hargrave D, Pritchard-Jones K, Maitland N, Chenevix-Trench G, Riggins GJ, Bigner DD, Palmieri G, Cossu A, Flanagan A, Nicholson A, Ho JW, Leung SY, Yuen ST, Weber BL, Seigler HF, Darrow TL, Paterson H, Marais R, Marshall CJ, Wooster R, Stratton MR, Futreal PA. Mutations of the BRAF gene in human cancer. Nature. 2002;417(6892):949-54. Epub 2002/06/18. doi: 10.1038/nature00766. PubMed PMID: 12068308.

167. Pollock PM, Harper UL, Hansen KS, Yudt LM, Stark M, Robbins CM, Moses TY, Hostetter G, Wagner U, Kakareka J, Salem G, Pohida T, Heenan P, Duray P, Kallioniemi O, Hayward NK, Trent JM, Meltzer PS. High frequency of BRAF mutations in nevi. Nat Genet. 2003;33(1):19-20. Epub 2002/11/26. doi: 10.1038/ng1054. PubMed PMID: 12447372.
168. Michaloglou C, Vredeveld LC, Soengas MS, Denoyelle C, Kuilman T, van der Horst CM, Majoor DM, Shay JW, Mooi WJ, Peeper DS. BRAFE600-associated senescence-like cell cycle arrest of human naevi. Nature. 2005;436(7051):720-4. Epub 2005/08/05. doi: 10.1038/nature03890. PubMed PMID: 16079850.
169. Gray-Schopfer VC, Cheong SC, Chong H, Chow J, Moss T, Abdel-Malek ZA, Marais R, Wynford-Thomas D, Bennett DC. Cellular senescence in naevi and immortalisation in melanoma: a role for p16? Br J Cancer. 2006;95(4):496-505. Epub 2006/08/02. doi: 10.1038/sj.bjc.6603283. PubMed PMID: 16880792; PMCID: PMC2360676.
170. Vergel M, Carnero A. Bypassing cellular senescence by genetic screening tools. Clin Transl Oncol. 2010;12(6):410-7. Epub 2010/06/11. doi: 10.1007/s12094-010-0528-2. PubMed PMID: 20534396.
171. Acosta JC, O'Loghlen A, Banito A, Guijarro MV, Augert A, Raguz S, Fumagalli M, Da Costa M, Brown C, Popov N, Takatsu Y, Melamed J, d'Adda di Fagagna F, Bernard D, Hernando E, Gil J. Chemokine signaling via the CXCR2 receptor reinforces senescence. Cell. 2008;133(6):1006-18. Epub 2008/06/17. doi: 10.1016/j.cell.2008.03.038. PubMed PMID: 18555777.
172. Lee S, Schmitt CA. The dynamic nature of senescence in cancer. Nat Cell Biol. 2019;21(1):94-101. Epub 2019/01/04. doi: 10.1038/s41556-018-0249-2. PubMed PMID: 30602768.
173. Funayama R, Saito M, Tanobe H, Ishikawa F. Loss of linker histone H1 in cellular senescence. J Cell Biol. 2006;175(6):869-80. Epub 2006/12/13. doi: 10.1083/jcb.200604005. PubMed PMID: 17158953; PMCID: PMC2064697.
174. Zhang R, Poustovoitov MV, Ye X, Santos HA, Chen W, Daganzo SM, Erzberger JP, Serebriiskii IG, Canutescu AA, Dunbrack RL, Pehrson JR, Berger JM, Kaufman PD, Adams PD. Formation of MacroH2A-containing senescence-associated heterochromatin foci and senescence driven by ASF1a and HIRA. Dev Cell. 2005;8(1):19-30. Epub 2004/12/29. doi: 10.1016/j.devcel.2004.10.019. PubMed PMID: 15621527.
175. Yu Y, Schleich K, Yue B, Ji S, Lohneis P, Kemper K, Silvis MR, Qutob N, van Rooijen E, Werner-Klein M, Li L, Dhawan D, Meierjohann S, Reimann M, Elkahloun A, Treitschke S, Dorken B, Speck C, Mallette FA, Zon LI, Holmen SL, Peeper DS, Samuels Y, Schmitt CA, Lee S. Targeting the Senescence-Overriding Cooperative Activity of Structurally Unrelated H3K9 Demethylases in Melanoma. Cancer Cell. 2018;33(2):322-36 e8. Epub 2018/02/14. doi: 10.1016/j.ccell.2018.01.002. PubMed PMID: 29438700; PMCID: PMC5977991.
176. Narita M, Narita M, Krizhanovsky V, Nunez S, Chicas A, Hearn SA, Myers MP, Lowe SW. A novel role for high-mobility group a proteins in cellular senescence and

heterochromatin formation. Cell. 2006;126(3):503-14. Epub 2006/08/12. doi: 10.1016/j.cell.2006.05.052. PubMed PMID: 16901784.
177. Di Micco R, Sulli G, Dobreva M, Liontos M, Botrugno OA, Gargiulo G, dal Zuffo R, Matti V, d'Ario G, Montani E, Mercurio C, Hahn WC, Gorgoulis V, Minucci S, d'Adda di Fagagna F. Interplay between oncogene-induced DNA damage response and heterochromatin in senescence and cancer. Nat Cell Biol. 2011;13(3):292-302. Epub 2011/02/22. doi: 10.1038/ncb2170. PubMed PMID: 21336312; PMCID: PMC3918344.
178. Salama R, Sadaie M, Hoare M, Narita M. Cellular senescence and its effector programs. Genes Dev. 2014;28(2):99-114. Epub 2014/01/23. doi: 10.1101/gad.235184.113. PubMed PMID: 24449267; PMCID: PMC3909793.
179. Coppe JP, Patil CK, Rodier F, Sun Y, Munoz DP, Goldstein J, Nelson PS, Desprez PY, Campisi J. Senescence-associated secretory phenotypes reveal cell-nonautonomous functions of oncogenic RAS and the p53 tumor suppressor. PLoS Biol. 2008;6(12):2853-68. Epub 2008/12/05. doi: 10.1371/journal.pbio.0060301. PubMed PMID: 19053174; PMCID: PMC2592359.
180. Rodier F, Coppe JP, Patil CK, Hoeijmakers WA, Munoz DP, Raza SR, Freund A, Campeau E, Davalos AR, Campisi J. Persistent DNA damage signalling triggers senescence-associated inflammatory cytokine secretion. Nat Cell Biol. 2009;11(8):973-9. Epub 2009/07/15. doi: 10.1038/ncb1909. PubMed PMID: 19597488; PMCID: PMC2743561.
181. Acosta JC, Banito A, Wuestefeld T, Georgilis A, Janich P, Morton JP, Athineos D, Kang TW, Lasitschka F, Andrulis M, Pascual G, Morris KJ, Khan S, Jin H, Dharmalingam G, Snijders AP, Carroll T, Capper D, Pritchard C, Inman GJ, Longerich T, Sansom OJ, Benitah SA, Zender L, Gil J. A complex secretory program orchestrated by the inflammasome controls paracrine senescence. Nat Cell Biol. 2013;15(8):978-90. Epub 2013/06/19. doi: 10.1038/ncb2784. PubMed PMID: 23770676; PMCID: PMC3732483.
182. Xue W, Zender L, Miething C, Dickins RA, Hernando E, Krizhanovsky V, Cordon-Cardo C, Lowe SW. Senescence and tumour clearance is triggered by p53 restoration in murine liver carcinomas. Nature. 2007;445(7128):656-60. Epub 2007/01/26. doi: 10.1038/nature05529. PubMed PMID: 17251933; PMCID: PMC4601097.
183. Coppe JP, Desprez PY, Krtolica A, Campisi J. The senescence-associated secretory phenotype: the dark side of tumor suppression. Annu Rev Pathol. 2010;5:99-118. Epub 2010/01/19. doi: 10.1146/annurev-pathol-121808-102144. PubMed PMID: 20078217; PMCID: PMC4166495.
184. Liu D, Hornsby PJ. Senescent human fibroblasts increase the early growth of xenograft tumors via matrix metalloproteinase secretion. Cancer Res. 2007;67(7):3117-26. Epub 2007/04/06. doi: 10.1158/0008-5472.CAN-06-3452. PubMed PMID: 17409418.
185. Marquardt JU, Andersen JB, Thorgeirsson SS. Functional and genetic deconstruction of the cellular origin in liver cancer. Nat Rev Cancer. 2015;15(11):653-67. Epub 2015/10/24. doi: 10.1038/nrc4017. PubMed PMID: 26493646.

186. Xue W, Wang XW. The search for precision models clinically relevant to human liver cancer. Hepat Oncol. 2015;2(4):315-9. Epub 2015/10/01. doi: 10.2217/hep.15.24. PubMed PMID: 30191010; PMCID: PMC6095146.
187. Martinez E, Palhan VB, Tjernberg A, Lymar ES, Gamper AM, Kundu TK, Chait BT, Roeder RG. Human STAGA complex is a chromatin-acetylating transcription coactivator that interacts with pre-mRNA splicing and DNA damage-binding factors in vivo. Mol Cell Biol. 2001;21(20):6782-95. Epub 2001/09/21. doi: 10.1128/MCB.21.20.6782-6795.2001. PubMed PMID: 11564863; PMCID: PMC99856.
188. Allard S, Utley RT, Savard J, Clarke A, Grant P, Brandl CJ, Pillus L, Workman JL, Cote J. NuA4, an essential transcription adaptor/histone H4 acetyltransferase complex containing Esa1p and the ATM-related cofactor Tra1p. EMBO J. 1999;18(18):5108-19. Epub 1999/09/16. doi: 10.1093/emboj/18.18.5108. PubMed PMID: 10487762; PMCID: PMC1171581.
189. Ikura T, Ogryzko VV, Grigoriev M, Groisman R, Wang J, Horikoshi M, Scully R, Qin J, Nakatani Y. Involvement of the TIP60 histone acetylase complex in DNA repair and apoptosis. Cell. 2000;102(4):463-73. Epub 2000/08/31. PubMed PMID: 10966108.
190. Wei X, Walia V, Lin JC, Teer JK, Prickett TD, Gartner J, Davis S, Program NCS, Stemke-Hale K, Davies MA, Gershenwald JE, Robinson W, Robinson S, Rosenberg SA, Samuels Y. Exome sequencing identifies GRIN2A as frequently mutated in melanoma. Nat Genet. 2011;43(5):442-6. Epub 2011/04/19. doi: 10.1038/ng.810. PubMed PMID: 21499247; PMCID: PMC3161250.
191. Hodis E, Watson IR, Kryukov GV, Arold ST, Imielinski M, Theurillat JP, Nickerson E, Auclair D, Li L, Place C, Dicara D, Ramos AH, Lawrence MS, Cibulskis K, Sivachenko A, Voet D, Saksena G, Stransky N, Onofrio RC, Winckler W, Ardlie K, Wagle N, Wargo J, Chong K, Morton DL, Stemke-Hale K, Chen G, Noble M, Meyerson M, Ladbury JE, Davies MA, Gershenwald JE, Wagner SN, Hoon DS, Schadendorf D, Lander ES, Gabriel SB, Getz G, Garraway LA, Chin L. A landscape of driver mutations in melanoma. Cell. 2012;150(2):251-63. Epub 2012/07/24. doi: 10.1016/j.cell.2012.06.024. PubMed PMID: 22817889; PMCID: PMC3600117.
192. Cancer Genome Atlas Research N, Kandoth C, Schultz N, Cherniack AD, Akbani R, Liu Y, Shen H, Robertson AG, Pashtan I, Shen R, Benz CC, Yau C, Laird PW, Ding L, Zhang W, Mills GB, Kucherlapati R, Mardis ER, Levine DA. Integrated genomic characterization of endometrial carcinoma. Nature. 2013;497(7447):67-73. Epub 2013/05/03. doi: 10.1038/nature12113. PubMed PMID: 23636398; PMCID: PMC3704730.
193. Kalkat M, Resetca D, Lourenco C, Chan PK, Wei Y, Shiah YJ, Vitkin N, Tong Y, Sunnerhagen M, Done SJ, Boutros PC, Raught B, Penn LZ. MYC Protein Interactome Profiling Reveals Functionally Distinct Regions that Cooperate to Drive Tumorigenesis. Mol Cell. 2018;72(5):836-48 e7. Epub 2018/11/13. doi: 10.1016/j.molcel.2018.09.031. PubMed PMID: 30415952.
194. Wurdak H, Zhu S, Romero A, Lorger M, Watson J, Chiang CY, Zhang J, Natu VS, Lairson LL, Walker JR, Trussell CM, Harsh GR, Vogel H, Felding-Habermann B, Orth AP, Miraglia LJ, Rines DR, Skirboll SL, Schultz PG. An RNAi screen identifies

TRRAP as a regulator of brain tumor-initiating cell differentiation. Cell Stem Cell. 2010;6(1):37-47. Epub 2010/01/21. doi: 10.1016/j.stem.2009.11.002. PubMed PMID: 20085741.
195. Jethwa A, Slabicki M, Hullein J, Jentzsch M, Dalal V, Rabe S, Wagner L, Walther T, Klapper W, Bohnenberger H, Rettel M, Lu J, Smits AH, Stein F, Savitski MM, Huber W, Aylon Y, Oren M, Zenz T. TRRAP is essential for regulating the accumulation of mutant and wild-type p53 in lymphoma. Blood. 2018. Epub 2018/04/15. doi: 10.1182/blood-2017-09-806679. PubMed PMID: 29653964.
196. Lin ZZ, Jeng YM, Hu FC, Pan HW, Tsao HW, Lai PL, Lee PH, Cheng AL, Hsu HC. Significance of Aurora B overexpression in hepatocellular carcinoma. Aurora B Overexpression in HCC. BMC Cancer. 2010;10:461. Epub 2010/08/31. doi: 10.1186/1471-2407-10-461. PubMed PMID: 20799978; PMCID: PMC2940801.
197. Yeh HW, Lee SS, Chang CY, Hu CM, Jou YS. Pyrimidine metabolic rate limiting enzymes in poorly-differentiated hepatocellular carcinoma are signature genes of cancer stemness and associated with poor prognosis. Oncotarget. 2017;8(44):77734-51. Epub 2017/11/05. doi: 10.18632/oncotarget.20774. PubMed PMID: 29100421; PMCID: PMC5652811.
198. Hu H, Zhu W, Qin J, Chen M, Gong L, Li L, Liu X, Tao Y, Yin H, Zhou H, Zhou L, Ye D, Ye Q, Gao D. Acetylation of PGK1 promotes liver cancer cell proliferation and tumorigenesis. Hepatology. 2017;65(2):515-28. Epub 2016/10/25. doi: 10.1002/hep.28887. PubMed PMID: 27774669.
199. Yang XM, Cao XY, He P, Li J, Feng MX, Zhang YL, Zhang XL, Wang YH, Yang Q, Zhu L, Nie HZ, Jiang SH, Tian GA, Zhang XX, Liu Q, Ji J, Zhu X, Xia Q, Zhang ZG. Overexpression of Rac GTPase Activating Protein 1 Contributes to Proliferation of Cancer Cells by Reducing Hippo Signaling to Promote Cytokinesis. Gastroenterology. 2018;155(4):1233-49 e22. Epub 2018/07/17. doi: 10.1053/j.gastro.2018.07.010. PubMed PMID: 30009820.
200. Lee N, Kwon JH, Kim YB, Kim SH, Park SJ, Xu W, Jung HY, Kim KT, Wang HJ, Choi KY. Vaccinia-related kinase 1 promotes hepatocellular carcinoma by controlling the levels of cell cycle regulators associated with G1/S transition. Oncotarget. 2015;6(30):30130-48. Epub 2015/09/17. doi: 10.18632/oncotarget.4967. PubMed PMID: 26375549; PMCID: PMC4745786.
201. Zender L, Spector MS, Xue W, Flemming P, Cordon-Cardo C, Silke J, Fan ST, Luk JM, Wigler M, Hannon GJ, Mu D, Lucito R, Powers S, Lowe SW. Identification and validation of oncogenes in liver cancer using an integrative oncogenomic approach. Cell. 2006;125(7):1253-67. Epub 2006/07/04. doi: 10.1016/j.cell.2006.05.030. PubMed PMID: 16814713; PMCID: PMC3026384.
202. Zhang Y, Shi J, Liu X, Feng L, Gong Z, Koppula P, Sirohi K, Li X, Wei Y, Lee H, Zhuang L, Chen G, Xiao ZD, Hung MC, Chen J, Huang P, Li W, Gan B. BAP1 links metabolic regulation of ferroptosis to tumour suppression. Nat Cell Biol. 2018;20(10):1181-92. Epub 2018/09/12. doi: 10.1038/s41556-018-0178-0. PubMed PMID: 30202049; PMCID: PMC6170713.

203. Ravens S, Yu C, Ye T, Stierle M, Tora L. Tip60 complex binds to active Pol II promoters and a subset of enhancers and co-regulates the c-Myc network in mouse embryonic stem cells. Epigenetics Chromatin. 2015;8:45. Epub 2015/11/10. doi: 10.1186/s13072-015-0039-z. PubMed PMID: 26550034; PMCID: PMC4636812.
204. Chen T, Sun Y, Ji P, Kopetz S, Zhang W. Topoisomerase IIalpha in chromosome instability and personalized cancer therapy. Oncogene. 2015;34(31):4019-31. Epub 2014/10/21. doi: 10.1038/onc.2014.332. PubMed PMID: 25328138; PMCID: PMC4404185.
205. Carter SL, Eklund AC, Kohane IS, Harris LN, Szallasi Z. A signature of chromosomal instability inferred from gene expression profiles predicts clinical outcome in multiple human cancers. Nat Genet. 2006;38(9):1043-8. Epub 2006/08/22. doi: 10.1038/ng1861. PubMed PMID: 16921376.
206. Weiler SME, Pinna F, Wolf T, Lutz T, Geldiyev A, Sticht C, Knaub M, Thomann S, Bissinger M, Wan S, Rossler S, Becker D, Gretz N, Lang H, Bergmann F, Ustiyan V, Kalin TV, Singer S, Lee JS, Marquardt JU, Schirmacher P, Kalinichenko VV, Breuhahn K. Induction of Chromosome Instability by Activation of Yes-Associated Protein and Forkhead Box M1 in Liver Cancer. Gastroenterology. 2017;152(8):2037-51 e22. Epub 2017/03/03. doi: 10.1053/j.gastro.2017.02.018. PubMed PMID: 28249813.
207. Mu X, Espanol-Suner R, Mederacke I, Affo S, Manco R, Sempoux C, Lemaigre FP, Adili A, Yuan D, Weber A, Unger K, Heikenwalder M, Leclercq IA, Schwabe RF. Hepatocellular carcinoma originates from hepatocytes and not from the progenitor/biliary compartment. J Clin Invest. 2015;125(10):3891-903. Epub 2015/09/09. doi: 10.1172/JCI77995. PubMed PMID: 26348897; PMCID: PMC4607132.
208. Yan T, Lu L, Xie C, Chen J, Peng X, Zhu L, Wang Y, Li Q, Shi J, Zhou F, Hu M, Liu Z. Severely Impaired and Dysregulated Cytochrome P450 Expression and Activities in Hepatocellular Carcinoma: Implications for Personalized Treatment in Patients. Mol Cancer Ther. 2015;14(12):2874-86. Epub 2015/10/31. doi: 10.1158/1535-7163.MCT-15-0274. PubMed PMID: 26516155; PMCID: PMC4674380.
209. Li T, Apte U. Bile Acid Metabolism and Signaling in Cholestasis, Inflammation, and Cancer. Adv Pharmacol. 2015;74:263-302. Epub 2015/08/04. doi: 10.1016/bs.apha.2015.04.003. PubMed PMID: 26233910; PMCID: PMC4615692.
210. Wang M, Han J, Xing H, Zhang H, Li Z, Liang L, Li C, Dai S, Wu M, Shen F, Yang T. Dysregulated fatty acid metabolism in hepatocellular carcinoma. Hepat Oncol. 2016;3(4):241-51. Epub 2016/10/01. doi: 10.2217/hep-2016-0012. PubMed PMID: 30191046; PMCID: PMC6095185.
211. Johnson MR, Barnes S, Kwakye JB, Diasio RB. Purification and characterization of bile acid-CoA:amino acid N-acyltransferase from human liver. J Biol Chem. 1991;266(16):10227-33. Epub 1991/06/05. PubMed PMID: 2037576.
212. Pellicoro A, van den Heuvel FA, Geuken M, Moshage H, Jansen PL, Faber KN. Human and rat bile acid-CoA:amino acid N-acyltransferase are liver-specific peroxisomal enzymes: implications for intracellular bile salt transport. Hepatology. 2007;45(2):340-8. Epub 2007/01/30. doi: 10.1002/hep.21528. PubMed PMID: 17256745.

213. Wang AG, Yoon SY, Oh JH, Jeon YJ, Kim M, Kim JM, Byun SS, Yang JO, Kim JH, Kim DG, Yeom YI, Yoo HS, Kim YS, Kim NS. Identification of intrahepatic cholangiocarcinoma related genes by comparison with normal liver tissues using expressed sequence tags. Biochem Biophys Res Commun. 2006;345(3):1022-32. Epub 2006/05/23. doi: 10.1016/j.bbrc.2006.04.175. PubMed PMID: 16712791.
214. Fan T, Rong Z, Dong J, Li J, Wang K, Wang X, Li H, Chen J, Wang F, Wang J, Wang A. Metabolomic and transcriptomic profiling of hepatocellular carcinomas in Hras12V transgenic mice. Cancer Med. 2017;6(10):2370-84. Epub 2017/09/25. doi: 10.1002/cam4.1177. PubMed PMID: 28941178; PMCID: PMC5633588.
215. Yang Y, Qin SK, Wu Q, Wang ZS, Zheng RS, Tong XH, Liu H, Tao L, He XD. Connexin-dependent gap junction enhancement is involved in the synergistic effect of sorafenib and all-trans retinoic acid on HCC growth inhibition. Oncol Rep. 2014;31(2):540-50. Epub 2013/12/10. doi: 10.3892/or.2013.2894. PubMed PMID: 24317203; PMCID: PMC3896525.
216. Udali S, Guarini P, Ruzzenente A, Ferrarini A, Guglielmi A, Lotto V, Tononi P, Pattini P, Moruzzi S, Campagnaro T, Conci S, Olivieri O, Corrocher R, Delledonne M, Choi SW, Friso S. DNA methylation and gene expression profiles show novel regulatory pathways in hepatocellular carcinoma. Clin Epigenetics. 2015;7:43. Epub 2015/05/07. doi: 10.1186/s13148-015-0077-1. PubMed PMID: 25945129; PMCID: PMC4419480.
217. Hu PS, Xia QS, Wu F, Li DK, Qi YJ, Hu Y, Wei ZZ, Li SS, Tian NY, Wei QF, Shen LJ, Yin B, Jiang T, Yuan JG, Qiang BQ, Han W, Peng XZ. NSPc1 promotes cancer stem cell self-renewal by repressing the synthesis of all-trans retinoic acid via targeting RDH16 in malignant glioma. Oncogene. 2017;36(33):4706-18. Epub 2017/04/11. doi: 10.1038/onc.2017.34. PubMed PMID: 28394339.
218. Zhuo L, Hascall VC, Kimata K. Inter-alpha-trypsin inhibitor, a covalent protein-glycosaminoglycan-protein complex. J Biol Chem. 2004;279(37):38079-82. Epub 2004/05/21. doi: 10.1074/jbc.R300039200. PubMed PMID: 15151994.
219. Subrungruanga I, Thawornkunob C, Chawalitchewinkoon-Petmitrc P, Pairojkul C, Wongkham S, Petmitrb S. Gene expression profiling of intrahepatic cholangiocarcinoma. Asian Pac J Cancer Prev. 2013;14(1):557-63. Epub 2013/03/29. PubMed PMID: 23534794.
220. Li Y, Jaramillo-Lambert A, Hao J, Yang Y, Zhu W. The stability of histone acetyltransferase general control non-derepressible (Gcn) 5 is regulated by Cullin4-RING E3 ubiquitin ligase. J Biol Chem. 2011;286(48):41344-52. Epub 2011/10/12. doi: 10.1074/jbc.M111.290767. PubMed PMID: 21987584; PMCID: PMC3308846.
221. Du T, Nagai Y, Xiao Y, Greene MI, Zhang H. Lysosome-dependent p300/FOXP3 degradation and limits Treg cell functions and enhances targeted therapy against cancers. Exp Mol Pathol. 2013;95(1):38-45. Epub 2013/05/07. doi: 10.1016/j.yexmp.2013.04.003. PubMed PMID: 23644046; PMCID: PMC3963828.
222. Wilkie GS, Dickson KS, Gray NK. Regulation of mRNA translation by 5'- and 3'-UTR-binding factors. Trends Biochem Sci. 2003;28(4):182-8. Epub 2003/04/26. doi: 10.1016/S0968-0004(03)00051-3. PubMed PMID: 12713901.

223. Chen M, Lyu G, Han M, Nie H, Shen T, Chen W, Niu Y, Song Y, Li X, Li H, Chen X, Wang Z, Xia Z, Li W, Tian XL, Ding C, Gu J, Zheng Y, Liu X, Hu J, Wei G, Tao W, Ni T. 3' UTR lengthening as a novel mechanism in regulating cellular senescence. Genome Res. 2018. Epub 2018/02/15. doi: 10.1101/gr.224451.117. PubMed PMID: 29440281; PMCID: PMC5848608.
224. Sun Y, Jiang X, Chen S, Fernandes N, Price BD. A role for the Tip60 histone acetyltransferase in the acetylation and activation of ATM. Proc Natl Acad Sci U S A. 2005;102(37):13182-7. Epub 2005/09/06. doi: 10.1073/pnas.0504211102. PubMed PMID: 16141325; PMCID: PMC1197271.
225. Acharya D, Hainer SJ, Yoon Y, Wang F, Bach I, Rivera-Perez JA, Fazzio TG. KAT-Independent Gene Regulation by Tip60 Promotes ESC Self-Renewal but Not Pluripotency. Cell Rep. 2017;19(4):671-9. Epub 2017/04/27. doi: 10.1016/j.celrep.2017.04.001. PubMed PMID: 28445719; PMCID: PMC5484067.
226. Wang X, Ahmad S, Zhang Z, Cote J, Cai G. Architecture of the Saccharomyces cerevisiae NuA4/TIP60 complex. Nat Commun. 2018;9(1):1147. Epub 2018/03/22. doi: 10.1038/s41467-018-03504-5. PubMed PMID: 29559617; PMCID: PMC5861120.
227. Gao C, Bourke E, Scobie M, Famme MA, Koolmeister T, Helleday T, Eriksson LA, Lowndes NF, Brown JA. Rational design and validation of a Tip60 histone acetyltransferase inhibitor. Sci Rep. 2014;4:5372. Epub 2014/06/21. doi: 10.1038/srep05372. PubMed PMID: 24947938; PMCID: PMC4064327.
228. Li W, Xu H, Xiao T, Cong L, Love MI, Zhang F, Irizarry RA, Liu JS, Brown M, Liu XS. MAGeCK enables robust identification of essential genes from genome-scale CRISPR/Cas9 knockout screens. Genome Biol. 2014;15(12):554. Epub 2014/12/06. doi: 10.1186/s13059-014-0554-4. PubMed PMID: 25476604; PMCID: PMC4290824.
229. Lee JS, Chu IS, Mikaelyan A, Calvisi DF, Heo J, Reddy JK, Thorgeirsson SS. Application of comparative functional genomics to identify best-fit mouse models to study human cancer. Nat Genet. 2004;36(12):1306-11. Epub 2004/11/27. doi: 10.1038/ng1481. PubMed PMID: 15565109.
230. Lee JS, Heo J, Libbrecht L, Chu IS, Kaposi-Novak P, Calvisi DF, Mikaelyan A, Roberts LR, Demetris AJ, Sun Z, Nevens F, Roskams T, Thorgeirsson SS. A novel prognostic subtype of human hepatocellular carcinoma derived from hepatic progenitor cells. Nat Med. 2006;12(4):410-6. Epub 2006/03/15. doi: 10.1038/nm1377. PubMed PMID: 16532004.
231. Weber J, Ollinger R, Friedrich M, Ehmer U, Barenboim M, Steiger K, Heid I, Mueller S, Maresch R, Engleitner T, Gross N, Geumann U, Fu B, Segler A, Yuan D, Lange S, Strong A, de la Rosa J, Esposito I, Liu P, Cadinanos J, Vassiliou GS, Schmid RM, Schneider G, Unger K, Yang F, Braren R, Heikenwalder M, Varela I, Saur D, Bradley A, Rad R. CRISPR/Cas9 somatic multiplex-mutagenesis for high-throughput functional cancer genomics in mice. Proc Natl Acad Sci U S A. 2015;112(45):13982-7. Epub 2015/10/29. doi: 10.1073/pnas.1512392112. PubMed PMID: 26508638; PMCID: PMC4653208.
232. Dobin A, Davis CA, Schlesinger F, Drenkow J, Zaleski C, Jha S, Batut P, Chaisson M, Gingeras TR. STAR: ultrafast universal RNA-seq aligner. Bioinformatics.

2013;29(1):15-21. Epub 2012/10/30. doi: 10.1093/bioinformatics/bts635. PubMed PMID: 23104886; PMCID: PMC3530905.
233. Li B, Dewey CN. RSEM: accurate transcript quantification from RNA-Seq data with or without a reference genome. BMC Bioinformatics. 2011;12:323. Epub 2011/08/06. doi: 10.1186/1471-2105-12-323. PubMed PMID: 21816040; PMCID: PMC3163565.
234. Love MI, Huber W, Anders S. Moderated estimation of fold change and dispersion for RNA-seq data with DESeq2. Genome Biol. 2014;15(12):550. Epub 2014/12/18. doi: 10.1186/s13059-014-0550-8. PubMed PMID: 25516281; PMCID: PMC4302049.
235. Anders S, Pyl PT, Huber W. HTSeq--a Python framework to work with high-throughput sequencing data. Bioinformatics. 2015;31(2):166-9. Epub 2014/09/28. doi: 10.1093/bioinformatics/btu638. PubMed PMID: 25260700; PMCID: PMC4287950.
236. Leduc C, Chemin G, Puget N, Sawan C, Moutahir M, Herceg Z, Khamlichi AA. Tissue-specific inactivation of HAT cofactor TRRAP reveals its essential role in B cells. Cell Cycle. 2014;13(10):1583-9. Epub 2014/03/29. doi: 10.4161/cc.28560. PubMed PMID: 24675885; PMCID: PMC4050163.
237. Tang Y, Luo J, Zhang W, Gu W. Tip60-dependent acetylation of p53 modulates the decision between cell-cycle arrest and apoptosis. Mol Cell. 2006;24(6):827-39. Epub 2006/12/26. doi: 10.1016/j.molcel.2006.11.021. PubMed PMID: 17189186.
238. Miyamoto N, Izumi H, Noguchi T, Nakajima Y, Ohmiya Y, Shiota M, Kidani A, Tawara A, Kohno K. Tip60 is regulated by circadian transcription factor clock and is involved in cisplatin resistance. J Biol Chem. 2008;283(26):18218-26. Epub 2008/05/07. doi: 10.1074/jbc.M802332200. PubMed PMID: 18458078.
239. Halkidou K, Gnanapragasam VJ, Mehta PB, Logan IR, Brady ME, Cook S, Leung HY, Neal DE, Robson CN. Expression of Tip60, an androgen receptor coactivator, and its role in prostate cancer development. Oncogene. 2003;22(16):2466-77. Epub 2003/04/30. doi: 10.1038/sj.onc.1206342. PubMed PMID: 12717424.
240. Hernandez-Segura A, Nehme J, Demaria M. Hallmarks of Cellular Senescence. Trends Cell Biol. 2018;28(6):436-53. Epub 2018/02/27. doi: 10.1016/j.tcb.2018.02.001. PubMed PMID: 29477613.
241. Munoz-Espin D, Serrano M. Cellular senescence: from physiology to pathology. Nat Rev Mol Cell Biol. 2014;15(7):482-96. Epub 2014/06/24. doi: 10.1038/nrm3823. PubMed PMID: 24954210.
242. Akimitsu N, Adachi N, Hirai H, Hossain MS, Hamamoto H, Kobayashi M, Aratani Y, Koyama H, Sekimizu K. Enforced cytokinesis without complete nuclear division in embryonic cells depleting the activity of DNA topoisomerase IIalpha. Genes Cells. 2003;8(4):393-402. Epub 2003/03/26. PubMed PMID: 12653966.
243. Carpenter AJ, Porter AC. Construction, characterization, and complementation of a conditional-lethal DNA topoisomerase IIalpha mutant human cell line. Mol Biol Cell. 2004;15(12):5700-11. Epub 2004/10/01. doi: 10.1091/mbc.e04-08-0732. PubMed PMID: 15456904; PMCID: PMC532048.

244. Negri C, Bernardi R, Donzelli M, Scovassi AI. Induction of apoptotic cell death by DNA topoisomerase II inhibitors. Biochimie. 1995;77(11):893-9. Epub 1995/01/01. PubMed PMID: 8824770.
245. Elmore LW, Rehder CW, Di X, McChesney PA, Jackson-Cook CK, Gewirtz DA, Holt SE. Adriamycin-induced senescence in breast tumor cells involves functional p53 and telomere dysfunction. J Biol Chem. 2002;277(38):35509-15. Epub 2002/07/09. doi: 10.1074/jbc.M205477200. PubMed PMID: 12101184.
246. Wang Y, Zhu S, Cloughesy TF, Liau LM, Mischel PS. p53 disruption profoundly alters the response of human glioblastoma cells to DNA topoisomerase I inhibition. Oncogene. 2004;23(6):1283-90. Epub 2004/02/13. doi: 10.1038/sj.onc.1207244. PubMed PMID: 14961077.
247. Lee JJ, Kim BC, Park MJ, Lee YS, Kim YN, Lee BL, Lee JS. PTEN status switches cell fate between premature senescence and apoptosis in glioma exposed to ionizing radiation. Cell Death Differ. 2011;18(4):666-77. Epub 2010/11/13. doi: 10.1038/cdd.2010.139. PubMed PMID: 21072054; PMCID: PMC3131905.
248. Eom YW, Kim MA, Park SS, Goo MJ, Kwon HJ, Sohn S, Kim WH, Yoon G, Choi KS. Two distinct modes of cell death induced by doxorubicin: apoptosis and cell death through mitotic catastrophe accompanied by senescence-like phenotype. Oncogene. 2005;24(30):4765-77. Epub 2005/05/05. doi: 10.1038/sj.onc.1208627. PubMed PMID: 15870702.
249. Young AP, Schlisio S, Minamishima YA, Zhang Q, Li L, Grisanzio C, Signoretti S, Kaelin WG, Jr. VHL loss actuates a HIF-independent senescence programme mediated by Rb and p400. Nat Cell Biol. 2008;10(3):361-9. Epub 2008/02/26. doi: 10.1038/ncb1699. PubMed PMID: 18297059.
250. Campaner S, Doni M, Hydbring P, Verrecchia A, Bianchi L, Sardella D, Schleker T, Perna D, Tronnersjo S, Murga M, Fernandez-Capetillo O, Barbacid M, Larsson LG, Amati B. Cdk2 suppresses cellular senescence induced by the c-myc oncogene. Nat Cell Biol. 2010;12(1):54-9; sup pp 1-14. Epub 2009/12/17. doi: 10.1038/ncb2004. PubMed PMID: 20010815.
251. Lin HK, Chen Z, Wang G, Nardella C, Lee SW, Chan CH, Yang WL, Wang J, Egia A, Nakayama KI, Cordon-Cardo C, Teruya-Feldstein J, Pandolfi PP. Skp2 targeting suppresses tumorigenesis by Arf-p53-independent cellular senescence. Nature. 2010;464(7287):374-9. Epub 2010/03/20. doi: 10.1038/nature08815. PubMed PMID: 20237562; PMCID: PMC2928066.
252. Senturk S, Mumcuoglu M, Gursoy-Yuzugullu O, Cingoz B, Akcali KC, Ozturk M. Transforming growth factor-beta induces senescence in hepatocellular carcinoma cells and inhibits tumor growth. Hepatology. 2010;52(3):966-74. Epub 2010/06/29. doi: 10.1002/hep.23769. PubMed PMID: 20583212.
253. Prieur A, Besnard E, Babled A, Lemaitre JM. p53 and p16(INK4A) independent induction of senescence by chromatin-dependent alteration of S-phase progression. Nat Commun. 2011;2:473. Epub 2011/09/15. doi: 10.1038/ncomms1473. PubMed PMID: 21915115.

254. Dou Z, Xu C, Donahue G, Shimi T, Pan JA, Zhu J, Ivanov A, Capell BC, Drake AM, Shah PP, Catanzaro JM, Ricketts MD, Lamark T, Adam SA, Marmorstein R, Zong WX, Johansen T, Goldman RD, Adams PD, Berger SL. Autophagy mediates degradation of nuclear lamina. Nature. 2015;527(7576):105-9. Epub 2015/11/03. doi: 10.1038/nature15548. PubMed PMID: 26524528; PMCID: PMC4824414.
255. Dou Z, Ghosh K, Vizioli MG, Zhu J, Sen P, Wangensteen KJ, Simithy J, Lan Y, Lin Y, Zhou Z, Capell BC, Xu C, Xu M, Kieckhaefer JE, Jiang T, Shoshkes-Carmel M, Tanim K, Barber GN, Seykora JT, Millar SE, Kaestner KH, Garcia BA, Adams PD, Berger SL. Cytoplasmic chromatin triggers inflammation in senescence and cancer. Nature. 2017;550(7676):402-6. Epub 2017/10/05. doi: 10.1038/nature24050. PubMed PMID: 28976970; PMCID: PMC5850938.
256. Takahashi A, Loo TM, Okada R, Kamachi F, Watanabe Y, Wakita M, Watanabe S, Kawamoto S, Miyata K, Barber GN, Ohtani N, Hara E. Downregulation of cytoplasmic DNases is implicated in cytoplasmic DNA accumulation and SASP in senescent cells. Nat Commun. 2018;9(1):1249. Epub 2018/03/30. doi: 10.1038/s41467-018-03555-8. PubMed PMID: 29593264; PMCID: PMC5871854.
257. Lan YY, Heather JM, Eisenhaure T, Garris CS, Lieb D, Raychowdhury R, Hacohen N. Extranuclear DNA accumulates in aged cells and contributes to senescence and inflammation. Aging Cell. 2019;18(2):e12901. Epub 2019/02/02. doi: 10.1111/acel.12901. PubMed PMID: 30706626; PMCID: PMC6413746.
258. Gire V, Dulic V. Senescence from G2 arrest, revisited. Cell Cycle. 2015;14(3):297-304. Epub 2015/01/08. doi: 10.1080/15384101.2014.1000134. PubMed PMID: 25564883; PMCID: PMC4353294.
259. Gunesdogan U, Jackle H, Herzig A. Histone supply regulates S phase timing and cell cycle progression. Elife. 2014;3:e02443. Epub 2014/09/11. doi: 10.7554/eLife.02443. PubMed PMID: 25205668; PMCID: PMC4157229.
260. Agarwal ML, Agarwal A, Taylor WR, Chernova O, Sharma Y, Stark GR. A p53-dependent S-phase checkpoint helps to protect cells from DNA damage in response to starvation for pyrimidine nucleotides. Proc Natl Acad Sci U S A. 1998;95(25):14775-80. Epub 1998/12/09. doi: 10.1073/pnas.95.25.14775. PubMed PMID: 9843965; PMCID: PMC24525.
261. Krenning L, Feringa FM, Shaltiel IA, van den Berg J, Medema RH. Transient activation of p53 in G2 phase is sufficient to induce senescence. Mol Cell. 2014;55(1):59-72. Epub 2014/06/10. doi: 10.1016/j.molcel.2014.05.007. PubMed PMID: 24910099.
262. Feringa FM, Raaijmakers JA, Hadders MA, Vaarting C, Macurek L, Heitink L, Krenning L, Medema RH. Persistent repair intermediates induce senescence. Nat Commun. 2018;9(1):3923. Epub 2018/09/27. doi: 10.1038/s41467-018-06308-9. PubMed PMID: 30254262; PMCID: PMC6156224.
263. Kotsantis P, Petermann E, Boulton SJ. Mechanisms of Oncogene-Induced Replication Stress: Jigsaw Falling into Place. Cancer Discov. 2018;8(5):537-55. Epub 2018/04/15. doi: 10.1158/2159-8290.CD-17-1461. PubMed PMID: 29653955; PMCID: PMC5935233.

264. Kang KT, Kwon YW, Kim DK, Lee SI, Kim KH, Suh DS, Kim JH. TRRAP stimulates the tumorigenic potential of ovarian cancer stem cells. BMB Rep. 2018;51(10):514-9. Epub 2018/06/26. PubMed PMID: 29936929; PMCID: PMC6235085.
265. Dang CV. MYC, metabolism, cell growth, and tumorigenesis. Cold Spring Harb Perspect Med. 2013;3(8). Epub 2013/08/03. doi: 10.1101/cshperspect.a014217. PubMed PMID: 23906881; PMCID: PMC3721271.
266. Loizou JI, Oser G, Shukla V, Sawan C, Murr R, Wang ZQ, Trumpp A, Herceg Z. Histone acetyltransferase cofactor Trrap is essential for maintaining the hematopoietic stem/progenitor cell pool. J Immunol. 2009;183(10):6422-31. Epub 2009/11/03. doi: 10.4049/jimmunol.0901969. PubMed PMID: 19880447.
267. Shachaf CM, Kopelman AM, Arvanitis C, Karlsson A, Beer S, Mandl S, Bachmann MH, Borowsky AD, Ruebner B, Cardiff RD, Yang Q, Bishop JM, Contag CH, Felsher DW. MYC inactivation uncovers pluripotent differentiation and tumour dormancy in hepatocellular cancer. Nature. 2004;431(7012):1112-7. Epub 2004/10/12. doi: 10.1038/nature03043. PubMed PMID: 15475948.
268. Unno A, Takada I, Takezawa S, Oishi H, Baba A, Shimizu T, Tokita A, Yanagisawa J, Kato S. TRRAP as a hepatic coactivator of LXR and FXR function. Biochem Biophys Res Commun. 2005;327(3):933-8. Epub 2005/01/15. doi: 10.1016/j.bbrc.2004.12.095. PubMed PMID: 15649435.
269. Sharov G, Voltz K, Durand A, Kolesnikova O, Papai G, Myasnikov AG, Dejaegere A, Ben Shem A, Schultz P. Structure of the transcription activator target Tra1 within the chromatin modifying complex SAGA. Nat Commun. 2017;8(1):1556. Epub 2017/11/18. doi: 10.1038/s41467-017-01564-7. PubMed PMID: 29146944; PMCID: PMC5691046.
270. Xu P, Li C, Chen Z, Jiang S, Fan S, Wang J, Dai J, Zhu P, Chen Z. The NuA4 Core Complex Acetylates Nucleosomal Histone H4 through a Double Recognition Mechanism. Mol Cell. 2016;63(6):965-75. Epub 2016/09/07. doi: 10.1016/j.molcel.2016.07.024. PubMed PMID: 27594449.
271. Turanov AA, Lo A, Hassler MR, Makris A, Ashar-Patel A, Alterman JF, Coles AH, Haraszti RA, Roux L, Godinho B, Echeverria D, Pears S, Iliopoulos J, Shanmugalingam R, Ogle R, Zsengeller ZK, Hennessy A, Karumanchi SA, Moore MJ, Khvorova A. RNAi modulation of placental sFLT1 for the treatment of preeclampsia. Nat Biotechnol. 2018. Epub 2018/11/20. doi: 10.1038/nbt.4297. PubMed PMID: 30451990; PMCID: PMC6526074.
272. Lazo JS, Sharlow ER. Drugging Undruggable Molecular Cancer Targets. Annu Rev Pharmacol Toxicol. 2016;56:23-40. Epub 2015/11/04. doi: 10.1146/annurev-pharmtox-010715-103440. PubMed PMID: 26527069.
273. Sun Y, Jiang X, Chen S, Price BD. Inhibition of histone acetyltransferase activity by anacardic acid sensitizes tumor cells to ionizing radiation. FEBS Lett. 2006;580(18):4353-6. Epub 2006/07/18. doi: 10.1016/j.febslet.2006.06.092. PubMed PMID: 16844118.

274. Kobayashi J, Kato A, Ota Y, Ohba R, Komatsu K. Bisbenzamidine derivative, pentamidine represses DNA damage response through inhibition of histone H2A acetylation. Mol Cancer. 2010;9:34. Epub 2010/02/11. doi: 10.1186/1476-4598-9-34. PubMed PMID: 20144237; PMCID: PMC2831819.
275. Coffey K, Blackburn TJ, Cook S, Golding BT, Griffin RJ, Hardcastle IR, Hewitt L, Huberman K, McNeill HV, Newell DR, Roche C, Ryan-Munden CA, Watson A, Robson CN. Characterisation of a Tip60 specific inhibitor, NU9056, in prostate cancer. PLoS One. 2012;7(10):e45539. Epub 2012/10/12. doi: 10.1371/journal.pone.0045539. PubMed PMID: 23056207; PMCID: PMC3466219.
276. Huang F, Abmayr SM, Workman JL. Regulation of KAT6 Acetyltransferases and Their Roles in Cell Cycle Progression, Stem Cell Maintenance, and Human Disease. Mol Cell Biol. 2016;36(14):1900-7. Epub 2016/05/18. doi: 10.1128/MCB.00055-16. PubMed PMID: 27185879; PMCID: PMC4936061.
277. Sheikh BN, Phipson B, El-Saafin F, Vanyai HK, Downer NL, Bird MJ, Kueh AJ, May RE, Smyth GK, Voss AK, Thomas T. MOZ (MYST3, KAT6A) inhibits senescence via the INK4A-ARF pathway. Oncogene. 2015;34(47):5807-20. Epub 2015/03/17. doi: 10.1038/onc.2015.33. PubMed PMID: 25772242.
278. Baell JB, Leaver DJ, Hermans SJ, Kelly GL, Brennan MS, Downer NL, Nguyen N, Wichmann J, McRae HM, Yang Y, Cleary B, Lagiakos HR, Mieruszynski S, Pacini G, Vanyai HK, Bergamasco MI, May RE, Davey BK, Morgan KJ, Sealey AJ, Wang B, Zamudio N, Wilcox S, Garnham AL, Sheikh BN, Aubrey BJ, Doggett K, Chung MC, de Silva M, Bentley J, Pilling P, Hattarki M, Dolezal O, Dennis ML, Falk H, Ren B, Charman SA, White KL, Rautela J, Newbold A, Hawkins ED, Johnstone RW, Huntington ND, Peat TS, Heath JK, Strasser A, Parker MW, Smyth GK, Street IP, Monahan BJ, Voss AK, Thomas T. Inhibitors of histone acetyltransferases KAT6A/B induce senescence and arrest tumour growth. Nature. 2018;560(7717):253-7. Epub 2018/08/03. doi: 10.1038/s41586-018-0387-5. PubMed PMID: 30069049.
279. Kalva SP, Iqbal SI, Yeddula K, Blaszkowsky LS, Akbar A, Wicky S, Zhu AX. Transarterial chemoembolization with Doxorubicin-eluting microspheres for inoperable hepatocellular carcinoma. Gastrointest Cancer Res. 2011;4(1):2-8. Epub 2011/04/06. PubMed PMID: 21464864; PMCID: PMC3070282.
280. Azarova AM, Lyu YL, Lin CP, Tsai YC, Lau JY, Wang JC, Liu LF. Roles of DNA topoisomerase II isozymes in chemotherapy and secondary malignancies. Proc Natl Acad Sci U S A. 2007;104(26):11014-9. Epub 2007/06/21. doi: 10.1073/pnas.0704002104. PubMed PMID: 17578914; PMCID: PMC1904155.
281. Lyu YL, Kerrigan JE, Lin CP, Azarova AM, Tsai YC, Ban Y, Liu LF. Topoisomerase IIbeta mediated DNA double-strand breaks: implications in doxorubicin cardiotoxicity and prevention by dexrazoxane. Cancer Res. 2007;67(18):8839-46. Epub 2007/09/19. doi: 10.1158/0008-5472.CAN-07-1649. PubMed PMID: 17875725.
282. Bose R, Verheij M, Haimovitz-Friedman A, Scotto K, Fuks Z, Kolesnick R. Ceramide synthase mediates daunorubicin-induced apoptosis: an alternative mechanism for generating death signals. Cell. 1995;82(3):405-14. Epub 1995/08/11. PubMed PMID: 7634330.

283. Toyoda E, Kagaya S, Cowell IG, Kurosawa A, Kamoshita K, Nishikawa K, Iiizumi S, Koyama H, Austin CA, Adachi N. NK314, a topoisomerase II inhibitor that specifically targets the alpha isoform. J Biol Chem. 2008;283(35):23711-20. Epub 2008/07/04. doi: 10.1074/jbc.M803936200. PubMed PMID: 18596031; PMCID: PMC3259784.
284. Childs BG, Baker DJ, Kirkland JL, Campisi J, van Deursen JM. Senescence and apoptosis: dueling or complementary cell fates? EMBO Rep. 2014;15(11):1139-53. Epub 2014/10/15. doi: 10.15252/embr.201439245. PubMed PMID: 25312810; PMCID: PMC4253488.
285. Chen QM, Liu J, Merrett JB. Apoptosis or senescence-like growth arrest: influence of cell-cycle position, p53, p21 and bax in H2O2 response of normal human fibroblasts. Biochem J. 2000;347(Pt 2):543-51. Epub 2000/04/06. doi: 10.1042/0264-6021:3470543. PubMed PMID: 10749685; PMCID: PMC1220988.
286. Purvis JE, Karhohs KW, Mock C, Batchelor E, Loewer A, Lahav G. p53 dynamics control cell fate. Science. 2012;336(6087):1440-4. Epub 2012/06/16. doi: 10.1126/science.1218351. PubMed PMID: 22700930; PMCID: PMC4162876.
287. Paek AL, Liu JC, Loewer A, Forrester WC, Lahav G. Cell-to-Cell Variation in p53 Dynamics Leads to Fractional Killing. Cell. 2016;165(3):631-42. Epub 2016/04/12. doi: 10.1016/j.cell.2016.03.025. PubMed PMID: 27062928; PMCID: PMC5217463.
288. Tang Y, Zhao W, Chen Y, Zhao Y, Gu W. Acetylation is indispensable for p53 activation. Cell. 2008;133(4):612-26. Epub 2008/05/20. doi: 10.1016/j.cell.2008.03.025. PubMed PMID: 18485870; PMCID: PMC2914560.
289. Li T, Kon N, Jiang L, Tan M, Ludwig T, Zhao Y, Baer R, Gu W. Tumor suppression in the absence of p53-mediated cell-cycle arrest, apoptosis, and senescence. Cell. 2012;149(6):1269-83. Epub 2012/06/12. doi: 10.1016/j.cell.2012.04.026. PubMed PMID: 22682249; PMCID: PMC3688046.
290. Timofeev O, Schlereth K, Wanzel M, Braun A, Nieswandt B, Pagenstecher A, Rosenwald A, Elsasser HP, Stiewe T. p53 DNA binding cooperativity is essential for apoptosis and tumor suppression in vivo. Cell Rep. 2013;3(5):1512-25. Epub 2013/05/15. doi: 10.1016/j.celrep.2013.04.008. PubMed PMID: 23665223.
291. Kagawa S, Fujiwara T, Kadowaki Y, Fukazawa T, Sok-Joo R, Roth JA, Tanaka N. Overexpression of the p21 sdi1 gene induces senescence-like state in human cancer cells: implication for senescence-directed molecular therapy for cancer. Cell Death Differ. 1999;6(8):765-72. Epub 1999/09/01. doi: 10.1038/sj.cdd.4400549. PubMed PMID: 10467350.
292. Chang BD, Watanabe K, Broude EV, Fang J, Poole JC, Kalinichenko TV, Roninson IB. Effects of p21Waf1/Cip1/Sdi1 on cellular gene expression: implications for carcinogenesis, senescence, and age-related diseases. Proc Natl Acad Sci U S A. 2000;97(8):4291-6. Epub 2000/04/13. doi: 10.1073/pnas.97.8.4291. PubMed PMID: 10760295; PMCID: PMC18232.
293. Zhou BP, Liao Y, Xia W, Spohn B, Lee MH, Hung MC. Cytoplasmic localization of p21Cip1/WAF1 by Akt-induced phosphorylation in HER-2/neu-overexpressing cells.

Nat Cell Biol. 2001;3(3):245-52. Epub 2001/03/07. doi: 10.1038/35060032. PubMed PMID: 11231573.
294. Brown JP, Wei W, Sedivy JM. Bypass of senescence after disruption of p21CIP1/WAF1 gene in normal diploid human fibroblasts. Science. 1997;277(5327):831-4. Epub 1997/08/08. PubMed PMID: 9242615.
295. Hsu C, Altschuler S.J., Wu, L.F. Patterns of Early p21 Dynamics Determine Proliferation-Senescence Cell Fate after Chemotherapy. Cell. 2019. doi: 10.1016/j.cell.201905.041.
296. Augello G, Puleio R, Emma MR, Cusimano A, Loria GR, McCubrey JA, Montalto G, Cervello M. A PTEN inhibitor displays preclinical activity against hepatocarcinoma cells. Cell Cycle. 2016;15(4):573-83. Epub 2016/01/23. doi: 10.1080/15384101.2016.1138183. PubMed PMID: 26794644; PMCID: PMC5056616.
297. Iglesias-Bartolome R, Patel V, Cotrim A, Leelahavanichkul K, Molinolo AA, Mitchell JB, Gutkind JS. mTOR inhibition prevents epithelial stem cell senescence and protects from radiation-induced mucositis. Cell Stem Cell. 2012;11(3):401-14. Epub 2012/09/11. doi: 10.1016/j.stem.2012.06.007. PubMed PMID: 22958932; PMCID: PMC3477550.
298. d'Adda di Fagagna F. Living on a break: cellular senescence as a DNA-damage response. Nat Rev Cancer. 2008;8(7):512-22. Epub 2008/06/25. doi: 10.1038/nrc2440. PubMed PMID: 18574463.
299. Biton S, Ashkenazi A. NEMO and RIP1 control cell fate in response to extensive DNA damage via TNF-alpha feedforward signaling. Cell. 2011;145(1):92-103. Epub 2011/04/05. doi: 10.1016/j.cell.2011.02.023. PubMed PMID: 21458669.
300. Herbig U, Jobling WA, Chen BP, Chen DJ, Sedivy JM. Telomere shortening triggers senescence of human cells through a pathway involving ATM, p53, and p21(CIP1), but not p16(INK4a). Mol Cell. 2004;14(4):501-13. Epub 2004/05/20. PubMed PMID: 15149599.
301. Bunz F, Dutriaux A, Lengauer C, Waldman T, Zhou S, Brown JP, Sedivy JM, Kinzler KW, Vogelstein B. Requirement for p53 and p21 to sustain G2 arrest after DNA damage. Science. 1998;282(5393):1497-501. Epub 1998/11/20. PubMed PMID: 9822382.
302. Wiebusch L, Hagemeier C. p53- and p21-dependent premature APC/C-Cdh1 activation in G2 is part of the long-term response to genotoxic stress. Oncogene. 2010;29(24):3477-89. Epub 2010/04/13. doi: 10.1038/onc.2010.99. PubMed PMID: 20383190.
303. Mao Z, Ke Z, Gorbunova V, Seluanov A. Replicatively senescent cells are arrested in G1 and G2 phases. Aging (Albany NY). 2012;4(6):431-5. Epub 2012/06/30. doi: 10.18632/aging.100467. PubMed PMID: 22745179; PMCID: PMC3409679.
304. Jullien L, Mestre M, Roux P, Gire V. Eroded human telomeres are more prone to remain uncapped and to trigger a G2 checkpoint response. Nucleic Acids Res. 2013;41(2):900-11. Epub 2012/11/30. doi: 10.1093/nar/gks1121. PubMed PMID: 23193277; PMCID: PMC3553962.

305. Toledo LI, Murga M, Gutierrez-Martinez P, Soria R, Fernandez-Capetillo O. ATR signaling can drive cells into senescence in the absence of DNA breaks. Genes Dev. 2008;22(3):297-302. Epub 2008/02/05. doi: 10.1101/gad.452308. PubMed PMID: 18245444; PMCID: PMC2216689.
306. Cipriano R, Kan CE, Graham J, Danielpour D, Stampfer M, Jackson MW. TGF-beta signaling engages an ATM-CHK2-p53-independent RAS-induced senescence and prevents malignant transformation in human mammary epithelial cells. Proc Natl Acad Sci U S A. 2011;108(21):8668-73. Epub 2011/05/11. doi: 10.1073/pnas.1015022108. PubMed PMID: 21555587; PMCID: PMC3102347.
307. Kang C, Xu Q, Martin TD, Li MZ, Demaria M, Aron L, Lu T, Yankner BA, Campisi J, Elledge SJ. The DNA damage response induces inflammation and senescence by inhibiting autophagy of GATA4. Science. 2015;349(6255):aaa5612. Epub 2015/09/26. doi: 10.1126/science.aaa5612. PubMed PMID: 26404840; PMCID: PMC4942138.
308. Dorr JR, Yu Y, Milanovic M, Beuster G, Zasada C, Dabritz JH, Lisec J, Lenze D, Gerhardt A, Schleicher K, Kratzat S, Purfurst B, Walenta S, Mueller-Klieser W, Graler M, Hummel M, Keller U, Buck AK, Dorken B, Willmitzer L, Reimann M, Kempa S, Lee S, Schmitt CA. Synthetic lethal metabolic targeting of cellular senescence in cancer therapy. Nature. 2013;501(7467):421-5. Epub 2013/08/16. doi: 10.1038/nature12437. PubMed PMID: 23945590.
309. Milanovic M, Fan DNY, Belenki D, Dabritz JHM, Zhao Z, Yu Y, Dorr JR, Dimitrova L, Lenze D, Monteiro Barbosa IA, Mendoza-Parra MA, Kanashova T, Metzner M, Pardon K, Reimann M, Trumpp A, Dorken B, Zuber J, Gronemeyer H, Hummel M, Dittmar G, Lee S, Schmitt CA. Senescence-associated reprogramming promotes cancer stemness. Nature. 2018;553(7686):96-100. Epub 2017/12/21. doi: 10.1038/nature25167. PubMed PMID: 29258294.
310. Park EJ, Lee JH, Yu GY, He G, Ali SR, Holzer RG, Osterreicher CH, Takahashi H, Karin M. Dietary and genetic obesity promote liver inflammation and tumorigenesis by enhancing IL-6 and TNF expression. Cell. 2010;140(2):197-208. Epub 2010/02/10. doi: 10.1016/j.cell.2009.12.052. PubMed PMID: 20141834; PMCID: PMC2836922.
311. Rao SG, Jackson JG. SASP: Tumor Suppressor or Promoter? Yes! Trends Cancer. 2016;2(11):676-87. Epub 2017/07/26. doi: 10.1016/j.trecan.2016.10.001. PubMed PMID: 28741506.
312. Yoshimoto S, Loo TM, Atarashi K, Kanda H, Sato S, Oyadomari S, Iwakura Y, Oshima K, Morita H, Hattori M, Honda K, Ishikawa Y, Hara E, Ohtani N. Obesity-induced gut microbial metabolite promotes liver cancer through senescence secretome. Nature. 2013;499(7456):97-101. Epub 2013/06/28. doi: 10.1038/nature12347. PubMed PMID: 23803760.
313. Xiao M, Chen W, Wang C, Wu Y, Zhu S, Zeng C, Cai Y, Liu C, He Z. Senescence and cell death in chronic liver injury: roles and mechanisms underlying hepatocarcinogenesis. Oncotarget. 2018;9(9):8772-84. Epub 2018/03/02. doi: 10.18632/oncotarget.23622. PubMed PMID: 29492237; PMCID: PMC5823588.
314. Hubackova S, Krejcikova K, Bartek J, Hodny Z. IL1- and TGFbeta-Nox4 signaling, oxidative stress and DNA damage response are shared features of replicative,

oncogene-induced, and drug-induced paracrine 'bystander senescence'. Aging (Albany NY). 2012;4(12):932-51. Epub 2013/02/07. doi: 10.18632/aging.100520. PubMed PMID: 23385065; PMCID: PMC3615160.
315. Dovey M, Patton EE, Bowman T, North T, Goessling W, Zhou Y, Zon LI. Topoisomerase II alpha is required for embryonic development and liver regeneration in zebrafish. Mol Cell Biol. 2009;29(13):3746-53. Epub 2009/04/22. doi: 10.1128/MCB.01684-08. PubMed PMID: 19380487; PMCID: PMC2698760.
316. Utani K, Kohno Y, Okamoto A, Shimizu N. Emergence of micronuclei and their effects on the fate of cells under replication stress. PLoS One. 2010;5(4):e10089. Epub 2010/04/14. doi: 10.1371/journal.pone.0010089. PubMed PMID: 20386692; PMCID: PMC2851613.
317. Fenech M, Kirsch-Volders M, Natarajan AT, Surralles J, Crott JW, Parry J, Norppa H, Eastmond DA, Tucker JD, Thomas P. Molecular mechanisms of micronucleus, nucleoplasmic bridge and nuclear bud formation in mammalian and human cells. Mutagenesis. 2011;26(1):125-32. Epub 2010/12/18. doi: 10.1093/mutage/geq052. PubMed PMID: 21164193.
318. Song CQ, Wang D, Jiang T, O'Connor K, Tang Q, Cai L, Li X, Weng Z, Yin H, Gao G, Mueller C, Flotte TR, Xue W. In Vivo Genome Editing Partially Restores Alpha1-Antitrypsin in a Murine Model of AAT Deficiency. Hum Gene Ther. 2018;29(8):853-60. Epub 2018/03/31. doi: 10.1089/hum.2017.225. PubMed PMID: 29597895; PMCID: PMC6110121.
319. Mou H, Ozata DM, Smith JL, Sheel A, Kwan SY, Hough S, Kucukural A, Kennedy Z, Cao Y, Xue W. CRISPR-SONIC: targeted somatic oncogene knock-in enables rapid in vivo cancer modeling. Genome Med. 2019;11(1):21. Epub 2019/04/17. doi: 10.1186/s13073-019-0627-9. PubMed PMID: 30987660; PMCID: PMC6466773.